CHARACTERIZATION OF CNT REINFORCED Al FUNCTIONALLY GRADED COMPOSITE LAMINATES

Thesis

Submitted in partial fulfilment of the requirements for the degree of

DOCTOR OF PHILOSOPHY

by

GURURAJA UDUPA

(Reg.No ME08F01)

DEPARTMENT OF MECHANICAL ENGINEERING

NATIONAL INSTITUTE OF TECHNOLOGY KARNATAKA,

SURATHKAL, MANGALORE - 575 025

August - 2017

DECLARATION

By the ph.D. Research Scholar

I hereby declare that the Research Thesis entitled ***"CHARACTERIZATION OF CNT REINFORCED AL FUNCTIONALLY GRADED LAMINATES" which*** is being submitted to **National Insttute of Technology Karnataka, Surathkal** in the partial fullfillment of the requirements of award of the degree **Doctor of Philosophy in Department of Mechanical Engineering** *is a bonafide report of the research work carried out by me.* The material contained in this Research Thesis has not been submitted to any University or Institution for the award of any degree.

Register Number **: ME08F01**

Name of the Research Scholar **: Gururaja Udupa**

Signature of the Research Scholar:

Department of Mechanical Engineering

Place :NITK - Surathkal

Date:

CERTIFICATE

This is to certify that the Research Thesis entitled ***"CHARACTERIZATION OF CNT REINFORCED Al FUNCTIONALLY GRADED COMPOSITE LAMINATES"*** submitted by **Mr. Gururaja Udupa (ME08F01)** as the record of the research work carried out by him, is accepted as the Research Thesis submission in partial fulfillment of the requirements for the award of the degree of **Doctor of Philosophy.**

Research Guides

Dr. Shrikantha S.Rao

Dr. K V Gangadharan

Date:

Chairman DRPC

Date:

ACKNOWLEDGEMENT

I would like to express my sincere thanks to my supervisors, Dr. Shrikantha S Rao and Dr. K.V. Gangadharan for their motivation and guidance throughout my research work. I am grateful to them for their keen interest in the preparation of this thesis. It has been my pleasure to work with them.

I wish to thank Prof. Karanam Uma Maheswar Rao, Director NITK Surathkal, Present Head of the department of Mechanical Engineering Prof. Narendranath and Prof. Jayakara Hegde, Prof. Appukuttan K.K., Prof. Mohanan, Prof. Ashok Babu, Prof. Mohan Kumar, Prof. Prasad Krishana, prof. K.V. Gangadharan former Heads of the Department, Mechanical Engineering for their support and encouragement throughout my stay at the NITK campus.

I wish to thank Prof. U. Sripati., Department of Electronic and Communication and Prof. S.M.Kulakarni, Department of Mechanical Engineering for being the members of Research Progress Assessment Committee and giving valuable suggestions. My thanks are due to Prof. A.O. Surendranathan, and Prof. Jagannath Nayak, Department of Metallurgy and Material Science Engineering, NITK for the help and support extended to conduct experiment in their laboratory

I wish to thank Prof. P.G. Mukunda, former Professor in the Department of Metallurgical and Materials Engineering at IIT Kharagpur for his valuable suggestions on developing the research ideas. Dr. Mervin. A. Herbet., Department of Mechanical Engineering for his valuable suggestions and encouraging throughout the project and thank all the Professors at NITK Surathkal, for passing their knowledge on to me.

I would like to thank all the non-teaching staff of Mechanical Engineering, Metallurgy & Material Science Engineering, Civil Engineering and Chemistry, NITK for their help in the experimental works. My thanks are due to Dr. Prithviraj, Incharge of Strength of Material laboratory, Department of Civil Engineering, NITK for the help and support extended to conduct experiment in their laboratory.

I am especially grateful to my colleagues and friends of Research Group, Dr. Saravana, Dr. Umashankar, Dr. Padiyar and importantly Mr. Abhinava Alva, one who initiated the concept of FGM project to be pursued.

I wish to thank my friends and colleagues at Department of Mechanical Engineering, NITK Dr. Vasudeva.M, Dr. Kumar G.N, Dr. Guruprasad K.R, Dr.P.Naveen karanth, Prof. Suresh Kumar Y, Prof. Suresh Hebbar. I wish to extend my thank to Dr. Veershetty, Dr. Shivananda naik, Dr. Vijaya kumar H, Dr. Sudhakar J. I am immensely indebted to the unending help and support I received from my co-research colleagues Mr. Umanath. P, Dr. Harsha Hegde, Mr. Avinash Pai and Mr. katari Kiran for their constant support and encouragements. The informal support and encouragement of many friends have been indispensable. I wish to extend my thank Junior research colleagues Dr. Manjayya, Dr. Arun kumar, Dr.Arun parameshwaran, Dr.Vignesh Naik, Dr.Kamal Babu, Mr. Karthik Rao, Mr.Subramanya prabu, Ms. Rashmi, Ms. Charitha. I wish to extend my thank to coordinator of C.S.D laboratory, helped to utilize the facility and all my colleagues at C.S.D lab at NITK for constant support during my stay.

At the end, I would like to thank Mr. Damodhara shetty, Foreman and Dr. R.P Reddy, Department of Mechanical Engineering, NITK, one who introduced me as a lecturer at NITK and constantly encouraging me to pursue my degree at NITK.

Finally and most importantly I thank my family, with whose constant encouragement and love, I have been successful in completing my thesis.

GURURAJA UDUPA

Dedicated

to

my parents

and

my family

Characterization of CNT reinforced Al Functionally Graded Composite Laminates

Abstract

Functionally graded composite laminate materials(FGCL) are special kind of new generation materials aimed at meeting new requirements of engineering applications. It contains, two or multi-phase particulate composites in which material composition and microstructure are characterized by continuous, smooth variations on macroscopic scale designed to meet desired functional performance. The absence of sharp interfaces in FGCL reduce chances of material property mismatch and thus leading to significant improvement in damage resistance and mechanical durability. Therefore, FGCL's are of great interest in disciplines as diverse as civil, electrical, mechanical, nuclear and nano engineering applications. However, the extent to which an FGCL can be tailored to meet the required performance –i.e., the design of FGCL strongly depends on the resultant effective properties and more importantly, on how these properties relate to its functional requirements. Hence, predicting mechanical, thermal or other relevant properties for given microstructure and its spatial distribution plays a significant role in the design of FGCL.

Objective and scope of the present work includes planning, preparation of CNT reinforced Al Functionally graded composite laminates by mechanical Powder Metallurgy technique and experimental testing for its characteristic properties. FG samples are prepared by varying the content of CNT (0.1,0.2,0.3,0.4 and 0.5 wt.%)in weight percentage and tested. Such prepared FGCL samples are tested for physical and mechanical properties. Before the FGCL samples are prepared, simple composite samples are prepared for same weight fraction of CNT reinforcement to characterize the microstructure and tested for the hardness. These composites are tested as per the ASTM guidelines. Once the results are confirmed, FGCL samples are designed for same weight fraction of reinforcement in layered fashion. The weight fraction is proportionally increased from 0.1 to 0.5wt.% from one end to the other end of the sample. The density, hardness and tensile behavior of FGCL samples are experimentally evaluated. These properties are found to be increasing with addition of CNT reinforcement. The damping ratio of composite and FGCL is estimated from impact hammer test, which demonstrated the significance of FGCL on the damping characteristics compared to a conventional composite material.

At present work, more focus on developing high wear resistance, light weight, good damping material with moderate good thermal conductivity material for brake rotor applications. Experimental investigation on FGCL proved good tensile stress properties with 0.5wt.% CNT reinforcement and these results are proven good agreement with characterization of microstructure. Microhardness for the cross-section of FG samples linearly varies with the increment in CNT reinforcement, which results in the variation of microstructure. Reduction in grain size found for 0.1 to 0.5wt.% CNT reinforcement, observed staggered layer of microstructure. The hardness of the developed material become high on the 0.5wt.% CNT reinforced side.

Wear properties are investigated with proper Design of Experiments by using Taguchi techniques for three parameters(Load, Abrasive grit size, Weight percent of CNT). It revealed that reinforcement of CNT affected reduction in the friction between the matting surface due to the formation of lubrication layers. Good wear resistance is observed for 0.25 to 0.4 wt.% CNT reinforcement. This result is in good agreement with the observation of SEM images for same weight fraction of CNT reinforcement. ANOVA results proved load, wear surface(Abrasive grit size) are the prominent factors for wear and CNT reinforcements improved the wear resistance in the materials. Finally, the improvement in thermal conductivity has been observed on CNT reinforcement.

Furthermore, FGCL's are associated with particulate composites where the weight fraction of particles varies in one or several directions. One of the advantages of a monotonous variation of weight fraction of constituent phases is the elimination of stress discontinuity that is often encountered in laminated composites and accordingly, avoiding delaminating-related problems. Investigation on developed FGCL samples found good agreement with the continuity in microstructure without step deviation as well as the hardness variation. Good damping behavior and wear resistance ability with improved thermal conductivity features could be a promising proposition for brake rotor materials. Insertion of developed light weight CNT reinforced FGCL between the cast iron plate on brake rotor make a huge impact on weight reduction and cost economics.

Keywords: FGM, FGCL, CNT, Al, Damping, Wear, Characterization, Composites, Brake rotor.

CONTENTS

LIST OF TABLES

LIST OF FIGURES

NOMENCLATURE

FGM	Functionally Graded Material
FG	Functionally Graded
FGCM	Functionally Graded Composite Material
FGCL	Functionally Graded Composite Laminates
CNT	Carbon Nano Tubes
SWCNT	Single Wall Carbon Nanotubes
MWCNT	Multi Wall Carbon Nanotubes
SDEV	Standard deviation
wt.%	Weight percent
E_c	Young's modulus of composite
E_f	Young's modulus of matrix
V_m	Volume fraction of matrix
V_f	Volume fraction of filler
£	Logarithmic decrement
ζ	Damping ratio
P	Density
GPa	Giga Pascal
TPa	Tera Pascal

CHAPTER 1
INTRODUCTION

1.1 Introduction

The concept of functionally graded materials (FGM) was proposed in 1984 by materials scientists in the Sendai area of Japan as a means of preparing thermal barrier materials. Since then, an effort to develop high-performance heat-resistant materials using functionally gradient technology has been continuing. In recent years, attempts to apply the FGM concept to enhance energy conversion efficiency have been initiated under the auspices of the Agency of Science and Technology (STA), Government of Japan. FGMs are composite materials, microscopically inhomogeneous, whose mechanical properties vary smoothly and continuously from one surface to the other (Koizumi1996). Under the same loading conditions, FGMs show better thermal properties than conventional composites. The concept of graded material is introduced to take advantage of its constituents, e.g. heat/corrosion resistance of ceramics on one side, and mechanical strength and toughness of metals on the other side of a plate-like body. FGMs provide superior thermo-mechanical performances under given loading circumstances. FGMs can be used to improve creep behavior, fracture toughness of machine tools, wear resistance, oxidation resistance in high-temperature aerospace and automotive components and so on. The accuracy of prediction of response of FGM structures will depend on both the kinematic modeling and the correctness of estimated effective material properties of the two-phase system. In order to achieve best performance, accurate material–property estimation is essential because the associated analysis and design for selecting an optimal volume–fraction variation definitely depends on its suitability. Apart from continuity, the performance of FGMs can be maximized by optimally tailoring the material composition (Kapuria et al. 2008).

1.2 Carbon Nanotube

The carbon nanotubes have high stiffness and axial strength due to carbon–carbon sp^2 bonding. It is one of the strongest materials (A.M.K. Esawi et al. 2011) having young's modulus of 1.4 TPa and tensile strength well above 100 GPa. CNT has excellent thermal properties with a thermal conductivity at least twice that of diamond and showing superconducting properties at lower temperatures. This shows unique electrical properties such as extremely low electrical resistance and can carry highest current density, measured as high as 109 A/cm^2. A comparison of Young's modulus of various reinforcing materials is shown in Table 1.1(Animesh bose 1985, I.Sridhar et al. 2008). Various techniques are being developed to synthesize of carbon nanotubes. Some of the basic methods used are the carbon-arc discharge method, the laser ablation method, the chemical vapor deposition (CVD) method, the flame synthesis, and Smalley's high-pressure carbon monoxide (HIP-CO) process. To produce CNTs of desired characteristics in large quantities is still a challenging task for the scientists and engineers**.**

Table 1.1. Comparison of Young's modulus for different reinforcements

(Animesh bose 1985, I.Sridhar et al. 2008).

Sl.No	Reinforcing material	Young's modulus (GPa)
1	Carbon particle	50
2	Aluminum	70
3	Wrought iron	210
4	Carbon fiber	250
5	Silicon carbide	450
6	Carbon Nanotube	1400

1.3 Aluminium and Alloys

Aluminum (Al) is one of the major industrial light weight metals available in abundance. It has gained significant commercial value since the last hundred years. The remarkable combination of useful properties suitable for a wide range of applications highlights the

importance of Al. The advancement in industrial technology has also contributed towards the growth in the usage of Al. The advantages of Al are so wide-ranging that they deserve to be applied where lightness, good mechanical and physical properties, durability, and workability are desired. The lightness of Al can also contribute to considerable weight savings in supporting structures (Anderi et al. 2006).

Apart from possessing good mechanical and physical properties, Al is also non-magnetic. These properties are invaluable in electronic industries and offshore structures. Because of the non-toxic nature, Al is also widely used in packaging industries. Other valuable properties include high reflectivity, heat barrier properties and heat conduction. The metal is malleable and can be easily worked by the common manufacturing and shaping processes (Gibson and Ashby 1988). The properties and characteristics of Al such as conductivity, corrosion resistance, finish, mechanical properties, and thermal expansion are modified by the addition of alloying elements. Alloying Al with small amounts of copper, magnesium, silicon, manganese, CNT imparts useful properties (Bishop et al. 2000).

Al as an engineering material has been of great interest for aerospace and automotive applications due to its high strength to weight ratio. The weight reduction of a vehicle by substituting Al for heavier materials results in 6-8% of weight savings. Even though there are improvements in materials other than Al, Al and its alloys still account for 80% of the structural weight of the most modern aircraft (Lloyd 1994). The alloys of 2xxx (Al & Cu) and 7xxx (Al & Zn) series have been used as main materials of construction for commercial aircraft even today. Al is also used in buildings, bridges, and other structural applications. Use of Al in automobiles is expected to grow, much faster due to the demand for a greener environment and greater fuel efficiency (Mondolfo 1976,La Delpha et al. 2008).

1.4 Composites

In the present day industry, there is a demand for a new material which can have combinations of most of the essential properties. The industry promotes the preparation of material made from two or more constituent materials with significantly different

physical and chemical properties which remain distinct at the macroscopic or microscopic scale. These materials are called composites whose properties depend on the constituent materials as well as the properties at the interface. More recently, the automotive, electronics and recreation industries have been working rigorously on the development of composites. The development of composites is a complex process and requires many considerations. Various parameters such as reinforcements and matrix types, tooling requirements and processes influence the fabrication (A.P. Meyer,1994). Composites provide interface when surfaces of dissimilar constituents interact with each other. Choice of fabrication method depends on matrix properties and the effect of matrix on the properties of reinforcement. One of the prime considerations in the selection and fabrication of composites is that the constituents should be chemically inert, non relative.

The composites are broadly classified as Metal matrix, polymer matrix and Ceramic matrix composites. The metal matrix composites that are currently produced and practically applied are based on light metal alloys, such as Magnesium (Mg) alloys, Aluminum (Al) alloys, Titanium (Ti) alloy and high temperature super alloys (J.E.Hatch, 1984). Reinforcements for the composites can be long fibers, short fibers and particles or whiskers. Fibers are essentially characterized by one very long axis with other two axes either often circular or near circular. Particles have no preferred orientation and shape. Whiskers have a preferred shape but are small, both in diameter and length as compared to fibers. It is understandable that properties of composite materials are improved versions of matrix materials due to presence of the dispersed phase.

1.4.1 Metal Matrix Composites

Metal matrix composites (MMCs) are a class of materials that are certain to play a significant role in the development of future engineering components. Most of the metals and alloys make good matrix for the composites due to their excellent mechanical properties, high thermal and electrical conductivity, and low coefficient of thermal expansion (Srivatsan et al. 1995). MMCs, in general, consist of two components, one is the metal matrix and the second is the reinforcement. While a variety of matrix materials have been used for making MMCs, the major emphasis has been on the development of

lighter MMCS using materials like Al, Ti, Mg, Zn and their alloys. This is due to the fact that they have significant potential for improvement in the thrust to weight ratio for the aerospace and automotive engines. Al alloy based MMCs are finding wide spread applications in industries. .

1.4.2 CNT reinforced functionally graded composite materials

CNT reinforced metal or ceramic matrix functional graded composites exhibit continuous improvements in properties such as thermo mechanical, light weight, dimensional stability, barrier properties, flame retarding abilities, heat resistance and electrical conductivity (Pindera et al. 1997, Suresh et al 1998). Compared to metals, these show higher strength-to-density ratios, higher stiffness-to-density ratios, better fatigue and wear resistance, better elevated temperature properties (Higher strength-Lower creep rate). In contrast to composite materials, FG-composites have new unique properties like, ability to mould directional mechanical properties, higher temperature capability (lower thermal expansion properties), excellent fatigue and fracture resistance. Relatively inadequate technology development and present complex fabrication methods are the major draw backs. It is difficult to meet stringent dimensional stability requirements during gradation and results in higher cost of the product.

1.5 Application of CNT in FGCM

CNT reinforced functionally graded-composite materials have the ability to function more efficiently than larger structures and machines. Due to functional variation of FGM-materials, their physical/chemical properties (e.g. stability, hardness, conductivity, reactivity, optical sensitivity, melting point, etc.) can be manipulated to improve the overall properties of conventional materials (Birman et al. 1995, Noda et al. 1999).

A material is called as nano-material when the size of the material is less than 100 nm in one direction. Carbon Nanotube (CNT) is an example for nano-material. It has many interesting physical and chemical properties and many of them have great potential in lot of applications. Due to small size, it has a large total surface area to volume ratio. The increasing of the surface area enhances the chemical reaction, the ability of surface

absorption and the catalytic ability of the material. In addition, the conductivity, mechanical strength, as well as optical property of the nano- materials are quite different from that of bulk system. The CNTs have a high potential to improve the mechanical, physical and electrical properties in composites.

Table 1.2. **Application of FGM (Miyamoto et al. 1999)**

Major areas	Application
Automobiles	Combustion chambers (SiC-SiC), Engine cylinder liners (Al-SiC), CNG storage cylinders, Diesel Engine pistons (SiCw/Al-alloy), Brake rotors, Leaf springs (E-glass/epoxy), Drive shafts (Al-C), Flywheels, Racing car brakes (Al-SiC), Motorcycle drive sprocket, Pulleys, Torque converter reactor, Shock absorbers (SiCp/Al-alloy), Radiator end caps.
Sub-Marine	Propulsion shaft (Carbon and glass fibers), Cylindrical pressure hull (Graphite/Epoxy), Sonar domes (Glass/Epoxy), Composite piping system, Scuba diving cylinders (Al-SiC), Floats, Boat hulls.
Commercial and Industrial	Pressure vessels, Fuel tanks, Cutting tool inserts, Laptop cases, Wind turbine blades, Electric motors, Firefighting air bottles, Artificial ligaments, MRI scanner cryogenic tubes, Wheelchairs, Hip joint implants, Eyeglass frames, camera tripods, Musical instruments, Drilling tubes, Drilling motor shaft, Drill casing, Crane components, High pressure hydraulic pipe, X-ray tables, Heart valves, Helmets, Crucibles, Beams.
Aerospace equipment and structures	Rocket nozzle (TiAl-SiC fibers), Heat exchanger panels, Engine parts (Be-Al), Wind tunnel blades, Spacecraft truss structure, Reflectors, Solar panels, Camera housing, Hublle space telescope metering truss assembly, Turbine rotor, Turbine wheels (operating above 40,000 rpm), Nose caps and leading edge of missiles and Space shuttle.
Aerospace	Wings, Rotary launchers, Engine casing, Rings (Al_2O_3 /Al-alloy), Drive shaft, Propeller blades, Landing gear doors, Thrust reverser(Carbon/Bismaleimide), Helicopter components viz. Rotor drive shaft, Mast mount, Main rotor blades (Carbon/Epoxy).
Sports	Racing bicycle frame (SiCw/6061), Racing vehicle frame.

The CNT exhibits an exceptionally high aspect ratio in combination with low density, as well as high strength, stiffness and energy absorbing capacity, which makes it a potential candidate for reinforcement materials. The determination of the geometrical structure of a nanotube can be combined with other measurement techniques to explore many physical properties at the nanotube level as a function of the nanotube diameter and chirality (Dresselhaus et al. 2003). High damping in a structure can often improve the performance in a dynamic loading environment. It is of particular interest to the designer concerned with the analysis and development of equipment which must function successfully with long durability in a mechanically dynamic environment. Improvement in damping characteristics of these materials makes them even more attractive. Materials possessing combination of good mechanical and physical properties along with good damping ability and better wear resistance with good thermal conductivity, in particular are required for applications requiring light weight. This leads to designing of new materials using light weight materials like Al as matrix and nano particles in the form of CNT as reinforcement, so that the properties can be enhanced to meet the requirements..

1.6 Processing Techniques

Functionally graded carbon Nanotube reinforced (FG-CNTRC) composites are prepared through a variety of processing techniques. Figure1.1 shows various processes that have been adopted for the synthesis of CNT-reinforced FG-composites. Powder metallurgy is the most popular and widely applied technique for preparing CNT Reinforced FG composites(Miyamoto et al. 1999). Electrodeposition and electroless deposition are the second most important techniques for deposition of thin coatings of Metal matrix-CNT composites as well as for deposition of metals on to CNTs. Following subsections shows relevant processing tasks adopted in the present work.

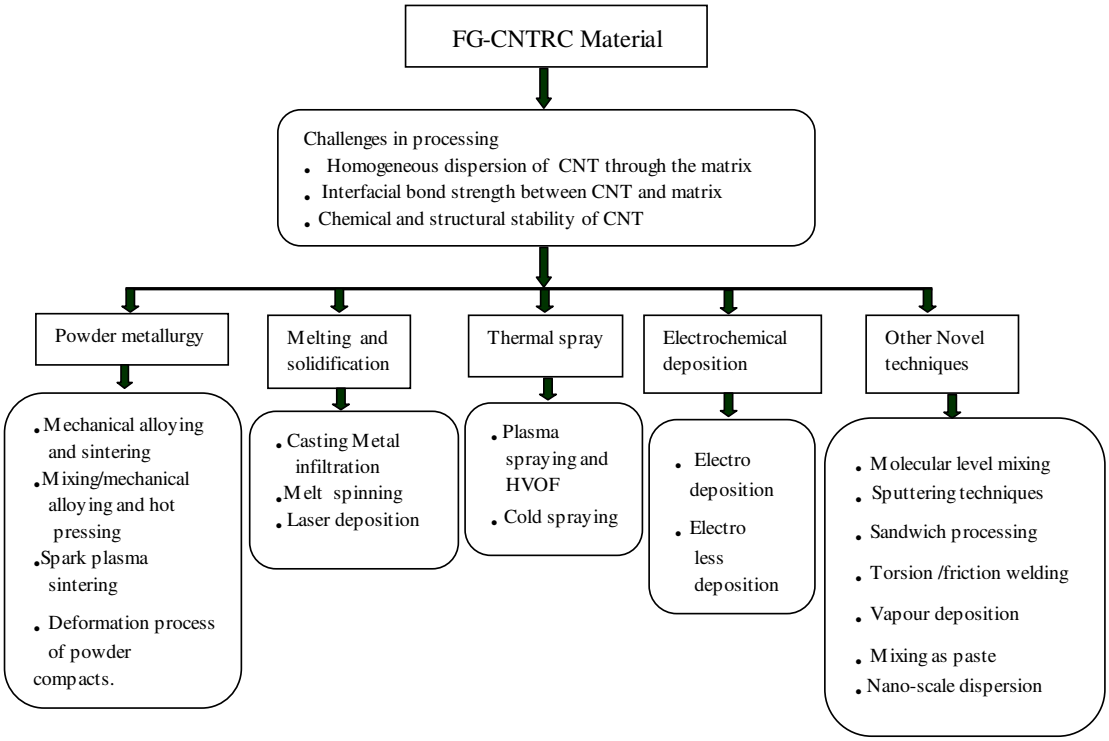

Figure 1.1. Different processing techniques

1.6.1 Powder Metallurgy

Powder Metallurgy is the process of blending fine powdered materials, compacting them into a desired shape, and then heating the compressed material in a controlled atmosphere to bond the material (sintering). The Powder Metallurgy process consists of four basic steps: (1) powder manufacture, (2) powder mixing and blending,(3) compacting, (4) sintering. Compacting is performed at room temperature, and the process of sintering is usually conducted at the atmospheric pressure. Recent developments have made it possible to use rapid manufacturing techniques which use the metal powder for the products. Because of this technique, the powder is melted and not sintered, so that better mechanical strength can be accomplished.

1.6.2 Sintering

Solid state sintering is the process of taking metal in the form of a powder and placing it into a mold or die. Once compacted into the mold, the material is exposed to a high temperature for a long period of time. The bonding takes place between the porous aggregate particles at elevated temperature and upon cooling, the powder mass would have bonded to form a solid piece. Sintering can be considered to proceed in three stages. During the first stage, neck growth proceeds rapidly but powder particles remain discrete. During the second stage, most of the densification occurs, the structure recrystallizes and particles diffuse into each other. During the third phase, isolated pores tend to become spheroidal and densification continues at a much lower rate. The word 'solid state' in Solid State Sintering simply refers to the state at which the material is in, when it bonds.

1.7 Outline of the thesis

The thesis is compiled and grouped in to 6 chapters. Chapter 1 gives a brief introduction of materials, methodologies and other aspects of the work that have been taken up. Chapter 2 forms the literature review. In this chapter, the work carried out by other researchers in relevant areas are identified and reviewed. It also deals with the objectives and scope of the work. Chapter 3 provides details on specimen preparation and characterization. In this chapter, the steps involved in producing Powder Metallurgy specimen of base Al and composites are detailed. Optical microscopy, TEM, XRD and mechanical property evaluation are also covered in this chapter. Characterization of Al matrix based CNT reinforced composites, result and discussion on macrostructure, density and hardness study are also presented. Chapter 4 focuses on the development and characterization of FGCL. A comparative study on experimental and model results is carried out. Conclusions on producing CNT reinforced Al matrix based FGCL through Powder Metallurgy route, dispersion of CNTs in the matrix and variation of wt.% gradation on materials prepared by studying SEM microstructure analysis, comparative study of damping on the composite and FGCL, variation of density and hardness in cross

section, result and discussion on tensile test, wear study, thermal study are also presented in chapter 5. Conclusion of the whole thesis is presented in chapter 6.

CHAPTER 2
LITERATURE REVIEW

2.1 Introduction

The development of suitable materials for different applications is still posing challenges in materials science engineering, which calls for increased focus on characterization of the developed materials for particular applications. Development of materials is carried out in three phases, i.e like, alloys, composites and functionally graded composites. Properties of the materials changed either as the reinforcement materials or with the change in percentage of reinforcement. Further studies on the direction of reinforcement led to functionally graded composites. Here, reinforcement material, method of reinforcement and direction of reinforcement matter a lot in getting good mechanical, physical as well as chemical properties. The material on which the study is carried out, the type of microstructure with continuous reinforcement, the type of damping mechanism, measurement methods also influence the properties. The recent advancement in fabrication methods and the applications are of great interest while developing new materials with new requirement of physical and chemical properties in materials. It is known that Aluminum (Al), its alloys and their composites as well as functionally graded composites are few of the most widely used materials for dynamic system environment applications such as aerospace and automotive industries. The processing of Al, its alloys and their composites containing different reinforcements, the study of mechanical properties and characterization of Functionally graded composites, and their enhancement, adaptability of such material for the engineering applications have been treated with great importance.

2.2 Aluminium and Aluminium Alloys

Aluminium (Al) is one of the most widely used non-ferrous materials in the manufacturing of different engineering and commercial products owing to its good strength to weight ratio. The significant weight savings and good mechanical properties

have made aluminium a potential material for most of the mechanical applications, especially in automobile and aeronautical industries (Sharma et al. 2004, Chunlei 2007, James and Edgar 2003). Progress in the metallurgy of Al and its alloys alongside the manufacturing processes has shown a significant landmark in the process of new materials development and as a possible replacement for steel family (Neubing et al. 2002).

Apart from possessing attractive material properties, like any other metal, Al can be easily cast, formed, or machined. It is a very lightweight metal with a density of around 2700 kg/m^3. It is highly impermeable and ductile in nature. Its strength can be adopted for the required application, by modifying the composition of its alloys (Lihua et al. 2007, Elwin 2004). Among the Al cast alloys, the Al-Si alloys themselves comprise 85% to 90%. They exhibit excellent ability to cast, very good mechanical and physical properties (Yijie et al. 2005a). The alloy constituents can be varied to achieve optimum mechanical properties (Ejiofor and Reddy 1997).

The alloys formed are grouped according to the major alloying elements. As per United Stated Aluminum Association system, the 4XXX Al alloy group is alloyed with silicon which promotes casting. Silicon increases fluidity of the melt, reduces the melting temperature and decreases the contraction associated with solidification. Silicon also has a low density($2.34\ g/cm^3$),which may be an advantage in reducing the overall weight of the cast component. Silicon has a very low solubility in Al and is retained as pure silicon. Silicon being hard, improves the abrasion resistance. Presence of fine distribution of Si crystals or coarsening contribute to the good damping property in Al-Si alloys (Kondo et al. 1999, Wei et al. 2002al).

The slow cooling of an Aluminum – silicon (Al-Si) alloy, starting from the liquid phase, leads to different microstructures being formed depending on whether the silicon content is lower than the eutectic composition (Hypoeutectic alloys) or higher than the eutectic composition (Hypereutectic) . In hypoeutectic alloys, the silicon content varies between 5.5 to 10.5%, and primary Al is the first phase to solidify while cooling. The micro-structure consists of primary Al dendrites within eutectic matrix. Eutectic alloys

contain 10.5 to 13.5% silicon and have micro structures consisting mainly of Al-Si eutectic. Hypereutectic alloys contain 16 to 23% silicon. Silicon reduces the thermal expansion coefficient, increases corrosion and wear resistance and improves casting and machining characteristics of the alloy (Massalski et al. 1990). All these properties blend Al perfectly to the manufacturing industry.

As far as aerospace and automobile industries are concerned, the broader focus is on the role of materials in creating lightweight structures (Haizhi 2003). Al-Si alloys are one of the important light metals, widely used in automotive, transportation, construction, and leisure industry due to their excellent wear resistance, pressure tightness, fluidity, and lower shrinkage (Ejiofor and Reddy 1997). It is reported that Al-Si alloys have relatively lower damping capacity compared to cast iron (Zhange et al. 1993, Rohatgi et al. 1994), which limits its ability to eliminate unwanted noise and vibration, enhancing vehicle and instrument stability in relevant applications. Such limitations can be overcome by choosing a composite material, a physical combination of two or more materials, tailored for certain properties.

2.3 Composites

A composite material is a mixture of two or more separate phases which have been intimately bound together and have properties superior to the individual constituents. According to ASM handbook, a composite is a "macroscopic combination of two or more distinct materials, having a recognizable interface between them" (ASM handbook 2001). Based on the type of matrix, they are grouped into metal matrix composites, polymer matrix composites and ceramic matrix composites. Depending on the size and shape of dispersed phase, they are classified as particulate-reinforced composites and fiber-reinforced composites. One more class of composites is structural composites, which includes laminates and sandwich structures. It is understandable that the properties of composite materials are nothing but improved version of properties of matrix materials in dispersed phase.

In the last few decades, development in composite materials has taken place rapidly, so as to meet the demands for better materials with higher standard of

performance and in-service reliability in structures, vehicles and machines. More recently, the automotive, electronics and recreation industries have also been intensively using composites, other than aerospace industries. Metal matrix composites (MMCs), in particular, have been receiving increasing attractiveness due to their highly specific mechanical and high temperature properties. However, the potential for widespread usage of MMCs is somewhat restricted owing to their relatively lower ductility and fracture toughness. Attention on MMC has started in 1960s, with the use of continuous reinforcement material (e.g. tungsten and boron fibers) and Al or copper as the matrix. In the 1980s, MMC production expanded and led to the development of discontinuously reinforced MMC (Clyne 1996).

2.3.1 Metal Matrix Composites

In the last two decades, MMCs have attracted considerable attention, mainly due to the availability of various types of reinforcements at competitive costs. The evolution of manufacturing processes to produce MMC's with reproducible structure and properties, and the availability of standard or near-standard metal working methods which can be utilized to fabricate these MMC's (Rack et al. 1988). The particulate reinforced MMC's are of particular interest due to their ease of fabrication, excellent combination of various mechanical properties and low processing costs and isotropic nature (Koczak and Premkumar 1993). Discontinuously reinforced MMC's have been observed to be a class of materials that exhibit a blend of properties of the reinforcement and the matrix (William and Harrigan 1998). Traditionally, discontinuously reinforced MMC's have been produced by several processing routes such as powder metallurgy, spray deposition, mechanical alloying (MA) and various casting techniques, i.e. squeeze casting, rheo casting, stir casting and compo casting (Tjong and Ma 2000). Commercial producers have concentrated on composites with particulate reinforcement because of cost issues (Lindroos and Trlvitie 1995).

Powder Metallurgy (PM) is one of the major processes used in processing of the MMCs (O' Donnell and Looney 2001). The process offers homogeneity in both composition and microstructure and also good yield to matrix (Hennessey et al. 2005).

This technique requires less energy input than the conventional ingot metallurgy process. In PM, it is important that the compaction process is correctly designed and implemented. This will ensure sufficient strength, porosity and density in the product. PM method comprises of blending of matrix powders and reinforcing elements and further cold pressing and sintering followed by plastic working (forging, extrusion). Plastic working is done primarily to achieve elimination and control of certain flaws and discontinuities. Most of the composite materials currently produced are based on light metal alloys, especially magnesium alloys, Al alloys and titanium matrices as well as high temperature super alloys based on nickel reinforced by stable ceramic dispersion particles. Composite materials based on light metal alloys are reinforced with dispersion particles, platelets, short fibers and continuous fibers (Kaczmar et al. 2000). Among the MMC's synthesized, Al metal matrix composites in general and discontinuously reinforced Al metal matrix composites in particular, have emerged as the forerunners for a variety of general and special engineering and structural applications (Das 2004). This trend has been attributed to their superior specific strength, specific stiffness, high temperature capability, lower coefficient of thermal expansion, better wear resistance, improved dimensional stability and amenability to conventional manufacturing techniques (Sathyanarayana et al. 1990, Allison and Cole 1993, Rohatgi 1995).

Although the micro mechanisms of particle interaction with matrix are complicated in composites, it is clear that local normal stresses acting on the particle interface are crucial for interfacial debonding between the particle and the matrix (Sun et al. 2003). Ramakrishna (1996) have reported on the relative importance of the load bearing effect of the reinforcement compared to the matrix – strengthening by the enhanced dislocation density in improving the yield strength of MMCs.

2.3.2 Al and Al alloy composites

Among the various metal matrix materials available, Aluminum and its alloys are widely used in the fabrication of MMCs for industrial use. They offer a large variety of mechanical properties which is depending on the chemical composition of the Al-matrix. Al-Si matrix composites, have resulted in comprehensive applications for the MMCs.

They have gained importance due to dimensional stability (Rohatgi 1995). It is reported that flake-graphite particles dispersed in the matrix of Al alloys increased the damping capacity; the improvement was better with higher amount of graphite (Rohatgi et al. 1976). The ratio between the damping capacity and the density of graphitic aluminium alloys is higher than that for cast iron, making them very attractive as light-weight, high-damping materials for possible aircraft applications.

Perez et al. (1993) studied the damping behavior of 6061Al/Gr metal matrix composites and observed that damping capacity improved with decrease in elastic modulus for the addition of graphite volume fractions from 0 to 0.1. Materials with high damping capacity have been identified to possess several advantages such as elimination of unwanted noise and vibration, enhancing vehicle and instrument stability (Rohatgi et al. 1994). The intrinsic damping of matrix and reinforcements is the main source of the damping of the composites found in preliminary damping studies of long graphite fiber, short graphite fiber and silicon carbide whisker reinforced Zn-Al alloy based composites (Mingyuan et al. 1994). Among high damping materials, Zn-Al alloys are considered as the most excellent non-ferromagnetic damping alloys and they possess low density.

SiC particles size of 62.4 μm and 28.5 μm were mixed with Al alloy (AA6061) powders of average size 71 and 16 μm, in different weight fractions and then subjected to uniaxial compaction and sintering (O'Donnell et al. 2001). The authors have observed that the size and distribution of the Aluminum powder affect strongly the sintering response of the green components. A narrow distribution of Aluminum powder size and an absolute size similar to SiC particles used should result in a composite, which is well sintered and does not exhibit particle clustering. The SiC particle size used must be minimized in order to reduce the possibility of particle fracture during in-service loading. Experiments have μm been carried out to investigate the damping behavior of foamed commercially pure Aluminium (Wei et al. 2002). The experimental value in terms of activation energy shows that this material has an enhanced damping capacity compared to bulk commercially pure aluminum due to the dislocation substructures intersecting and interacting with grain boundaries.

Couteau and Schaller 2004, carried out investigations on thermal stress relaxation in metal matrix composites using mechanical spectroscopy. It has been shown that thermal stress relaxation in MMCs can be interpreted in term of dislocation motion, controlled by a solid friction mechanism. A model was developed to achieve relaxation of thermal stresses by dislocation motion controlled by a solid friction mechanism to interpret the experimental results. The model results were found to be in good agreement with experimental values.

In their experimental studies on damping properties of coated continuous carbon fibers reinforced Aluminum matrix composites(Jinhai Gu et al. 2004), have reported that a Chemical Vapour Deposition (CVD) carbon coating on the surface of T300 carbon fibers greatly improves the overall damping capacity of C_f/Al composites. The improvement is mainly attributed to the interface micro-slip mechanism and the intrinsic high damping of the CVD pyrocarbon coating.

The effect of the presence of germanium (Ge) particles in the Aluminium matrix has been studied in terms of variation in overall damping property, significant to the internal friction arising at the matrix-particle interface. Results showed that compared to pure Al, 1.9 vol.% of Ge in the Al matrix increases the damping capacity by 46%. This is equal to the improvement obtained using 10.2 vol.% of SiC particulates. The experimental observation of this enhancement in damping characteristics has been rationalized in terms of the changes in the microstructure, such as the presence of plastic zones at the matrix-reinforcement interface (Narasimalu Srikanth and Manoj Gupta 2005).

The damping capacity test on Mg-Al-Si alloy was carried out using Dynamic mechanical Thermal Analyzer (DMTA) in three-point flexure mode (Lihua et al. 2005). The damping characteristic of Mg-Al-Si was investigated in terms of microstructure and micro hardness. The addition of Si resulted in the reduction of ratio of discontinuous precipitates. Strain-independent damping improved after treatment and strain-dependent damping decreases alloy with ageing time. The onset of increasing strain amplitude showed the shift of damping curve to bigger amplitudes.

The variation in damping capacity and tensile properties of Al-7Si-0.3 Mg aluminum alloy due to the effect of age hardening was studied by Choong 2005. The dislocation damping mechanism based on the Granato-Lucke theory due to age hardening process has shown marked influence on damping behavior of Al-7Si-0.3Mg. The high temperature background damping in metals occurs over a wider range of frequency or temperature caused by a combination of thermally activated dislocation mechanisms.

Studies have been conducted to find the effect of continuous/ discontinuous/ hybrid reinforcement on the damping characteristics of pure Al alloy composites (Narasimalu Srikanth et al. 2006). The samples were prepared using alumina particles in the size range of 10 μm to 50 μm and volume fraction of 10-13, 1.47 and 0.94 dispersed in Al-4 wt.% Mg matrix. Damping per unit volume percentage of alumina particles in the Al-Mg matrix increased by 58%,30% and 3% for the alumina particles size of 50 nm, 0.3 µm and 10µm, respectively, compared to the monolithic Al-Mg specimen. Such increase in damping has been rationalized in terms of microstructural changes that arise due to the presence of the alumina particles in the composite samples compared to that of unreinforced sample.

Composites of eutectic Al-Si alloy reinforced with sub-micron TiB_2 particles were successfully fabricated by means of reaction processing method (Hongzhan et al. 2006a). The ultimate tensile strength of the composites showed higher value than that of Al-Si master alloy at temperatures ranging from 25 to 400^0C, and the contribution ratio of the particles to the ultimate tensile strength reached its peak value at 260^0C.

The modules of Al-Si alloys A356 and A132 can be improved notably by producing their composites using TiB_2 particles. The incremental of the moduli of the two composites are close to each other at lower fractions of TiB_2 particles. However, the increment in modulus of 9.5 vol.% A 132/TiB_{2p} can reach 24GPa, which is 41.2% higher than that of 9.5 vol.% A356/TiB_{2p} (Hongzhan 2006b)

The composites of Al-Si (LM6) based alloy with Al_2O_3 particles as a reinforcement were produced using pressure die-casting technique. Three particle sizes and three volume fractions were used (huseyin Sevik and Can Kurnaz 2006). The density

values of the composites increased by adding Al_2O_3 particle. The hardness of the composites increased with increasing particle volume fraction and with decreasing particle size whereas the tensile strength decreased both with increasing particle volume fractions and size.

The spherical shaped fly ash particle reinforced Al6061 composites produces 40 vol.% porosities with hollow sphere of different diameters. The damping properties have been measured by using the forced vibration mode and the bending vibration mode on the multifunctional internal friction apparatus (We et al. 2006). The results indicate that the damping capacity of the fly ash/ Al 6061 composite with smaller reinforcement diameter is higher in both the vibration modes.

The Al356-fly ash particle composites were fabricated using stir-cast technique and hot extrusion (Sudarshan and Surappa 2008). Composites with 6 and 10 vol.% of fly ash were processed. Narrow size range (53-106/mu m) and wide size range (0.5-400/mu m) fly ash particles were used. Hardness, tensile strength, compressive strength and damping characteristics of the unreinforced alloy and composites were measured. Addition of fly ash resulted in increased hardness, elastic modulus and 0.2% proof stress. Composites reinforced with narrow size range fly ash particle exhibited superior, mechanical properties compared to composites with wide size range particles. A356 Al-Fly ash MMCs were found to exhibit improved damping capacity when compared to unreinforced alloy at ambient temperature.

The effect of macroscopic graphite (Gr) particulates of sizes 0.5-1.0 mm and up to 63 vol.% as reinforcement in eutectoid alloy of Zn-Al is evaluated for the damping behavior (wei et al. 2007). In this work, the damping behavior of the Zn-Al/Gr has been characterized by internal friction (IF) on a multifunction internal friction apparatus (MFIFA) at frequencies of 0.5,1.0 and 3.0 Hz over the temperature range of 25 to 400^0C, while continuously changing the temperature at each frequency. The damping capacity of the materials increased with reinforcement of macroscopic graphite particulates. The dominant damping mechanisms identified were dislocation damping and particulate/matrix interface damping. It was observed that, at higher temperatures,

dislocations, grain boundary gliding and interface sliding were operative more effectively.

The quartz-silicon dioxide particulate reinforced LM6 composites produced through carbon dioxide molding process, showed hardness to be increasing with increasing volume fraction of particulate. The tensile strength of the composites decreased with the increased addition of the particulate (Sulaiman et al. 2008). Fractographs of the tensile test specimen showed the particle pullout from the matrix due to lack of bonding and load deformation characteristic mechanism.

Among the various reinforcements in Al and Al-Si alloys, the dispersion of graphite particles in Al-Si alloys provides the alloy with antifriction properties, good wear properties, high damping characteristics, and good machinability. As a result, most developmental activities on this class of composites have focused more on microstructure and tribological characteristics than on mechanical properties (Das 2004). As regards to damping improvement due to porosity, alloying elements can greatly influence porosity formation via a few mechanisms. Firstly, an alloying element can change the freezing range of Al-Si alloy so that the porosity can be changed. When the freezing range is decreased, the "Mushy zone" in the solidifying material is reduced and thus the porosity is reduced. Secondly, alloying element can form dendritic intermetallics during solidification. Porosity can occur along these intermetallic dendrites. A study of the microstructure of an Al-9 wt.% Si-3 wt.% Cu alloy reveals that pores can nucleate along the long sides of the $\beta - Al_5FeSi$ needles (Roy et al. 1996). Thirdly, alloying elements can form a low melting point phase and cannot be filled when solidifying between dendrites. A study of an Al-Si-Mg alloy modified with Cu content over 0.2% resulted in a 7-fold increase of the dispersed microporosity (Caceres et al. 1999). The cause for the formation of dispersed microporosity is that, Cu forms some interdendritic Cu-rich phases, which solidify at a lower temperature and thus cannot be fully filled.

Silicon refining also has an influence on the formation of the porosity. Results of the work revealed that, the addition of 19 ppm phosphorus noticeably reduces the percentage porosity in the Al-9 wt.% Si-3 wt.% Cu alloy(Roy et al. 1996).

Recent studies have shown that improvement in mechanical properties can be achieved through the reduction of the scale of reinforcement size(Kiser et al. 1996, Kamat et al. 1991). The yield strength and plastic work hardening rate of the composites increase with decreasing particle size. It is found that the particle size has a significant effect on the dislocation strengthening mechanism, but little on the load transfer strengthening mechanism (Yan et al.2007). It is well established that the properties of MMCs are controlled by the size and volume fraction of the reinforcements as well as the nature of the matrix-reinforcement interfaces.

2.4 Carbon Nanotubes

Carbon Nanotubes are nanosize anisotropic material belonging to fullerence family identified in 1991 by Sumio Iijima, a Japanese physicist (Iijima 1991) and has proved very attractive in terms of properties like weight, strength, modulus values and dynamic behavior. Thereafter, different methods have been developed to produce Carbon Nanotubes. Iijima first observed the Multi-Walled Nanotube. The synthesis of Single Walled Nanotubes has been reported independently by Iijima and Ichlhashi (1993) and Bethune et al (1993).

Arc discharge method, Laser ablation and Chemical vapour deposition are the primary synthesis methods for single & multiwall carbon Nanotubes (Melissa Paradise and Tarun Goswami 2007). Multi-wall carbon Nanotubes were first produced by arc discharge method (Liu and Gao 2005).

Carbon nanotubes have been given a great deal of attention because of their unique properties that are leading to many promising applications (Erik et al. 2001, Rouff wt al. 2003, Kin et al. 2006a). The mechanical properties reported on carbon Nanotubes have given way for developing an entirely new class of composite materials. Although many research works report on the development of Nanotube based polymer composites (Kin et al. 2006b), attempts have also been made to produce composites using metals such as Al(Erik et al. 2001), lead (Nai et al. 2006), Silver (Fengs et al. 2005), copper (Kyung et al. 2006), magnesium (Peigney et al. 2007) as matrix materials with Nanotubes as reinforcement. Some of the key challenges in the fabrication of CNT composites include,

adequate dispersion of CNTs within the matrix and the tendency of CNTs to form bundles due to inter atomic forces (Gong et al. 2000, Zhu et al. 2003). Adhesion of the CNTs to the matrix has also been identified as another key issue (Star et al. 2001, Jin et al. 1998).

Salvetat Delmotte and Angel Rubio (2002) have discussed about mechanical properties of CNT's through a condensed review of important mechanical properties such as high elastic modulus and low weight. Authors have concluded CNTs to be a front-runner as reinforcement.

2.4.1 Carbon Nanotube Reinforced Composite

Composites of uniaxially oriented multi walled carbon nanotubes embedded in polymer matrices were fabricated and analyzed using transmission electron microscopy (Bower et al. 1999). In the strained composite films, buckling was observed universally in bent Nanotubes, the onset buckling strain and fracture strain were estimated to be 5% and 18%, respectively. The buckling wavelengths are reported to be proportional to the dimensions of the nanotubes. The carbon nanotubes have been found less than a nanometer in diameter for a single-walled nanotube with the elastic modulus and tensile strength as large as 0.8 TPa and 5 TPa, respectively. However, the superiority of the mechanical properties of nanotubes alone does not ensure mechanically superior composites because the composite properties are strongly influenced by the mechanics that govern the nanotube-polymer interface. The structural strength characteristics of composite materials greatly depend on the mechanical load transfer from the matrix (polymer interface) to the nanotube and the strength of the interface. The nature and mechanics of load transfer between Nanotube and polymer is critical for the manufacturing of carbon nanotube-polymer composites and will enable the tailoring of the interface for specific applications or superior mechanical properties (Desai and Haque 2005).

The review on exploring the progress in the area of reinforcement of polymers using carbon Nanotubes suggests that the effective processing is a great challenge. The mechanical properties of the polymer composites and the quality of reinforcement depend

on the processing techniques. The Multiwall Carbon Nanotubes have been dispersed homogeneously throughout polystyrene matrix by a simple solution evaporation method without destroying the integrity of the Nanotubes. Tensile tests on composite films show that 14 wt.% Nanotube additions result in 36%-42% and ~25% increase in elastic modulus and ultimate tensile stress respectively, indicating significant load transfer across the Nanotube-matrix interface (Coleman et al. 2006). It is concluded that carbon Nanotubes can be used in conjunction with carbon fibers in a hybrid polymer composite, in order to achieve elastic modulus values in the range 170-450 GPa. (Amal et al. 2007).

The force required to separate a carbon Nanotube from a solid polymer matrix has been measured by performing reproducible Nanopullout experiments using atomic force microscopy. The results imply that the polymer matrix in close vicinity of the carbon Nanotube is able to withstand stresses that would otherwise cause considerable yield in a bulk polymer specimen (Asa et al. 2003).

The effects of spatial distribution and geometry of carbon Nanotubes (CNTs) on the macroscopic stiffness and microscopic stresses of CNT reinforced polymer composites are investigated based on the multi-scale homogenization theory. An effective fiber model with transversely isotropic constitutive relationship is utilized to describe the nanotube including the surrounding thin matrix layer. The results reveal that, the staggered array of fibers given higher stiffness than regular array of fibers. Small end gap between two coaxial fibers can significantly enhance the macroscopic modulus. The effects of fiber volume fraction and fiber aspect ratio on the stiffness and stresses are similar to those of conventional short fiber reinforced composites. The fiber aspect ratio and fiber volume fraction on the distribution of micro-stresses along the fiber length show that large aspect ratio causes higher fiber axial stress than small aspect ratio for fiber volume fraction 20%. The stress concentration can be seen near the fiber ends with small aspect ratio giving higher shear stress than large aspect ratio. The region with high shear stress is limited to a very region for large aspect ratio. The fiber waviness significantly reduces the average fiber axial stress, which leads to a low macroscopic modulus. The concentration of shear stress is limited to a very small nano-size region,

which seems to be a beneficial characteristic of nanocomposites (Dongmeri Luo et al. 2007)

Attempts have also been made to develop the advanced engineering materials with improved properties through the incorporation of carbon Nanotubes in selected ceramics and metals matrices. The fully dense nanocomposites of signal-wall carbon nanotubes with nanocrystalline alumina (Al_2O_3) matrix at sintering temperatures as low as 1150^{o}C by spark-plasma sintering was prepared. A fracture toughness of 9.7 MPa/m^2, nearly three times higher than that of pure nanocrystalline alumina, and a 25% increase in toughness have been observed (Guo-Dong et al. 2002).

A review of carbon Nanotubes reinforced metal matrix and ceramic matrix nanocomposite was done by Peigney et al. 2000. Based on the structure, synthesis and physical properties of Carbon Nanotubes, the authors have reported that, a wide range of techniques have been used to fabricate these composites. The characterization of composites produced by different techniques has revealed that considerable improvements in electrical/ thermal properties can be achieved, but only a few studies have demonstrated significant improvements in macro-scale mechanical properties of ceramics such as fracture toughness (Arsecularatne and Zhang 2007).

Carbon Nanotube (CNT) reinforced magnesium was synthesized using the powder metallurgy technique followed by hot extrusion (Goh et al. 2006). Up to 0.3 wt.% of CNTs were added as reinforcements. The thermo-mechanical property results showed an increase in thermal stability with increasing amount of CNTs in the Mg nanocomposites. The mechanical property evaluation revealed an improvement of yield strength, ductility and work of fracture, the ratio of fracture toughness to Young's modulus with higher weight percentages of CNT.

The stiffening effect of carbon Nanotubes is quantitatively investigated by micromechanics methods. The effects of the extensively observed waviness and agglomeration of carbon Nanotubes are examined theoretically. The Mori-Tanaka effective-field method is first employed to calculate the effective elastic Moduli of composites with aligned or randomly oriented straight Nanotubes. The waviness or

curviness effect of Nanotubes are assumed to have a helical shape. Analytical expressions are derived for the effective elastic stiffness of Carbon Nanotube reinforced composites with effects of waviness and agglomeration showing reduction in the stiffening effect of Nanotubes significantly (Dong–Li Shi et al. 2004).

Copper with Carbon Nanotube (CNT/Cu) nanocomposites fabricated by the modified molecular-level mixing process, showed homogeneous dispersion of CNTs in a fine grained metal matrix. The nanocomposites consisting of 1.5μm Cu matrix grains and 5 vol.% of multiwall CNTs, showed a higher strengthening capability, enhanced the yield strength of unreinforced Cu by 2.3 times. The enhanced yield strength was due to the reinforcing effect of CNTs and additional hardening of the Cu matrix by grain refinement. The results revealed that the metallurgical treatment of the matrix is important for the development of high strength CNT/metal nanocomposites (Kim et al. 2008). High energy ball-milled nano-sized Cu powder reinforced with multiwall CNTs was cold rolled and sintered by spark plasma sintering (SPS) to produce the nanocomposites. The composite showed two-step yielding behavior on the stress-stain curves. This is caused from the micro structural characteristics consisting of two regions and the load transfer between these regions. The CNT/Cu nanocomposites showed a tensile strength of 281MPa, which is approximately 1.6 times than that of monolithic Cu (Kyung Tae Kim et al. 2006).

Powder Metallurgy method was used to produce composites of carbon Nanotubes in silver matrix. The effects of different Nanotube contents on the relative density, hardness, bend strength and electrical resistivity of the composites were investigated. The results showed that the addition of 8% by volume of carbon Nanotubes to the silver matrix increases the Vickers hardness and the bend strength by about 27% and 9%, respectively. The Nanotubes contributed less to the increase in bend strength than the hardness. The electrical resistivity of the composites increased slightly with increasing Nanotube volume fraction when the volume content of the Nanotubes was less than 10 vol.%. However, as the volume content increased from 10% to 25%, the resistivity experienced a sharp increase (Yi Frng et al. 2005).

A study has been made to demonstrate the ability to fabricate lightweight and ductile, but mechanically strong magnesium alloy(AZ91D) composites by introducing a small quantity of high crystalline multiwall carbon Nanotubes. It was observed that 1 wt.% of relatively short and straight carbon Nanotubes, distributed homogeneously on the outer surface of magnesium powders act as an effective reinforcing filler to prevent deformation. This enhances the tensile strength of magnesium alloy from 315 to 388 MPa (Shimizu et al. 2008).

Most of the review papers on CNT reinforced composites have highlighted that, carbon nanofibers are promising to revolutionize several fields in material science and are a major component of nanotechnology. Further, the development will depend on material availability at reasonable prices. Nanotubes have a wide range of unexplored potential applications in various technological areas such as aerospace, energy, automobile, medicine and chemical industry, in which they can be used as gas adsorbents, actuators, composite reinforcements, catalyst supports, probes, chemical sensors, nanopipes, nano-reactors etc (Rupesh Khare and Suryasarathi Bos 2005). The fundamental work in processing, characterization and analysis is important before the structural properties of this new class of nanocomposites are optimized (Subhranshu Sekhar Samal and Smrutisikha Bal, 2008). The dispersion of the filler and interaction between the matrix and the filler are the most important factors governing the improvement in physical properties of the nanocomposites structure (Bal and Samal 2007).

2.4.2 Processing and Characterization of CNT Reinforced Al/Al-Si Composites

The processing and the property evaluation of carbon Nanotube-reinforced Al-based composites, prepared by hot pressing followed by hot extrusion were carried out (Kuzumaki et al. 1998). His work indicated that the carbon Nanotubes in the composites were not damaged during the composite preparation and also no reaction product was visible at the Nanotube/Al interface after annealing for 24 hrs at 983 K. The strength of the composites was slightly affected with the annealing time at 873 K, while the strength of pure Al decreased significantly with time at the same temperature.

The aluminum-carbon nanotube (CNT) composites were prepared by hot-pressing the mixture of Al powder and CNT using powder metallurgy method (Xu et al. 1999) to study the micro structural characteristics and the distribution of carbon Nanotubes in the aluminum matrix. The electrical resistively of the composites was measured at temperatures varying from room temperature to 4.5 K. the electrical resistivity at room temperature increased slightly with increasing volume fraction of the Carbon Nanotubes in the aluminum. At about 80K, their resistivity abruptly dropped by more than 90%, but at lower temperatures, the resistivity did not show any fluctuation.

The study on the microstructure and interfacial reactions in an Al-fullerene (Al/C60) composite produced by pressurized liquid metal infiltration (squeeze casting) of a tap-packed C60 powder was conducted by Khalid et al. (2003). The composite showed a homogenous distribution of C60 crystals in the Al matrix, indicating that the original aggregated crystalline structure of the C60 fullerenes was not damaged during the composite fabrication process, though there was evidence of partial sublimation of C60. The C60 crystals had well integrated in the matrix and there was no hint either of porosity or of weak interfacial bonding. At the interface between Al and C60 rod-shaped and hexagonal plate-like phases were occasionally observed under TEM. These phases were identified as Al_4C_3 by XRD and Raman spectroscopy and were observed to nucleate on very thin layers of amorphous at the surface of the C60 crystals.

(Rong Zhong et al. 2003) produced the SWNT/ Nano-Al composites by mixing nano-Al particles and SWNTs. The cold consolidation and hot consolidation indicate that SWNTs can be used as an excellent reinforcing phase in a nano-Al matrix. The Vickers hardness measured using MVK – H3 hardness testing machine showed peak value of hardness as 2.89 GPa at 380^0C in comparison to 1.42 GPa at room temperature, proving that SWNTs are a promising reinforcement for metal matrices.

(Noguchi et al. 2004) employed the Nano-Scale Dispersion (NSD) method to disperse various fillers such as whiskers, ceramic fibers, and powders in metal matrices and to successfully produce nano-scale composites. It was observed that the carbon Nanotubes are uniformly dispersed in Al matrices. It is also noticed that, the

homogeneous dispersion of CNT, suppression of carbide formation and improvement of compatibility of CNT with Al were achieved by N-EP method (Nisshin Industry elastomer precursor method) (Noguchi tooru and Beppu Junichi 2004). In the first step, a precursor was made in which CNTs were uniformly dispersed. In the second step, molten Al was poured into the precursor to penetrate the precursor by capillary phenomenon and the mixture was cooled. The nanocomposite material made by N-EP method displayed improved elastic moduli, compression proof stress, and bending strength.

The free standing structures of Al-based nanostructured composite with carbon nanotubes as second phase particles have been synthesized by plasma spray forming technique (Laha et al. 2004). Microscopy and X-ray diffraction were carried out to analyze the composite structure and to verify the retention of carbon nanotubes. Besides, density and microhardness measurements were made to understand the effect of carbon Nanotube reinforcement on the mechanical properties of the composite. The characterization confirmed the presence of unmelted and chemically unreacted carbon nanotubes in the composite. Moreover, the composite showed an increase in relative microhardness due to the presence of carbon nanotube.

The inferences that powder metallurgy technique can be used for producing NT reinforced composite preparation and the Carbon Nanotubes (CNT) having Young's modulus of 1TPa, can be ideal reinforcements for composite materials have been presented by George et al. (2005). In this work, Multiwalled and single-walled Nanotubes synthesized by arc evaporation method were reinforced in commercial purity Aluminum. A mixture of CNT and Aluminum powder (200 mesh) was ball milled at 200 rpm for 5 min. The milled powder was compacted and the billets were sintered in an inert gas environment (nitrogen) for 45 min at 580^0C before finally hot extruding at 560^{o}C. Based on the geometry and physical properties of Multiwalled Nanotubes, three strengthening mechanisms were considered for the CNT/Al composite system, namely, thermal mismatch, Orowan looping and shear lag models. The results indicated that mechanical properties of the CNT/Al composite, including Young's modulus had improved. With the

increase in Young's modulus, the shear lag model seems to be applicable, since the other two models are not associated with Young's modulus, not an increase in yield strength could imply the additional applicability of Orowan looping and thermal mismatch models to the composite system. Hence the strengthening of the composite was considered as a synergistic effect of these mechanisms.

The Aluminum (Al)/ carbon (CNT) composite films were fabricated by sputtering pure Al on the surface of aligned multi-walled CNT arrays (Lijie Ci et al. 2006). Heat treatment was performed in the temperature range 400-950^0C. The interfacial reaction between the Al and the CNTs was investigated by annealing the samples at various temperatures. The results indicated that Aluminum carbide (Al_4C_3) formed at the interface between the Al and CNT layers and microscopic observation revealed that the reaction generally occurred at locations containing an amorphous carbon coating, at defect sites, and at open ends of CNTs. Because the nanosized CNTs are precursors for carbide formation, the Al_4C_3formed is also nanoscale in size. The carbide formed on the surface as well as at the tips of the CNTs improves the interfacial interaction between the CNTs and the Al layers. This also contributes to the enhancement of the mechanical properties of the composite. The authors concluded that chemical vapor deposited CNTs are a suitable candidate as reinforcing material for Al and other metal matrices.

The process of mechanical alloying (MA) to generate a homogenous distribution of 2 wt.% CNT within Al powders was carried out using Al (99.7% pure – 75 μm) and Multiwall Carbon Nanotubes (MWNT) (approximately 140 nm in diameter and 3-4μm in length, supplied by the MER corporation (Esawi and Morsi 2007). The effect of milling time (up to 48 hrs) on the morphological development of the powders and dispersion of CNTs were studied. The results showed that the MA technique is effective in dispersing the nanotubes within the soft Al matrix that simultaneously protects the nanotubes form damage under the impact of the milling balls. The result were encouraging for their processing of CNT-reinforced metal-matrix composites in general.

CNTs reinforced Al composites with 0 to 20% volume fraction of CNTs were produced by pressureless infiltration process to investigate the tribological properties of

the composites (Sheng-ming Zhou et al. 2007). The experimental results indicated that the friction coefficient of the composite decreases with increasing volume fraction of CNTs due to the self-lubrication and unique topological structure of CNTs. The hardness of the composites increased with increasing volume fraction.

Composites of Fe_3Al/CNT containing 5 vol.% of CNT were produced by spark plasma sintering (SPS). Samples of Fe_3Al/CNT were synthesized at a pressure of 30 MPa and temperature of 1273 K. These composites showed very promising mechanical properties like microhardness of 8.7 GPa and compressive yield strength of 3175 MPa which are about 95% and 56% higher than monolithic Fe_3Al(Lai –Xue Pang et al. 2007). The authors have indicated that CNTs are an effective nanoscale reinforcement for the inter metallics matrix composites which make an attractive material for future applications.

Perez-Bustamante et al., (2008) successfully produced the Al-based nanocomposites reinforced with Multiwalled Carbon Nanotubes by mechanical milling followed by pressureless sintering at 823 K under vacuum. Transmission electron microscopy at the interface showed that the nanotubes were not damaged during the preparation and no reaction products were after sintering. The yield stress (σ_y) and the maximum strength (σ_{max}) of the composites were considerably higher than those reported in the literature for pure Al prepared by the same route. The values for σ_y and σ_{max} increased with volume fraction of Nanotubes. The milling time and the concentration of nanotubes also contributed to the mechanical properties of the nanocomposites.

Using 5 wt.% MWNTs with 50 μm 2024 Al alloy powder, Deng et al., (2007) produced composites to study the apparent activation energy and reaction order by Kissinger equation and Crane equation under non-isothermal condition using the differential scanning calorimeter (DSC). The reaction product was examined under X-ray diffraction (XRD) and transmission electron microscopy (TEM). The experimental results showed that the Carbon Nanotubes react with aluminum and form Al_4C_3 phases with needle shape. The peak temperature of the reaction of carbon nanotubes and

aluminum was found to depend on the heating rate during the continuous heating. Apparent activation energy and reaction order of the reaction of Carbon Nanotubes and aluminum were found to be 194.01 and 0.92 kJ/mol, respectively.

The interfacial phenomena in thermally sprayed (plasma and high-velocity oxyfuel spraying) hypereutectic Al-Si composite reinforced with multiwalled carbon nanotube (CNT), analyzed both theoretically and experimentally, confirmed the formation of an ultra thin $\beta - SiC$ reaction layer at the interface (Laha et al. 2007b). Plasma sprayed composite exhibits a thicker Six layer (~ 5 nm) than the high velocity oxyfuel sprayed composite (~ 2nm). The formation of $\beta - SiC$ is identified as a factor responsible for the improved wettability of the molten Al-Si alloy matrix with MWNT reinforcement.

The carbon nanotube reinforced matrix composites were produced by isostatic pressing followed by hot extrusion techniques (Deng et al. 2007d). Microstructural results showed homogeneous distribution of nanotubes in the matrix, with some nanotubes acting as bridges across cracks; while a few pulled out on fracture surfaces of composites. The nanotubes wt.% showed significant effect on mechanical properties of composites. 1.0 wt.% Nanotube/ 2024 Al composite is found to exhibit the highest tensile strength and Young's modulus with increments of 35.7% and 41.3% respectively, higher than those with 2024Al matrix.

The fracture surfaces of the tensile test specimens were examined using field emission scanning electron microscope (Deng et al. 2007). Tensile strength and Young's modulus of the composite improved remarkably at 1.0 wt.% of CNT reinforcement but observed pull out of CNT's in Al matrix composite.

The coefficient of thermal expansion (CTE) studied for 1.0 wt.% multiwall Carbon Nanotubes reinforced aluminum matrix composite (Deng et al. 2008), had shown that the CTE of the composite reduces in relation to those of pure aluminum and 2024Al matrix decreases the CTE by 12% compared with those of pure aluminum and 2024Al matrix composites.

The same authors studied the damping behavior of CNTs reinforced 2024Al composite (Deng et al. 2007b). The damping behavior of the composites was investigated at frequencies of 0.5, 1.0, 5.0, 10, 30 Hz, in a temperature range of 25 – 400^0C. The frequency significantly affected the damping capacity of the composite with a frequency 0.5 Hz reached 975×10^{-3}. The storage modulus reached 82.3 GPa when the temperature was 400^0C. This shows that CNTs are a promising reinforcement for metal matrix composites to obtain high damping capabilities at an elevated temperature without sacrificing the mechanical strength and stiffness of a metal matrix.

The aluminum borate whisker (ABOw) and CNTs hybrid composites were produced through squeeze casting process (Zhang et al. 2007a). The results showed that CNTs decrease the compressive deformation in the composite. A small amount of CNTs, effectively improved the modulus, strength and elongation of the hybrid composite. Although the content of ABOw in ABOw/Al composite (40.8%) is higher than that in ABOw+CNTs/Al composite (35.1%), the young's modulus of the hybrid composite increased from 107.08 Gpa to 111 Gpa..

The free standing composite structures of hypereutectic Al-Si alloy with multiwalled carbon nanotubes (MWCNT) reinforcement, were produced by two different thermal spraying techniques viz Plasma spray Forming (PSF) and High velocity OXY-Fuel (HVOF) Spray Forming (Laha et al. 2007a). The microstructural and mechanical property evaluation of the two thermally spray formed nanocomposites indicated the presence of nanosized grains in the A-Si alloy matrix and physically intact and undamaged carbon nanotubes were observed in both the nanocomposites. This indicates the excellent interfacial bonding between alloy matrix and CNT. The elastic modulus and hardness of HVOF sprayed nanocomposite was reported to be higher than PSF sprayed composites.

CNTs were dispersed in Al powder by ball milling technique and composites were produced by hot extrusion (Choi et al. 2008). Transmission electron microscope results revealed that CNTs were distributed uniformly and the distribution improved with higher ball milling duration. The CNTs did not affect the grain refinement process during

the ball milling. In composites having grains of 200 nm and 70 nm size, load is transferred effectively, and the strengthening efficiency matched well with the rule of mixture for discontinuous fibers.

Powder rolling technique was used to fabricate the carbon nanotube reinforced Al strips. The Al-CNT mixtures were blended either in a mixer-shaker at a rotary speed of 46 rpm, or in a planetary mill at a rotary speed of 300 rpm in argon atmosphere, prior to rolling (Amal et al. 2008). The dispersion of the Nanotubes in the matrix was observed to be better when the blending was under higher energy planetary mill action. The strength of the rolled strips was evaluated for various wt.% of CNT. Out of the three CNT wt.% (0.5, 1, and 2), Al-0.5 wt.% composite strips exhibited enhanced mechanical properties.

The Multiwalled Carbon Nanotube reinforced Al Nanocomposite coatings was prepared using cold gas kinetic spraying (Srinivasa et al. 2008). Spray drying was used to obtain a good dispersion of the nanotubes in micron-sized gas atomized Al-Si eutectic powders with the compositions of 0.5 wt.% and 1 wt.%. Cold spraying resulted in coatings of the order of 500μm in thickness. Fracture surfaces of deposits showed that the Nanotubes were uniformly distributed in the matrix. nanotubes of shorter length were fractured due to impact and shearing between Al-Si particles and Al matrix during the deposition process. Nanoindentation showed a distribution of elastic modulus values from 40-229 GPa which was attributed to microstructural heterogeneity of the coatings, that comprised the pure Al, Al-Si eutectic, porosity and CNTs.

The Al-based composite containing carbon nanotubes (CNTs) were produced using a process of severe plastic deformation through high –pressure torsion (HPT) (Tomoharu Tokunaga et al. 2008). A significant increase in hardness was recorded through straining in the HPT process. A tensile strength of more than 200MPa was reported along with reasonable ductility. Transmission electron microscopy showed that the grain size was reduced to approximately 100 nm and this was much smaller than the grain size without CNTs and the grain size reported on a bulk sample.

Extruded (un-annealed) samples of Al-2wt.% CNT composites demonstrated high notch-sensitivity and also fractured consistently outside the gauge length during tensile

testing. In contrast, extruded samples annealed at 400°C and at 500°C for 10 hr prior to testing, exhibited more ductile behavior and no notch sensitivity (Esawi et al. 2009). The composites were processed through powder metallurgy route and for homogeneous dispersion of particles, planetary ball milling was used.

Hansang Kwon et al. (2009) produced highly densified Aluminum/carbon nanotube composites with nanoscale dispersion and regular orientation of the CNTs by spark plasma sintering and subsequent hot extrusion process. Microstructural observations confirmed that both the sintered Al/CNT compact and the extruded bulk material had a good dispersion of oriented CNTs. Raman spectroscopy showed that the processing did little damage to the CNTs. As a result, the composites exhibited tensile strengths that were thrice larger than pure Al.

The homogenous dispersion of carbon nanotubes in micron sized Al-Si alloy powders was achieved by spray drying (Srinivasa et al. 2006). Excellent flowability of the powders allowed fabrication of thick composite coatings and hollow cylinders (5 mm thick) containing 5wt.% and 10 wt.% CNT by plasma spraying. Two-phase microstructure with matrix having good distribution of CNT and CNT rich clusters has been observed. Partial CNT surface damage was observed in case of the 10 wt.% CNT coating due to CNT mesh formation and smaller size of spray dried agglomerate. Increase in the elastic modulus and improvement in the yield strength and elastic recovery properties due to CNT addition is established through nanoindentation.

2.4.3 Damping

Problems involving vibration occur in many areas of mechanical, civil and aerospace engineering. Characterization of damping forces in a vibrating structure has long been an active area of research in structural dynamics. Damping is an important feature of the dynamic behavior of composite structures, involving minimization of resonant and non-resonant vibrations. Generally, in metals, damping is comparatively low, resulting in high vibration amplitudes. High amplitude usually results in increased noise level and fatigue, which is undesirable. Damping measurement and prediction is very important from system design point of view (Marchetti et al. 1987).

The development of high damping metallic materials is possible only when the microscopic mechanism that controls the mechanical strength are also responsible for internal friction. One way of achieving such a compromise is the use of two-phase composites, in which damping or strengthening phase plays a specific role (Schaller 2003).

All metals individually possess certain amount of internal damping, manifested as dissipation of energy under vibration (Jeary 1977). The energy is either translated into heat or radiated away from the system. Material or internal damping contributes to about 10-15% of the total system damping (Rao, 1990). In forced vibration, the energy supplied by the excitation balances the energy loss.

To design materials with good damping properties it is necessary to understand the interaction between the intrinsic damping capacity and design parameters of the material such as internal structure and the manufacturing parameters controlling the structure (Aberg et al. 2004).

In engineering designs, (Ritchie et al. 1987) the focus is on new materials exhibiting good mechanical properties and high damping simultaneously. The damping capacity of metals is considered to be connected with the presence, movement and interaction of crystal lattice defects, such as dislocations, grain boundaries, secondary phases, impure atoms and vacancies (Zhang et al. 1994a). The most important of these is dislocation damping and it is extremely influenced by the distribution of the strong pinning points in dislocations (Granato and lucke 1956).

It has been found that the damping capacity of porous, sintered Fe-Cr alloys increases with increasing porosity to about 20%, and is three times greater than that of pore-free cast/wrought materials (Suzuki et al. 1977).

The stiffer metallic compound like Mg_2Si is introduced to enhance the damping capacity of pure magnesium and its alloys and the damping capacity increases with increasing amount of Si. The damping capacities at high temperature have been improved greatly with increasing Si, which should be attributed to higher dislocation density and refinement of grain size (Liao et al. 2007b).

The particulate-reinforced metal matrix composite (PMMC) is one of the very important high damping materials, with both structural and functional features (Gu et al. 2004a). It is pointed out that the overall damping capacity of PMMCs is closely related to the individual constituents, namely, reinforcing particulate, matrix and inter phase.

The shape memory alloys also exhibit high damping capacity or internal friction due to thermos-elastic martensitic transformation, which is related to the hysteretic movement of interfaces (Van Humbeeck 2003). The effect of surface coatings of particulates and the large aspect ratio of particulates are beneficial for the improvement of damping (Jinhai et al. 2006).

Hence, the vibration damping of a structure can be achieved by active damping that senses and suppresses vibrations in real time or by passive damping, through structures and materials that absorb the vibrational energy (Chung 2001). So the components of the vibration damping structures are selected among the materials exhibiting high damping capacity including a large selection of high damping metallic materials (Ashby 1999).

Damping mechanisms in composite materials differ from those observed in usual materials. At the constituent level, the energy dissipation in composites is induced by different mechanisms such as viscoelastic nature of matrix and reinforcement, the damping at the matrix-reinforcement interface, the damping due to damage, etc (Jean-Marie and Youssef 2004). The first equipment for measuring the damping of composite materials was developed by Adams et al. (1970) and Adams and Bacon (1973). The impulse method was initially developed by Suarez et al. (1984) and Crane and Gillespie (1991). The test specimen to characterize is supported as a flat cantilever beam in a clamping block. Impulsive excitation is applied using an electromagnetic hammer and the transverse displacement of the beam is measured versus time by means of non- contact eddy current probe positioned near the tip of the beam. Then, Fourier transform is performed to obtain the frequency response function. Curve fitting to Fourier transform is used by Suarez et al. (1984) to yield the complex modulus, when damping is evaluated by Crane and Gillespie (1991) form the loss factor determined by the half-power bandwidth

method. The evaluation of damping from the logarithmic decrement of the free vibration of cantilever beams is considered by Hadi and Ashton (1996) using the experimental process developed by Wray et al. (1990). The evaluation of damping from flexural vibrations of plates is considered by Sol et.al. (1994) and De Visscher (1995) using a procedure which estimates the complex bending stiffness of plates. The problems of free vibrations, wave propagation, and static deformations in FG beams are solved using finite element accounting for power law and other alternative variations of elastic and thermal properties in the thickness direction are mentioned in (Chakraborty et al. 2003, Chakraborty and Gopalakrishnan 2003). A recent paper by park and Kim (2006) contains FEA of free vibrations of geometrically nonlinear FEM plates. Dynamic response of FGM initially Prestressed rectangular plate subjected to an impulsive lateral load as well as well as free vibrations of such plate are considered for the cases where two opposite edges are clamped, while two other edges could be clamped, simply supported or elastically clamped (Yang and Shen 2001). Other papers elucidating problems of free vibrations and stress analysis are vividly available (Liew et al. 2002, Chen and Ding 2002).

2.5 Functionally Graded Materials

FGM's are two or multi-phase particulate composites in which the material composition and microstructure vary spatially in the macroscopic length scale to meet a desired functional performance as mentioned in earlier section. The absence of sharp interfaces in FGM reduces material property mismatch which can lead to significant improvement in damage resistance and mechanical durability (Suresh and Mortensen 1998). However, the extent to which an FGM can be tailored to produce a target mechanical performance –i.e., the design of FGM strongly depends on the resultant effective properties and more importantly, on how these properties relate to its microstructure. Therefore, predicting mechanical, thermal or other relevant properties for given microstructure and its spatial distribution plays a significant role in the design of FGM.

A number of reviews dealing with various aspects of FGM have been published in recent years (Pinders at al. 1995, Markworth et al. 1995, Aboudi et al. 1997, Miyamoto et al. 1999, Paulino et al. 2003). At present, FGM's are associated with particulate composites where the volume/weight fraction of particles varies in one or several directions. One of the advantages of a monotonous variation of volume fraction of constituent phases is the elimination of stress discontinuity that is often encountered in laminated composites and accordingly, avoiding delaminating-related problems. FGM may also be developed using fiber-reinforced layers with a volume fraction of fibers that is coordinate dependent, rather than constant, producing the optimal set of properties.

An FGM can also have a skeletal microstructure (Vel and Batra 2002). FGM may have a different architecture that results in an orthotropic behavior. Typical examples of orthotropic FGM have lamellar and columnar microstructures obtained by plasma spray and electron beam physical vapor deposition manufacturing processes respectively (Kayseer and Ilschner 1995). While particulate FG composite materials may be locally isotropic, they are also heterogeneous due to spatial variations of volume fractions of the phases, where spherical or nearly spherical particles are embedded within an isotropic matrix (Yin et al. 2004). FGM may include more than two constituent phases. In the recent past, material consisting of a ceramic and two different metallic phases whose volume fraction varied in the thickness direction according to a power law is analyzed (Nemat-Alla 2003).

2.5.1 History of Functionally Graded Materials

FGM's are characterized by continuous, smooth variations in composition(reinforcing material) and/or microstructure within the material so as to meet functional performance requirements that vary with locations within the part. This shows that their transition profiles have been designed and introduced intentionally in such a way that the desired properties are achieved. This separated the FGM's from the conventionally homogenous composite materials (B. Kieback et al. 2003).

From the historical point of view, the production of FGM's dates back to 1972 (Bever et al. 1972). Research work carried out by Nath et al indicate that mica particles are gradiently dispersed in Al-Cu-Mg in centrifugally cast hollow cylinders (Nath et al. 1981). The authors have illustrated that the mica particles near the inner periphery can serve as good as a solid lubricant, whereas the mica free zone having nearly the same strength as the matrix alloy would serve as a good backing material. However the concept of Functionally Gradient Materials was proposed in 1984 by a materials scientist in Sendai, Japan as a means of preparing thermal barrier materials (Koizumi 1997).

Also many potential applications were reported by many researchers in the field of electrical, chemical, optical, nuclear and biomedical areas (Pompe et al. 2003, Mishina et al. 2003,Kato et al. 2006, Muller et al. 2003, Zhou et al. 2010).

2.5.2 FGM Processing Techniques

FGMs can meet functional performance requirement that vary with the location within a work piece such as in a turbine blade, rocket nozzle, medical implant, tool inserts and optical devices (Birman et al. 2007). Nowadays with the usefulness of FGMs being established, more attention is paid to research on production techniques of FGMs.

The manufacturing process of a FGM is classified according to methodology of obtaining spatially inhomogeneous structure known as "Gradation' and transformation of this structure into a bulk material known as "Consolidation'. Segregating processes start with macroscopically homogenous material which is converted by an external field (viz. gravity or electric field). Homogenizing and segregating processes produce continuous gradients, but have limitations concerning the types of gradients which can be produced (Kiebact et al. 2003) and in the following sections these techniques are explained detail. Kawasaki et al have extensively worked on FGM from the late 1990s. An overview of the processing techniques (Kiebact et al. 2003) is tabulated in Table 2.1.

Table 2.1. Overview of processing techniques for FGMs

Process	Variability of transition function	Layer thickness	Versatility in phase content	Type of FGM	component geometry versatility
Power stacking	Very good	M, L	Very good	Bulk	Moderate
Sheet lamination	Very good	T,M[b]	Very good	Bulk	Moderate
Wet powder spraying	Very good	UT,T[b]	Very good	Bulk[C]	Moderate
Slurry dipping	Very good	UT,T[b]	Very good	Coating	Good
Jet solidification	Very good	M, L	Very good	Bulk	Very good
Sedimentation/ Centrifuging	Good	C	Very good	Bulk	Poor
Filtration /Slip casting	Very good	C	Very good	Bulk[C]	Good
Laser cladding	Very good	M	Very good	Bulk, Coating	Very good
Thermal spraying	Very good	T	Very good	Coating, Bulk	Good
Diffusion	Moderate	C	Very good	Joint, Coating	Good
Directed solidification	Moderate	C	Moderate	Bulk	Poor
Electrochemical gradation	Moderate	C	Good	Bulk	Good
Foaming of polymers	Moderate	C	Good	Bulk[C]	Good
PVD,CVD	Very good	C	Very good	Coating	Moderate
GMFC process	Very good	M,L,C	Moderate	Bulk	Good

L: Large (>lmm); Medium (100-1000μm); T: Thin (10-100μm); UT: very Thin (<10μm); C: continuous [b] Depending on a available power size,[c] Maximum thickness is limited.

Powder Metallurgy (Kawasaki el al. 1990) technique involved the selection of a material combination of metals and ceramics, optimum compositional distribution, stepwise or

continuous stacking followed by die compaction, isostatic pressing and sintering. Among all the steps, sintering is the most important process. Any imbalance in sintering process will cause various faults such as warping, frustum formation, splitting and cracking. Later the authors have shown that this imbalance can be avoided by pressure sintering i.e., by hot pressing and hot isostatic pressing (Kawasaki et al. 1997). Since the consolidation of the green party during sintering or pressing requires high temperature, there may be adverse microstructural features associated with the sintering, in particular porosity any interfacial reaction products.

Lin el al developed a mechanical working process which eliminates the need for sintering (Lin et al. 1999). This working process was successfully employed for the production of SiC/Al 2124 FGMs. The vibration process also improved local homogeneity by breaking up the coarse SiC agglomerates which tend to form in high SiC content regions of the FGMs. Jingchuan Zhu and others produced ZrO_2-Ni FGM by hot pressing and pressure less sintering (Zhu et al. 2001). The FGM produced has continuity of both components and eliminated the macroscopic interface. Xie et al.2002 have extensively worked on W-Cu FGMs and reported that by increasing the holding time and sintering temperature, the sintering quality of W-Cu composites improves. It develops structural homogeneity and changes the quality of composites.

The graded coatings are mainly used to protect metallic or ceramic substrates used in space shuttles, jet engines, nuclear fusion equipment and gas turbines against oxidation, heat protection, wear and corrosion (Cetinel et al. 2003). Depending on application and the specific loading conditions, various approaches are used to generate the gradients (Schulz et al. 2003). The coating through thermal spray techniques like High-Velocity Oxy-Fuel (HVOF) spraying, Low-velocity Oxy-Fuel (LVOF), etc.. used as an alternative approach to the conventional thermal barrier coatings in order to reduce the mismatch effect, thermal expansion and interfacial stresses (Wayne et al. 1990,Pintsuk et al. 2007). An alternative technique for FGM is Layered Manufacture Technique (LMT). This technology can produce virtually free form geometries using different materials. Selective laser sintering, direct laser remelting and laser cladding

which are based on powder and laser interaction are the processes used under LMT (Beal et al 2006).

Song et al.(2006) developed a new process called electromagnetic separation method for in situ multilayer FGMs. Smaller force will be induced in the primary particles of the alloy such as Si in Al-Si alloy, due to their lower electrical conductivity. The interfaces between the layers show gradient transition in the microstructure form one layer to another in the situ multilayer FGM.

The method of preparing Al-Si alloy containing 18% Si FGM using power ultrasonic field and water cooling system was reported by Zhang et al. (2009). Ultrasonic vibrations lead to vigorous migration of primary Si, and water cooling increases the solicitation velocity. The primary Si particles are rapidly trapped in the outer region by the engulfment of solidification interphase, which causes the graded distribution of primary Si in the sample. It was shown that volume fraction of primary Si varies from 30% to zero from outer to the inner side of the FGM sample. In accordance to this even the hardness and water resistance also showed better graded character(Gupta et al. 2000).

The application of centrifugal force to a metal as it solidifies can be used to distribute the molten into mold cavities and to achieve a dense sound casting (Janco 1998). In classical micromechanics, a wide variety of models exists for predicting effective elastic properties of heterogeneous materials, such as rules of mixture and their bounds (Mura 1991, Nemat-Nasser and Hori 1999), the Hashin- Shtrikman model (Hashin and Strikman 1963), the Eshelby's equivalent inclusion theory (Weng 1984) and the Mori-Tanaka model (Mori and Tanaka 1973). For FGM applications, a higher order thermoelastic theory is developed by coupling local and global effects (Aboudi et al. 1996). Recently, an elastic model including pair-wise particle interaction and gradient effects of phase volume fraction has also been studied (Yin et al. 2004). The determination of effective properties has also been demonstrated using the Voronoi cell finite element method (VCFEM) (Grujicic and Zhang 1998). These models being deterministic in nature, Rahman and Chakraborty (2007) presented a stochastic micromechanical model for elastic properties of FGM's.

2.5.3 Different physical tests on FGM

Hardness, simple normal indentation provides a basic tool for approximately gauging the resistance of surfaces to contact damage, impact or penetration. Few publications available in recent past focus on hardness studies on metallic FGM's (Jaworska et al. 2006, Dobrzanski et al. 2007. Choia et al.2008). These studies are focused on cutting tool applications. Noraiham Mohamad et al. (2008) produced epoxidised natural rubber-alumina nanoparticles composites by melt compounding by varying alumina nanoparticle from 10-60 parts per hundred rubber (pphr) and investigated the mechanical properties. They found that increase in alumina nanoparticles content resulted in increase in hardness compared to unfilled counterparts. Similar research is carried out by Oleiwi et al. (2009) wherein they analyzed the effect of adding silica particles and alumina particles separately with different ratio of styrene butadiene rubber. Scarce literature on graded complaint composites prompted for the present study on hardness testing of FG rubber composites.

Tensile behavior is another measure of the ability of a material to be deformed. Compression testing is a useful procedure for measuring the plastic state behavior. Several experimental and analytical studies on compressive behavior of syntactic foams are found in the published literature (Bunn and Mottram 1993, Rizzi et al. 2000, Karthikeyan et al. 2001, Gupta et al. 2001, Gupta et al. 2007). The present study explores possibility by investigating the tensile properties of composite system.

(Castro et al. 2002) conducted tensile tests on FGMs at various levels of reinforcement content. The effect of SiC particulate reinforcement on strengthening of the alloy is limited up to a certain volume fraction. There is a continuous increase in tensile and yield strength at corresponding increments of SiC_P volume fraction in the range of 20-30%. On the contrary there is a reduction in tensile and yield strength for SiC_P concentration in the range of 30 – 40% volume fractions

Fracture mechanics tests were conducted on Al/SiC_P FGMs with cracks oriented parallel to the gradation and it was observed that for this orientation, the crack growth resistance improved. It was attributed to higher absorption of the energy imposed on the

external loads and as a result, the fracture toughness of the composite was increased(Castro et al. 2000). Bollono et al, investigated the cylinder linear made from Al-Si alloy and Al-Al_2O_3 composite for different process parameters in order to optimize the reinforcement distribution at the inner surface of the liner (Bollono et al 2004).

2.5.4 Static Analysis of Functionally Graded Materials

Because of the wide material variations and applications of FGM's, it is important to study the static and dynamic analysis of functionally graded materials. Cho and Park (2002) presented finite element analysis on thermo elastic characteristics of High strength FGM cutting tools. They found out the possibility of FGM for improving the thermal strength of metal cutting tools, according to the parametric analysis by two-dimensional thermo elastic finite element method.

Rosso et al. (1999) conducted studies on graded cemented carbides components to evaluate hardness properties as well as the shrinkage due to sintering process, which are functions of the employed grades and show gradual change between the single values of each of the coupled grades. They proved that fine carbide grain mixes have a higher hardness compared to coarse grain ones with the same cobalt content, even if their abrasion resistant factor and transverse rupture strength are lower.

Chen et al. (2009) discussed on the feasibility of functionally graded hard materials for tool applications. By studying phase diagrams, phase stability, phase equilibrium and metallurgical reactions during sintering, they produced graded WC-Co hardmetals and graded Silicon ceramics (Si3N4), with increased Co contents and increased p7a phase ratio inwards respectively, recently from homogenous powder compact. Toshio Nomura et al.(1999) used material design method for the functionally graded cemented carbide tool. Narasimhan et al. (1995) described a coating scheme for a cemented carbide substrate containing a high percentage of cobalt binder. Their results showed that a multilayer coating based on this scheme provides excellent resistance against tool deformation and greatly improves the efficiency of metal cutting.

Jaworska et al. (2006) have presented functionally graded cermets. They found that the FGM obtained by powders forming method should be sintered using pressure

processes in a closed container because of high porosity of the material, which is a result of various chemical contents. A nonlinear analysis of functionally graded beams to examine the effect of geometric nonlinearity on displacements and stresses in beams made of functionally graded materials (FGMs) was conducted by Tahani et al. (2006). It was observed that for the maximum deflection greater than 0.3 times the thickness, a non linear solution is required.

Fatemeh et al. (2009) determined the thermo-mechanical stress distribution by using analytical and numerical methods for a three layered composite beam having a middle layer of functionally graded material (FGM). They also found that different values of power index (m) has considerable effect on profile of thermo-mechanical stress distribution and stress distribution in a FGM beam across the inhomogeneous layer is nonlinear.

Cho and Ha (2001) used averaging and finite-element discretization approaches in the numerical analysis of functionally graded materials. They estimated the thermo mechanical properties and responses of dual-phase functionally graded materials by conventional averaging approaches, such as rules of mixtures, mean-field micromechanics and so on. An analytical solution for bi-material beam with graded intermediate layer is presented by Wang et al. (2010). They investigated the bending problem of a bi-material beam with a graded intermediate layer and developed an elasticity solution for a bi-material beam with a graded intermediate layer by means of the Airy stress function.

A general solution of a cantilever functionally graded beam with arbitrary graded variations of material property distribution based on two-dimensional theory of elasticity was presented by Zheng and Tao (2007). They studied the problem of a cantilever functionally graded beam subjected to different loads. They presented a general two-dimensional solution for a cantilever functionally graded beam, assuming that all the elastic moduli of the material have the same variations along the beam-thickness direction, in terms of Airy stress function. Apart from that, Naghdabadi et al. (2005) presented a finite element formulation for the thermo elastic analysis of functionally

graded plates and shells. Kang et al. (2009) have presented bending of functionally graded cantilever beam with power-law non-linearity subjected to an end force.

Walter et al. (2002) presented one of the latest developments in the field of hard metals and cermets used for metal cutting operations, i.e. the establishment of a functional gradient in near-surface areas of cutting tools leading to functional gradient hard metals (FGHMs). Dobrzanski and Dolzanska (2010) used palm quist method to evaluate WC-Co tool gradient materials. They described the propagation characteristic of cracks produced at the corners of Vickers indent and the toughness change in functionally graded WC–Co cemented carbide with high disproportion of cobalt matrix portion between core and surface layer.

2.5.5 Dynamic Analysis of Functionally Graded Materials

Considering the importance of free vibration and dynamic analysis of functionally graded beams, Kapuria et al. (2008) have presented a theoretical model and its experimental validation of bending and free vibration response of layered functionally graded beams. They used third order zigzag theory based model for layered functionally graded beams in conjunction with the modified rule of mixtures (MROM) for effective modulus of elasticity , and validated through experiments for static and free vibration response. It demonstrates the capability of the zigzag theory in accurately modeling the mechanics of such beams.

Li (2010) presented a higher-order theory for static and dynamic analyses of functionally graded beams to suit FGMs subjected to various end conditions including free, hinged, clamped and elastically restrained beams. Simsek (2010) has presented a fundamental frequency analysis of functionally graded beams by using different higher-order beam theories. In his study, he examined the effects of slenderness ratio, material variations, the different formulations and the beam theories on the fundamental frequencies.

Yaman (2006) carried out theoretical investigation of the dynamical behaviour of a cantilever beam, partially covered by damping and constraining layers, with

concentrated mass at the free end. He used a finite element method in order to obtain the resonant frequencies and loss factors.

Amal et al. (2010) presented the dynamic characteristics of functionally graded beam with material graduation in axially or transversally through the thickness based on the power law. The model obtained by them is more effective for replacing the non-uniform geometrical beam with axially or transversally uniform geometrical graded beam. Simsek et al. (2009) investigated free vibration characteristics and the dynamic behaviour of a functionally graded simply supported beam under a concentrated moving harmonic load. They derived the system of equations of motion by using Lagrange's equations under the assumptions of the Euler–Bernoulli beam theory. Sina et al. (2009) presented an analytical method for free vibration analysis of functionally graded beams. They used a new beam theory to analyze free vibration of functionally graded beams by assuming that the beam properties are varied through the thickness following a simple power law distribution in terms of volume fraction of material constituents.

One of the most prominent properties investigated by number of researches is the vibration analysis. A comprehensive study of large amplitude free vibrations of plates using approximate analytical and numerical methods (finite element) is presented in the literature (Ambartsumyan 1970, Chandra and Raju 1975, Chandra 1976, Sathyamoorthy 1983). Finite analysis is used to solve amplitude free vibration analysis of anisotropic composite plates by using the first-order shear deformation theory (Reddy and Chao 1981 and 1982). Khatua and Cheung (1973) presented a finite element formulation for bending and vibration of multilayer beams and plates, with constrained cores. Sadasiva Rao and Nakra (1974) carried out analysis of vibration of unsymmetrical sandwich beams and plates with viscoelastic cores. Rao (1978) derived the complete set of equations of motion and boundary conditions governing the vibration of sandwich beams using energy approach. Recently, Banerjee (2003) has used the dynamic stiffness method for free vibration analysis of three layer sandwich beams. The simplest sandwich beam model utilizes Euler-Bernoulli theory for the face layers and only allows the core to deform only in shear (Ahmed 1971 and 1972, Hashemi and Adique 2009).Sandwich systems are not

been fully exploited in structural applications due to damage tolerance concerns (Avery and Sankar 2000). Zenkour (2005) dealt with FG sandwich panels for bucking and free vibrations. In particular, free vibration analysis of sandwich composites has been carried out by a number of investigators (Ahmed 1971, Avery and Sanker 2000). The concept of FG material as core made of rubber (natural latex) and its influence on mechanical performance of sandwiches is scarcely available in early literature (Evans et al. 2001, Wadley et al. (2003). In particular, free vibration analysis of sandwich composites is carried out by a number of investigators (Ahmed 1971, Rao 1978, Rahmani et al. 2010). But these studies restrict themselves by focusing on the use of homogeneous core. In recent past, few studies dscussed about behavior of sandwiches for FG cores (Li et al. 2008, Rahmani et al. 2009, Kashtalyan and menshykova 2009, Sh. Hosseini-Hashemi et al. 2011) focusing on numerical studies. Although sandwich structures offer advantages over other types of structures, it is important to develop new types of materials in order to obtain the absolute minimum weight for given conditions such as structural geometry and loadings.

The work carried out by Wang Kai aimed at segregating 20% SiC particles in a Z1104 (Z1104: Si9.24%, Mg 0.54%) aluminum alloy using compo-casting technique to achieve uniformly distributed SiC_P/Z1104 composites (Kai et al 2009). Microstructural characteristics of these centrifugally cast composites were studied as a function of position along the radial direction of casting in order to investigate the effect of differing centrifugal force along the radial direction(Fukui et al 1997).

2.5.6 Hardness

The Al based FGMs made by using different processing techniques have reported variation in hardness from one end of the specimen to the other. A variation of hardness from 70 HV to 122 HV is reported for Al-28 wt%. Si, produced by magnetic separation method (Song et al 2007). Al-18 wt% Si processed by power ultrasonic field technique showed a gradient of 80 HV to 55 HV from outer to inner region on the sample, having a primary Si volume fraction of 30% at the outer region (Zhang et al 2009). Al-Al_3Ni in situ FG composites casting using centrifugal method have shown that as the

concentration of nickel increases, the hardness of the specimen increases. Al-20 wt.% Ni system has exhibited the maximum hardness gradation from 55BHN near outer periphery to 46 BHN near the inner periphery followed by Al- 10 wt% Ni (45- 39 BHN). This aspect is also clearly revealed in their respective microstructure (Rajan et al 2008, Melgarejo et al 2005, Gupta et al 2002). Mehdi Estili (2008) reported the gradual and homogeneous CNT incorporation within an alumina ceramic promises to effectively cause in-depth gradients in microstructure, grain size and hardness varies from 17.32 GPa for 3.5 vol% of CNT to 15.20 GPa for 9 vol% CNT and 12.53 GPa for 15 vol% CNT with less thermo-mechanical mismatch were pure alumina had13.38 GPa of Vickers hardness value. These achievements strongly suggest that CNTs should be employed as a novel multi-functional candidate for manipulating and designing graded functionalities and properties within the conventional ceramics. Meanwhile, FGM laminated with five layers composing of Al, Ti and Al_3Ti confirmed the average value of Vickers hardness for each laminated layer of the FGM increases with increasing content of Al_3Ti phase in the layer. (Takekazu Nagae et al 2000). Umashankar (2012) also worked extensively on Al and Al alloy reinforced CNT composites and reported variation of hardness.

2.5.7 Wear

Publications on the dry sliding wear of homogenous Al-Si system show that researchers have tried to optimize the Si content, study the transition in wear rate as a function of variations in sliding wear parameters, such as applied load and sliding distance. In the study of dry sliding wear of two Al-Si alloys(10.9 and 22.1 % Si) against a steel counter face, two wear regimes were observed (Sarkar et al1975).The first wear regime was described as a mixed mode of elastic - plastic contact where Archard's law is obeyed. The second regime, activated at a critical applied load, was characterized by gross plastic flow where the wear rate was not directly proportional to the load. It was also stated that the hyper- eutectic alloy experienced a higher wear rate than the hypo- eutectic alloy(Clarke et al 1979). Wear mechanisms in the dry sliding of Al-Si alloys have been classified as oxidative wear and metallic wear (Shivanath et al 1977);

- Oxidative wear occurred at lower applied loads. In this, aluminium oxide layer formed on both the wearing Al-Si surface and the counter face. Wear occurred firstly by oxidation of the asperities and then secondly by fracture and compaction of the oxidized wear debris into this film.
- Metallic wear mechanism was more predominant at higher applied loads. The Al-Si wear surface was characterized by plastic deformation and fracture, significant transfer of material between the sliding surfaces and wear debris formation.
- Al-Si alloy and CNT reinforced Al composites samples were subjected to wear studies on a pin on Disc machine using steel disc. Three distinct wear regimes were identified as a function of applied load(Reddy et al. 1994).

In case of mild wear conditions, the 1 wt.% CNTs reinforced Al6061 composite displayed lower wear rate and friction coefficient compared to the monolithic Al6061(A.M. Al-Qutub et al 2012). High erwear rate was oobserved and friction coefficient compared to the monolithic alloy for severe wear condition(A.M. Al-Qutub et al. 2012). In case of Seizure wear regime, temperatures near the surface were high enough to lower the shear strength in the sub-surface layer which promoted extensive material transfer from the wearing alloy to the steel counter face.

Regarding topographical features of worn Al-Si alloys in dry sliding, the mutual transfer of material between the wearing Al-Si and the steel counter face appears to be a feature of all wear regimes and becomes more significant as load increases. The transition from mild to severe (metallic) wear is associated with the existence of a delamination wear process (Sarkar et al. 1975). Although some papers reported that Si additions(4-24%Si) improved wear resistance of aluminium, no relationship between wear rates as a function of Si content was found (Reddy et al. 1994). Wear rate increased linearly with applied pressure but was independent of sliding velocity. The value of the friction coefficient was found to be insensitive to applied pressure, Si content and sliding velocity (Clarke et al. 1979). It was also reported that seizure was associated with features like rapid increase in wear rate, transfer of pin material to the counter face, increased face, increased noise and vibration (Reddy et al. 1995).However,(Kim et al. 2009) observed

mixed abrasive and adhesive wear for Al-CNT composites with different CNT content at fixed load and sliding speed. They also reported minimal oxidation wear for the composite containing 1 wt.% CNTs.

A few efforts have been made to find the effect of Si in Al based FGM. Wear resistance of the FGM sample produced by Al-18wt.% Si, power ultrasonic method decreased gradually from outer to inner. The wear resistance distribution of the FGM sample is in good accordance with the microstructure distribution (Zhang et al. 2009). In case of Al-Mg-B, it was shown that the wear resistance increased in trend with hardness observed in the outer region. The SEM analysis revealed abrasive and oxidative wear modes, the extent of which was dependent upon the boron content (Melgarejo et al. 2006). The wear rate of the FGM is not significantly affected by the presence of the aqueous solution (Gomes et al 2005).A tribological study carried out on Al/SiC_p FGM with water as lubricating medium showed that it played as a carried agent for transfer of material. To improve the wear resistance of thermal barrier coatings, hard particles were successfully introduced in to the surface area by employing the HVOF technique. A graded alunina particle profile was produced in the surface area, with 20% particles in the surface area proving to be the optimum, regarding good thermal shock and wear resistance (Schulz et al 2003,Gupta et al 2003).Micro ploughing and delamination wear reported as the dominant wear modes for Al-CNT composites by Choi et al. 2010. Oxidation is the main wear mechanism observed and explained this through the formation of alumina layer on the on the composite and its subsequent delamination causing abrasion between the specimen and the counter face (Zhou et al 2007).

It can be concluded that many mechanisms can play a significant role in the sliding wear behavior of complex polyphase alloys and that it is not a simple function of composition. The wear is a complex phenomenon which depends on different parameters viz., type of the matrix material, type of the reinforcement, surface roughness, processing technique, pressure, temperature, environment, sliding speed, type of friction etc (Bialo et al 2000).

2.5.8 Motivation

However, little is known on CNT reinforced Al composites through experimental route in case of Powder Metallurgy. Quantitative understanding on CNT reinforced Al FGCL stab resistance performance is also not yet available in open literature.

FGCLs resist high-temperature environments while maintaining toughness and other required mechanical properties. FGMs are being intensively extended to many applications, such as aeronautics, industrial materials (high-strength cutting tools), optoelectronics, energy materials, biomaterials and so on (Kapuria et al. 2008). In order to explore functionally graded cutting tool, Cho et.al. (2002) presented a new concept of FGM to metal cutting tools for relaxing thermal stress concentration near the tip-shank material interface. So, it is important to study the mechanical and microstructural analysis of FG structures. Since reinforcement of CNT in Al FGCLs provides superior thermo-mechanical performances under given loading circumstances, it can be used to improve hardness, wear resistance and fracture toughness of braking pad, brake rotors and many more applications. In this background, the motto of my work is to carry out investigative studies on the mechanical properties through microstructural analysis of CNT reinforced Al FGCL with simple cold compacting technique.

2.5.9 Objectives and Scope of the Present Work

From the literature survey, it is clear that the research work on development of low cost light weight materials for brake rotor is not sufficient. A cost effective CNT reinforced Al functionally graded composite brake rotor is proposed for the applications like light weight, wear resistance.

The perusal of FGMs literature review prompted a thorough and systematic study on these FGCLs by performing experimental characterization of various physical and mechanical properties including thermal conductivity. Therefore the work undertaken pursues the following objectives:

1. To prepare functionally graded Al composite with CNT reinforcement and study the physical properties of FGCL like density, hardness and damping behavior over gradation, under different weight fractions of reinforcement.
2. To carry out metallography studies on the effect of weight fraction of reinforcement on FGCL.
3. To study the behavior of FGCL in terms of wear and thermal conductivity under gradation.

Scope of the present work includes, processing of CNT reinforced Al samples with varying % by weight fraction of CNT. The study also involves an attempt to establish the gradation of reinforcement by physical and mechanical properties such as density, hardness and damping.

Developed FGM are utilized to further characterize their suitability in real world applications. Experiments are prepared as per design of experiments approach so that multiple factors (CNT weight fraction, Load and Abrasive grit size) at three different levels can be simultaneously analyzed to study wear behavior of the FG composites. Further, these samples are subjected to different tests including density, tensile, bending, damping and finally thermal conductivity test. In the end, combination of factors for low wear rate is proposed. Few samples are subjected to mechanical test and the response is averaged out for these. Thermal conductivity test is carried out on the FGCL samples to confirm the heat dissipation capacity of the developed material.

CHAPTER 3

MATERIAL PREPARATION AND EXPERIMENTAL METHODOLOGY

3.1 Introduction

In recent years, Nano reinforcements have gained considerable attention over conventional micron-sized reinforcements, because of the enhanced mechanical properties that can be imparted to the metal matrix composites (Aniruddha ram et al. 2013). Tubular structured reinforcements such as Carbon Nanotubes (CNTs) are considered as strengthening the matrix more effectively than spherical reinforcements owing to the resultant shorter inter-reinforcement spacing (Liu et al. 2012). As in conventional composites, the orientation of the CNTs, homogeneity of the composite, nanotube matrix adhesion, nanotube aspect ratio, and the volume fraction of nanotubes are expected to have significant influences on the properties of the nanocomposites. Controlling such factors to obtain a composite with exceptional properties is very challenging (Sridar et al. 2009). Theoretical and experimental results show that Multiwalled Carbon Nanotubes (MWCNTs), which are chemically more robust than their single-walled counterparts, are also the stiffest among known fibers, with a measured Young's modulus of ~1.8 TPa (Heekyu Choi et al. 2013). In addition, the elongation failure for CNTs is of the order of 0.4 (failure strain), which when combined with the stiffness, suggests high tensile strengths of ~55.5 GPa/mg/m^3 (Laha et al. 2009). Several fabrication techniques, namely ball milling, extrusion, hot pressing, equal channel angular pressing, spark plasma sintering, electrodeposition, electroless deposition, and thermal spraying, have been used to synthesize the metal matrix composites reinforced by CNTs (Pérez-Bustamante et al. 2009,Javadi et al. 2012).

In the present work, the CNT reinforced Al composites are prepared through Powder Metallurgy(PM) route. High energy ball milling was used to mix Al particles and the CNTs mechanically. In the next stage, Composite consisting of different layers with different weight fraction of CNT reinforcement is prepared as a functionally graded composite material. The composition is determined through Energy Dispersive

Spectroscopy (EDS) and X-ray Diffraction (XRD). The morphology and distribution of CNT in the base material is studied using optical microscopy. The distribution of CNT in the composite matrix is observed through Scaning Electron Microscope (SEM). Vickers hardness machine (CLEMEX-500) is used to study the variation of hardness on each layer of composites. The structure observed by a field-emission scanning electron microscope revealed an attachment of CNTs to the surface of the Al-flakes. SEM results showed that particle size and morphology of CNT reinforced Al varied with milling time for different mass fraction of reinforcing element. Finally, the composite powders were processed into bulk material by compaction and sintering. Further, the developed FGCL specimen is tested for studying hardness, young's modulus, damping, wear and thermal conductivity.

3.2 Materials and Methodology

3.2.1 Matrix Materials: Aluminium

Pure aluminium is soft, ductile, corrosion resistant and has a high electrical conductivity. Its properties are given in Table 3.1 In consequence it is widely used for many applications, but alloying with other elements is necessary to provide the higher strengths needed for other applications. CNT is used as reinforcement material and its properties are given in Table 3.2.

3.2.2 Methodology

The CNTs used in the present study were synthesized via chemical vapor deposition (Chengdu Co. Ltd, China). The flowchart for the specimen preparation was given in Figure 3.1.The Al powders (Acros, purity 99%, 200 mesh, Code: 300935001) were irregular in shape with a flake morphology (Figure 3.2a). The CNTs are 20-30 nm in diameter and 10-30 μm in length (Figure 3.2b).

CNT-Al powder mixtures were prepared by a mixing process that involved an intensive sonication in ethanol. Then, the solution was heated to a temperature of 55^{o}C and ultrasonicated until most of the ethanol had evaporated. In the next step, the

mechanical mixing process produced relatively homogeneous mixtures of CNTs and Al powders.

Table 3.1. Physical properties of Al

Sl.No	Properties	Value
1	Atomic Number	13
2	Atomic weight (g/mol)	26.98
3	Valency	3
4	Crystal structure	FCC
5	Melting point (^{o}C)	660.2
6	Boiling point (^{o}C)	2480
7	Mean Specific Heat (0-100°C) (cal/g.°C)	0.219
8	Thermal Conductivity (0-100°C) (cal/cms. °C)	0.57
9	Co-efficient of Linear Expansion (0-100°C) (x10-6/°C)	23.5
10	Electrical Resistivity at 20°C (μΩcm)	2.69
11	Density (g/cm^3)	2.6898
12	Modulus of Elasticity (GPa)	68.3
13	Poisson's Ratio	0.34

3.2.3 Properties of CNT

Table 3.2. Physical properties of CNT

Properties	Value
Purity	Carbon > 90% (trace metal basis)
OD × ID × L	10-15 nm × 2-6 nm × 0.1-10 μm
Total Impurities	Amorphous carbon, none detected by transmission electron microscope (TEM))
Melting Point	3652-3697 °C
Density	~2.1 g/mL at 25 °C

After the mixing process, the mixtures of 0.1% to 0.5% mass fraction CNTs and Al powders were placed in 300 ml mixing jars containing 25 stainless steel milling balls of 10 mm in diameter giving an initial ball-to-powder weight ratio (BPR = 10:1). The jar

was filled with argon and was then agitated in a horizontal ball milling at 250 rpm/min for various time intervals. Based on the literature study, the mixing duration for pure Al and CNT-Al composites for mechanical alloying was chosen to be 6 hrs. Homogeneously well dispersed CNT-Al composite powders containing different wt.% CNT were prepared by a planetary ball milling process (Retsch GmbH, PM400). Methanol was added as a process control agent (PCA) in order to minimize cold welding of the Al particles. The ball-milled powder mixtures were compacted in a cylindrical-diameter compaction die as shown in Figure 3.4 (Umashankar 2011). Based on the relationship between green density and compaction pressure of the Al alloys, the compaction pressure of the samples was chosen to be 120 kN for pure Al (Umashankar 2011). Finally, the samples were sintered in a vacuum furnace. The starting materials were characterized by field-emission scanning electron microscopy (FE-SEM) (using a Hitachi model SE 4160) to examine the dispersion of the CNTs within the Al matrix and to characterize the composites, morphology, and size of raw materials. The microstructures of the samples after every step were observed with an optical microscope (leica Co. DM 4000 M) and a scanning electron microscope (Camscan model MV2300)equipped with energy-dispersive spectrometry (EDS model Oxford). The microhardness of the sintered specimen were measured by a Vickers hardness tester (Wolpert, 1-30 kg). Next stage, FGCL was prepared based on the same process but the Al-CNT composite powders were assembled in a layered structure inside a 25 mm diameter die, with compositions ranging from pure Al to composite containing 0.5wt.% CNT, followed by cold-pressing (UTM Testing machine, 40 ton) for 60 sec under an uniaxial pressure of 400 kN.

3.2.3.1 Selection of Die and Powder weights

ASTM B-92503 standard has been adopted for the preparation of hardness test specimen. The design specification of die is depicted in Figure 3.3. Figure 3.4 shows the actual images of the die used for preparation of test specimens. The matrix material of 35 g (as per the requirement of billet size) and reinforcement based on the weight percentage are used for specimen preparation. Table 3.3 represents the weight percentage of reinforcement and corresponding weights.

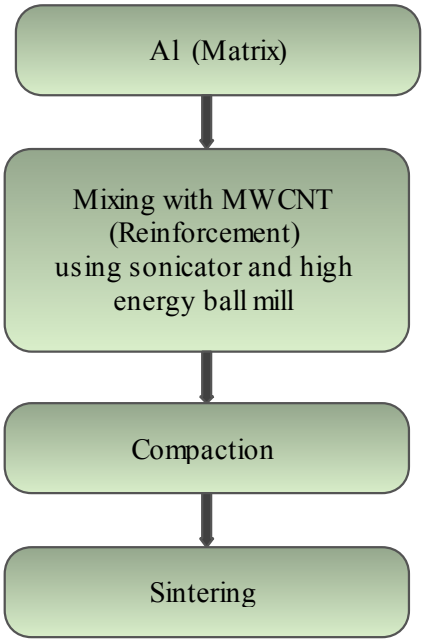

Figure 3.1. Flow chart for specimen preparation

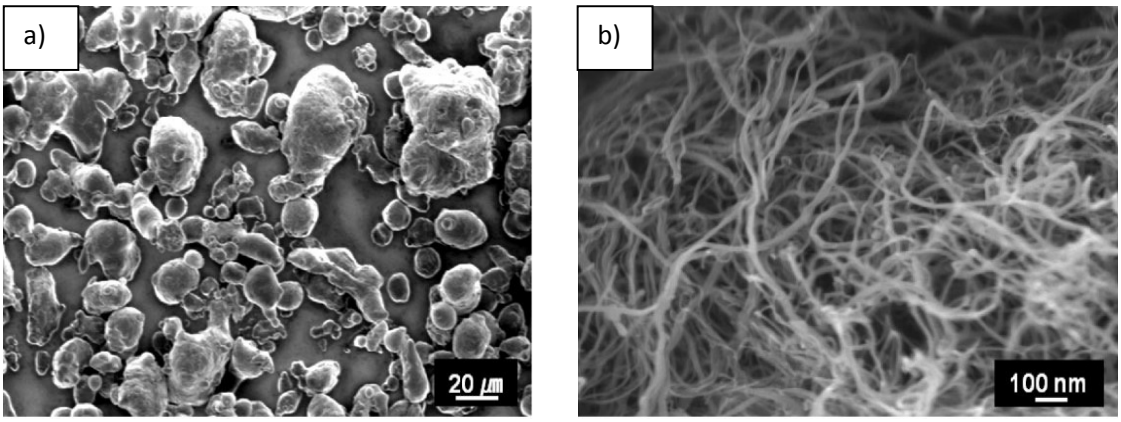

Figure 3.2.(a) SEM micrographs of as-received Al and (b) TEM micrograph of CNT

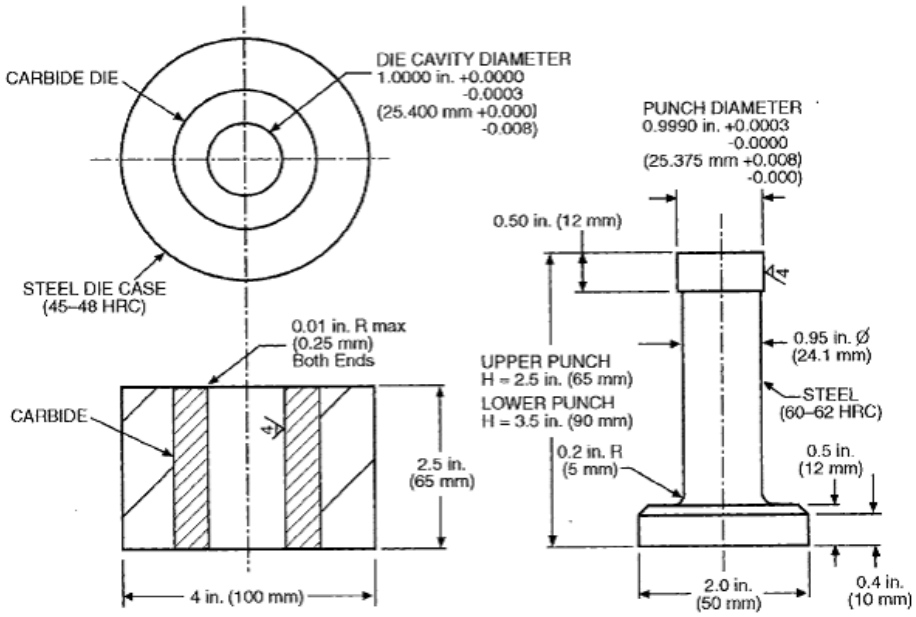

Figure 3.3. Detailed drawing of designed Die for preparation of specimen

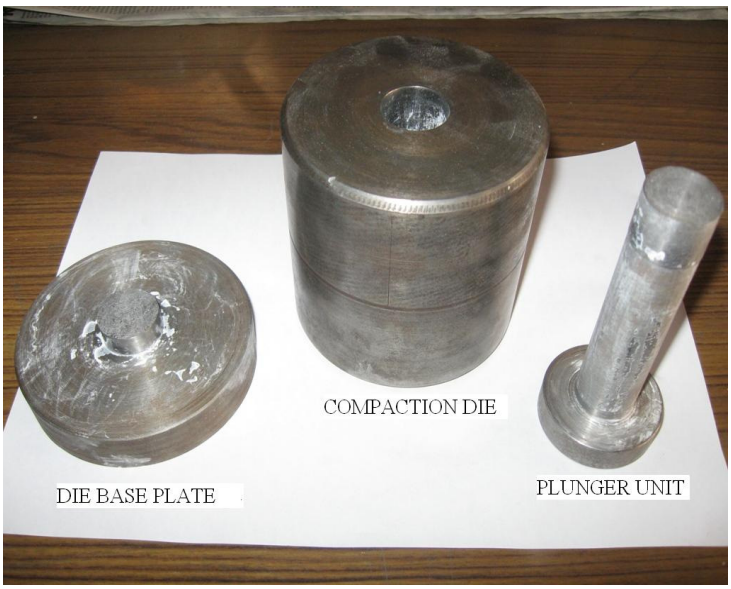

Figure 3.4. Compaction die set up

Table 3.3. Weight percentages of CNT

Weight percentage of reinforcement (wt. %)	Weight of reinforcement in g
0.25	0.0875
0.5	0.175
0.75	0.2625
1	0.35
1.5	0.525

3.2.3.2 Mixing of CNT and Al

The matrix Al and the reinforcement CNT are initially cleaned and mixed in a porcelain jar under controlled ambience. 35 g of Al powder (weight of powder as per the requirement of size of billet required) as matrix and a particular weight of CNT, say 0.175 g (0.5 wt.%), are put together and mixed using ball mill in a controlled atmosphere. Figure 3.5 shows Al and CNT before mixing.

Figure 3.5. Raw powder of Al and CNT before mixing

The manually mixed powders are then added to ethanol and further mixing is carried out by mechanical stirring assisted with ultrasonic shaker. Sonics VIBROCELL VC 750, having frequency of 20 KHz has been used to mix the powders for 30 minutes. Finally,

the mixed powders were dried at 120 ^{o}C in vacuum (less than 0.01 Pa) and broken up using High Energy ball milling for 15 hrs at 200 rpm, using Retsch PM-100 ball mill shown in Figure 3.6. A ratio of 1:10 in terms of weight of the mix and the weight of the balls is maintained in the steel jar of the Ball mill.

Figure 3.6. High-energy ball milling machine

3.2.3.3 TEM study

Transmission Electron Microscope (Make PHILIPS Model CM 200), having operating voltages of 20-200 kV with an image resolution of 0.23 nm, is used to identify the mixing condition and distribution of CNT in the metal matrix composite.

The Figure 3.7 represents the TEM images of Al-CNT reinforced composites for 0.5,1.0 and 1.5 wt.% of CNT. It is observed from the images of TEM that at 0.5wt.% of CNT, they appear to be fairly dense and uniform in terms of their distribution. When the wt.% increases to 1%, there is an indication of agglomeration or clustering. At 1.5 wt.%, the agglomeration is very predominant as shown by the TEM images. CNT needs to be denser and without much agglomeration in the matrix for better properties of the

composite. Similar results have also been reported by earlier researchers (Amal et al. 2008, Umashankar 2008).

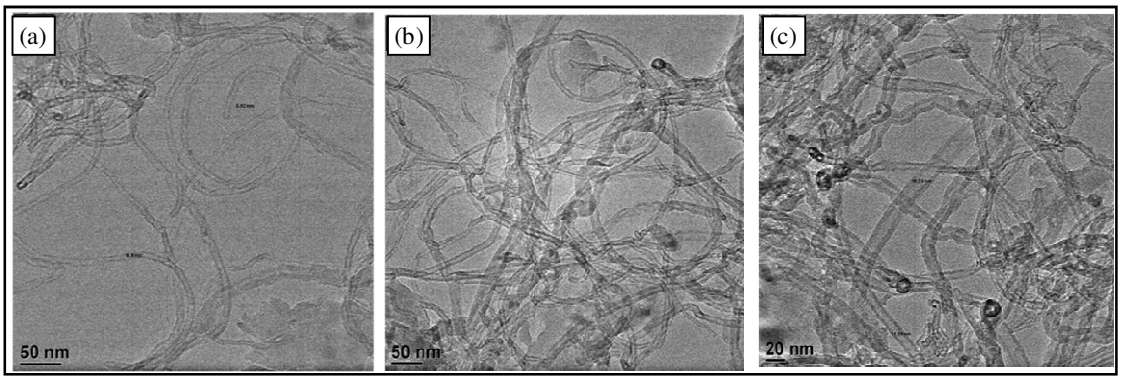

Figure 3.7. TEM images of (a) Al - 0.5wt.% CNT(b) Al - 1.0 wt.% CNT (c) Al - 1.5wt.% CNT

3.2.3.4 Compaction

Initially Al powder of 200 mesh size is mixed with different weight fraction of CNT as reinforcement and its density behavior is studied. Zinc stearate coating is applied to die and punch to minimize friction during the compaction process. Universal Testing Machine (UTM) of 40 ton capacities is used to apply load at the rate of 10 kN/min. The UTM used for compaction operation is shown in Figure 3.8.

For each compaction, 8.2 g (as per the requirement of billet size) of powder was used and poured into the die cavity. Care was taken to make sure that the powder got dispersed properly within the die cavity. Circular specimens with the size of 25 mm diameter and 6 mm length (8.2 g of powder) were pressed at pressures in the range of 12 tones for the mixed powders in order to study the compaction properties and consequently to observe the best compaction pressure for sintering. Similarly, rectangular bars of dimension 75 X 5 X 6 mm used for mechanical testing. A single performing hydraulic press UTM (40 ton Carver) was employed for compaction. Sintering was carried out under vacuum condition at a temperature of 550 °C for 1hr. The specimen densities before and after sintering were calculated by measuring the dimensions and weight of the specimens respectively.

Figure 3.8. Specimen Compaction Setup

The specimen obtained after compaction is shown in Figure 3.9. Billet obtained is cleaned and its density is determined by Archimedes principle. Figure 3.10(a) shows prepared FGCL specimen and Figure 3.10(b) shows polished cross-section view of FGCL.

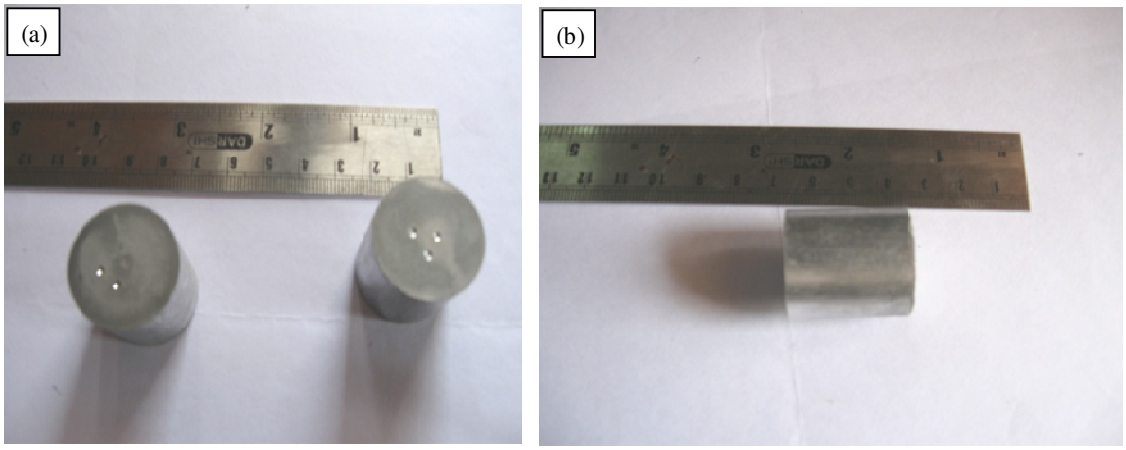

Figure 3.9. (a) - (b) Composite Specimen Obtained After Compacting (Diameter and Length)

Well mixed pure Al powders were compacted at different pressures in the range of 60 KN to 220 KN to study their compressibility. The optimum compaction load is obtained and standardized from the plot of density versus compaction load. The optimum compaction load is calculated only for the base materials and the same values used for the

composites also. This is due to the cost consideration of CNTs. Figure 3.11 shows densities for different compaction loads in case of Al.

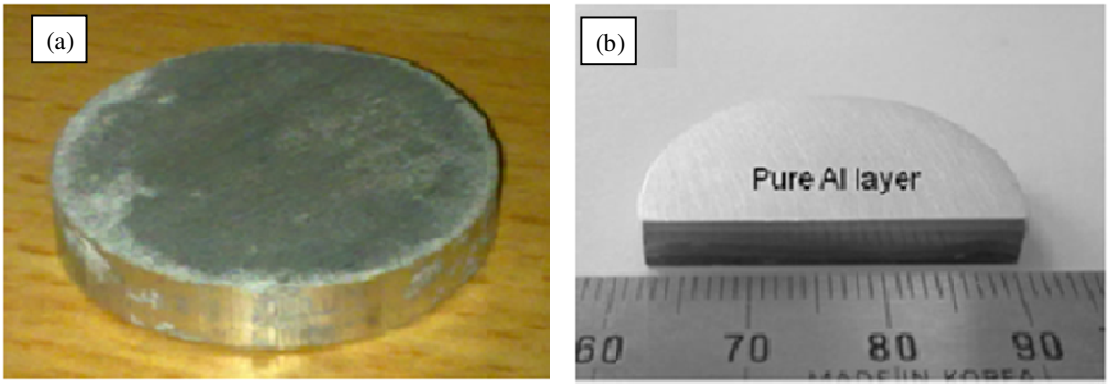

Figure 3.10. (a) FGCL specimen (b) Polished Layered FGCL specimen

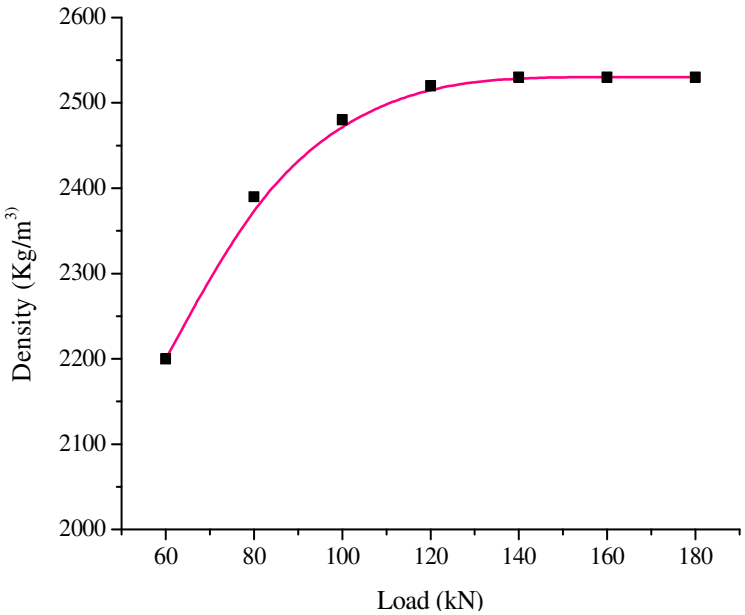

Figure 3.11. Compaction Density for Al

3.2.3.5 Sintering

After the compaction, the billets are sintered in a vacuum furnace in an inert atmosphere. The vacuum furnace shown in Figure 3.12 is used for sintering. The furnace has a

pressure capacity of 0.01 bar, maximum temperature of 750 ^{o}C with the temperature increment rate of 10 ^{o} C/min.

Figure 3.12. Vacuum Furnace used for Sintering

Based on literature study, (Umashankar 2011) the sintering temperature (0.8 to 0.85 times the melting temperature) and the time for Al materials are fixed as shown in the Table 3.4.

Table 3.4. Sintering Temperature and Time

Specimen	Sintering Temperature in ^{o}C	Sintering time in minutes
Al	550	60

The billets were successfully sintered without the occurrence of intrinsic melting. The billets containing a high weight percent (1.5 wt.%) of CNT showed a surface with fine microscopic cracks coupled with the ability to be easily chipped off at the edges. The lower density and use of compaction load of the base material appear to be the reason for such a phenomenon.

3.2.3.6 EDS Analysis

Energy Dispersive Spectroscopy (EDS) was performed on sintered specimen. JEOL 6380 LV Scanning Electron Microscope was used for this purpose. The microscope column is equipped with a tungsten-hairpin filament gun. The accelerating voltage for determining the energy and wavelength of electrons in the electron beam can be varied between 0.2 and 40 KV.

3.2.3.7 XRD Analysis

XRD studies are carried out on JEOL-JDX-8P diffractometer using copper Kα radiation with nickel filter. 30 kV tube voltage and 20 mA tube current are chosen. A scan speed of 0.5 degree per minute is employed over an angular 2θ range of 20-80^{o}. XRD analysis has been carried out on Al and CNT reinforced Al composites. XRD results are discussed in chapter 5.

CHAPTER 4

FUNCTIONALLY GRADED CNT REINFORCED Al COMPOSITE LAMINATES

4.1 Introduction

Functionally Graded Composite Laminates (FGCLs) are inhomogeneous materials, consisting of two (or more) different materials, engineered to have a continuously varying spatial composition. This chapter describes the FGCL basic concepts, classification, properties and preparation methods in detail. An overview of the current trends in research and application of FGCL is presented. Based upon the current trends, FGCLs have a huge potential in the future application in different areas of application like aerospace industry, defense, chemical industry, etc. CNT reinforced aluminium functionally graded composite laminates prepared in this regard and detailed characterization has been done.

The FGCL is the one which can solve practical problems arising from production and application of a new type of composite material. FGCL based materials are used in new generation spacecraft because of their 'high performance' and 'multi-functional' role (Suresh. S et.al. 1997). It is one the fastest emerging areas in materials science field (Pindera et.al. 1997). These materials also have great potential in space shuttles and similar vehicles. For example: When the space shuttle enters the atmosphere, the flight speed is more than 25 Mach and its surface temperature is as high as 2000 ^{o}C. Its exhaust gases from the combustion chamber also has a temperature of about 2000^{o}C with heat flux greater than 5MW/m^2 and its air near the front entrance has a thermal capacity 5MW/m^2 (Noda et.al. 1999). Conventional materials are incapable in handling such high temperature. FGCL based materials are capable of this and have great potential in this area (Birman.V 1995). Thus formation of gradients of chemical composition, phase distribution or microstructure represent a new fervently pursued concept in the design of advanced engineering components (Kaysser et al. 1995). In this regard, the main challenge is to combine irreconcilable properties in the same component, such as high hardness at high temperatures and structural toughness at low temperatures. A possible

concept to meet this demand is that of functionally graded materials (Cho et.al. 2001), where the use of a multi-phase composite material such as metal-based ceramic coating material, as each phase constitutes different thermal expansion coefficient and thermal stress variation in particular direction (Yin et al. 2005). It is easy to peel off coating occurring at the phase boundary or cracking the specimen between the substrate. To address such a conventional heat-resistant materials under extreme conditions and their inadequacies, the Japanese scholars, Hirai Toshio Watanabe Long trio (1987) first proposed the concept of functionally gradient materials, With the continuous deepening of the study, the concept of functionally gradient composite materials have been developed with reference to computer-aided materials design based on the use of advanced composite technology to constitute the material elements (composition, structure) along the thickness direction of the one side to the other side, with a continuous change, so that the nature of the material gradient changes and as well as functional aspects (Liu et.al 2001).

4.1.1 FGCL Concept Design

Two types of FGM can be prepared as shown in Figure 4.1(a) and stepwise structure sho wn in Figure 4.1(b).

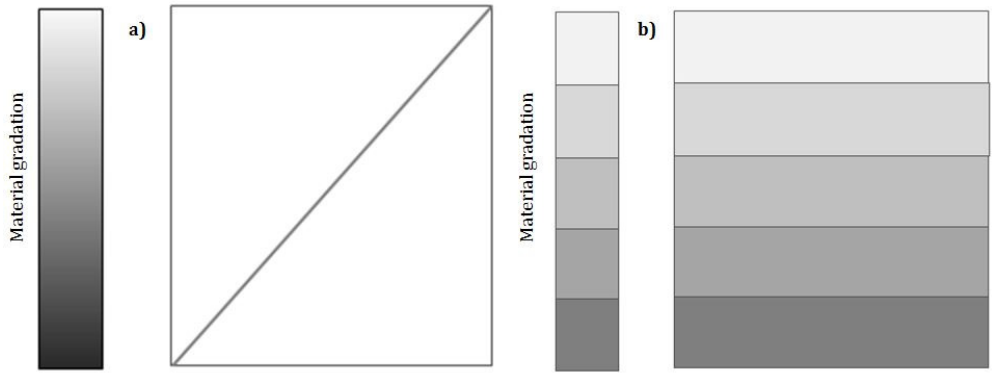

Figure 4.1. (a-b) Schematic representation of concept of gradation

In the case of continuous graded structure, the change in composition and microstructure occurs continuously with position. On the other hand, in the case of step wise, microstruc

ture feature changes in a stepwise manner, giving rise to a multilayered structure with int erface existing between discrete layers(FGCL). Figure 4.1(a,b) shows the schematic view of both structures relative to FGM (B. Kieback.et.al. 2003).

4.1.2 Methodology

To prepare the sample, 3 g of Al powder is placed inside the die. In order to maintain the gradient properties, 3 g of Al is mixed with 0.1% to 0.5% weight fraction of CNT separately. The powders mixed with different wt.% percentages of CNT are placed on top of the pure Al powder varying from 0.1% to 0.5% to maintain the gradient in property. All these layers of the powder are compacted by loading it to 620 kN using UTM for 60 s.

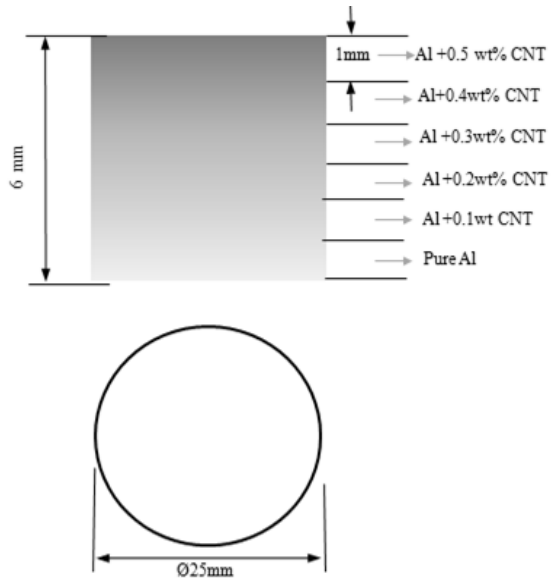

Figure 4.2. Schematic diagram of FGM

Zinc stearate coating is applied to die and punch to minimize the friction during compaction. Universal Testing Machine (UTM) of 40 ton capacity is used to apply load at the rate of 10 kN/min. The removed component of the die is sintered at 550^{o} C in vacuum furnace for 1hour.

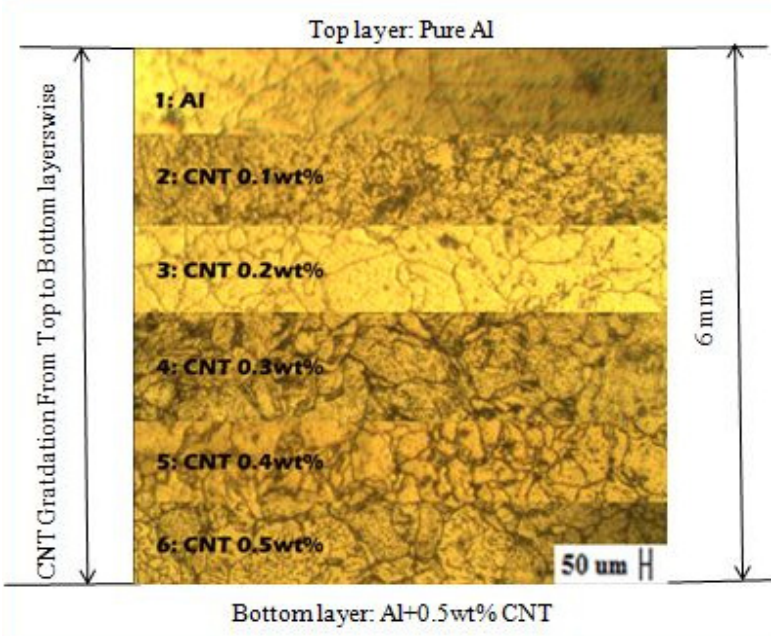

Figure 4.3. Microstructure of FGCL of Al with CNT reinforcement with different layers

Schematic diagram of FGCL sample is shown in Figure 4.2 showing variation of CNT reinforcement from pure Al to 0.5wt.% CNT from one end to another end of the specimen. The variation of microstructure is as shown in Figure 4.3. Grain size variation are observed clearly as the CNT reinforcement increases which in turn change the hardness of the specimen from one end to another end.

4.1.3 Analysis

First layer of pure Al shows an average hardness of 31HV and second layer of Al and 0.1wt. % CNT shows average of 38HV. It clearly reveals the effect of CNT reinforcement. Consequent third layer of 0.2 wt. % of CNT reinforcement shows average of 45 HV hardness value. Fourth layer shows 53 HV with 0.3 wt. % CNT reinforcement. Fifth and sixth layer hardness also increased linearly with 0.4 and 0.5 wt. % of CNT to 63 HV and 71 HV respectively. This confirms that the average hardness of each layer is improved with small reinforcement of CNT. The interfacial bond strength would be maintained by proper compacting load of 22 ton. This shows the sudden variation of hardness due to non lianear variation of CNT reinforcement. Controlled reinforcement of

CNT and high compacting load is necessary to achieve good material strength in case of functionally graded composite laminates.

4.1.4 Interface Layer

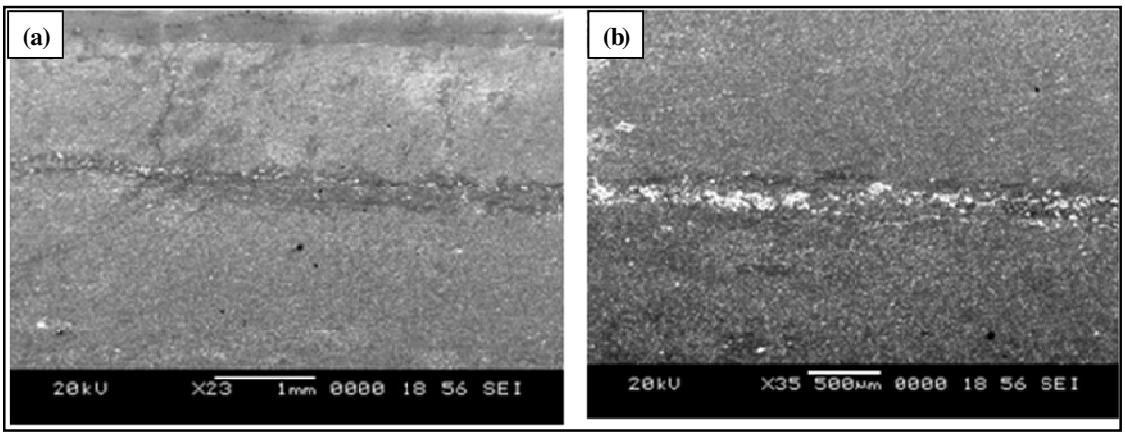

Figure 4.4(a). Interface of first and second layer (b) Interface of second and third layer

If the applied load is very less, the strength of interface of FGCL specimen would be very weak as shown in Figure 4.4(a) and (b). To maintain a good strength, a load of at least 22 tones is required. It depends on the matrix material compaction capacity.

4.1.5 Microstructure Analysis

From the Optical microscopic microstructure of the CNT/Al composites shown in Figure 4.5(f) and (h), the entangled CNTs (the black blocks shown by the arrows) became less with 6 hrs of ball-milling time. The aluminium powders got thinner as ball milling time was increased (Figure 4.5b.) and the high surface area and flat morphology of powders could provide more sites for CNT dispersion and thus were beneficial to the uniform distribution of CNTs (Shimizu et al. 2008). A network structure of CNTs around the Al powders was formed after 6hrs ball-milling (Figure 4.5e).

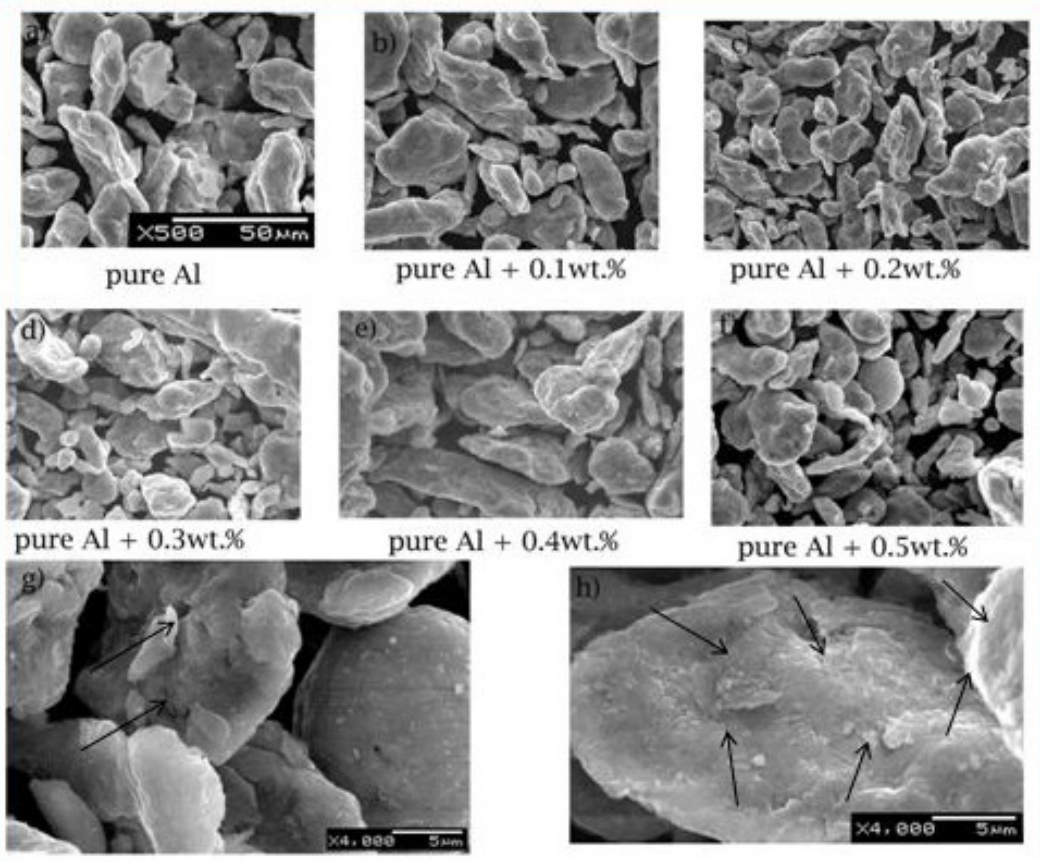

Figure 4.5. SEM micrographs of Al-CNT composite powders with different amounts of CNT

The change in the dispersion style of CNTs is attributed to the deformation of the mixture powders. The mixture powders were flattened gradually by shearing force during ball-milling (Figure 4.5h.), resulting in greatly increased specific surface areas of aluminium powders. In the preliminary stage of ball-milling some CNTs were distributed at the original powder boundaries. As the ball-milling time increased, the CNTs were gradually separated and dispersed into the Al powders (Figure 4.5f.), and finally a uniform dispersion of the CNTs was achieved when ball-milled for an appropriate time (15hrs). If the ball milling time is further increased, high energy ball-milling could change the structures of CNTs (Z.Y. Liu et al. 2012) and induce more impurities like Al_2O_3 and Fe. Thinner the flaky aluminum particle was, larger the surfaces areas, which would then lead to more Al_2O_3. Too much Al_2O_3 would reduce the bonding of Al powders and

decrease the ductility of the Al matrix, which would adversely affect the mechanical properties of the composites.

The mechanical properties of the CNT/Al composites are mainly affected by four factors: matrix strength, interface reaction, dispersion of CNTs and damage of CNTs. Increasing the ball-milling time results in more uniform dispersion of the CNTs and tighter bonding between the CNTs and Al resulting in higher Young's modulus of CNT/Al composites. This is because the strengthening of the composites by CNTs was improved first with the good dispersion of the CNTs; however, the improvement of dispersion uniformity was not obvious after 15 h ball-milling. Further increasing the ball-milling led to more serious damage to the CNTs, even the interface reaction between the damaged CNTs and Al matrix, resulting in reduced mechanical properties of the CNT/Al composites.

4.1.6 SEM image Analysis

The etched metallographic specimen of layered graded composite were observed under Scanning Electron Microscope (JEOL 6830) with magnification of 100X and 2000X.The topology of the polished surfaces are shown in below Figure 4.6.

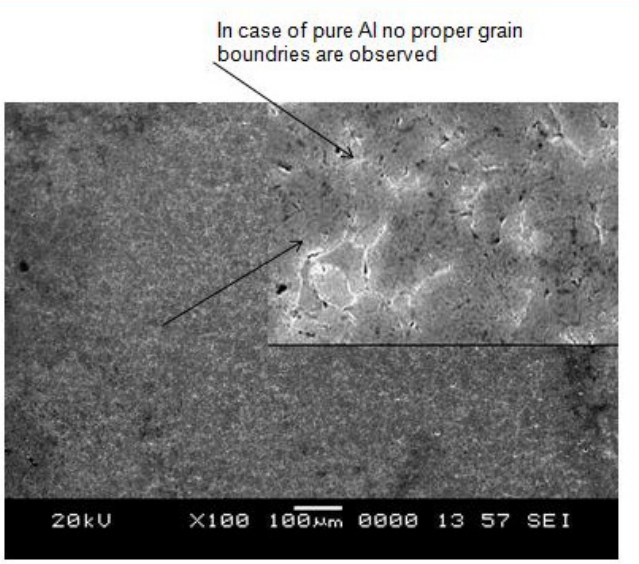

Figure 4.6. SEM microstructure image of Pure Al layer

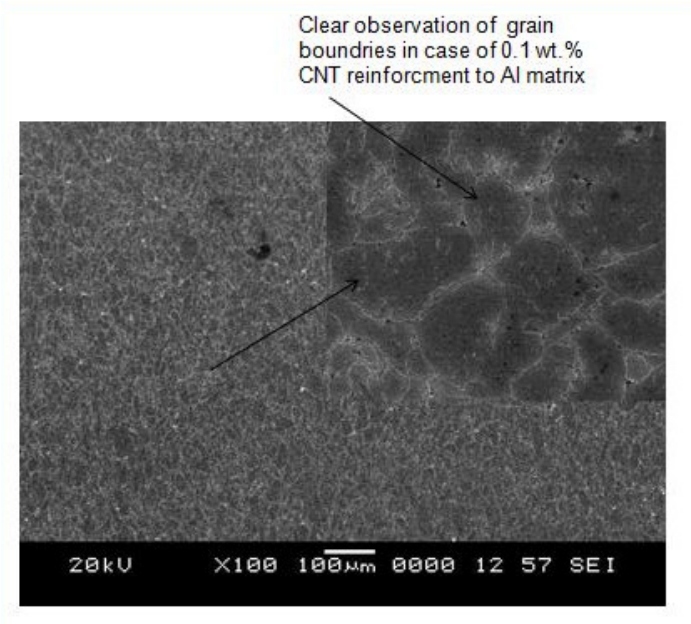

Figure 4.7. SEM micro structure of Al matrix composite with 0.1 wt.% CNT reinforcement

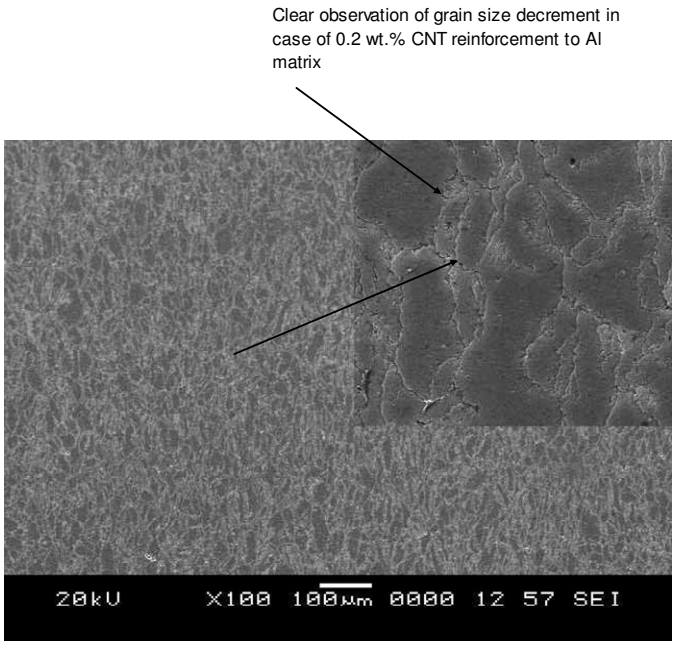

Figure 4.8. SEM microstructure of Al matrix composite with 0.2 wt.% CNT reinforcement

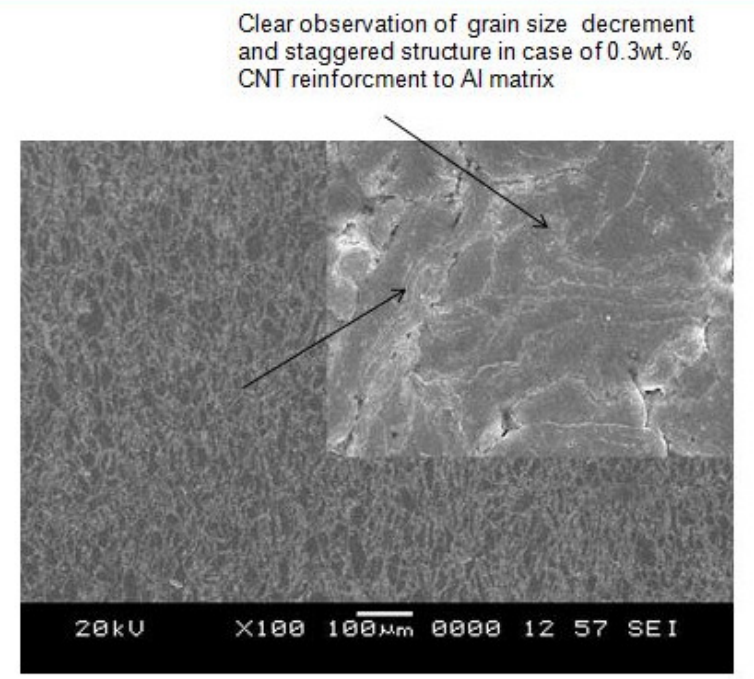

Figure 4.9. SEM microstructure of Al matrix composite with 0.3 wt.% CNT reinforcement

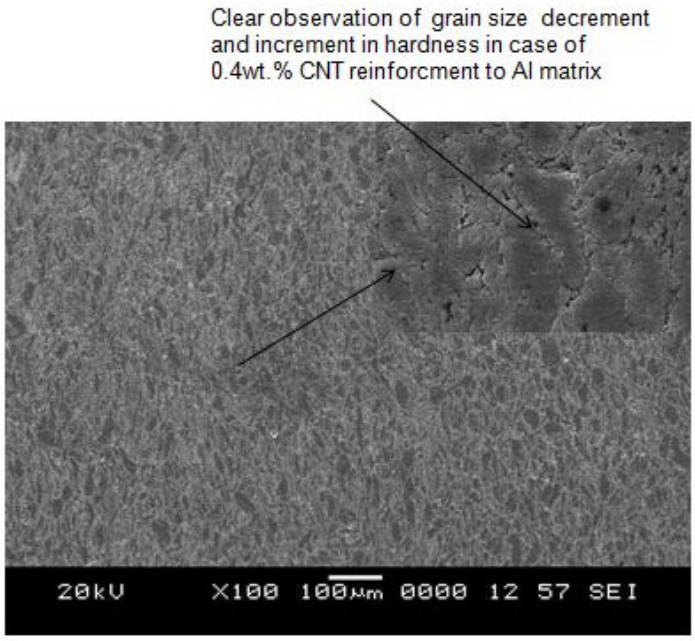

Figure 4.10. SEM microstructure of Al matrix composite with 0.4 wt.% CNT reinforcement

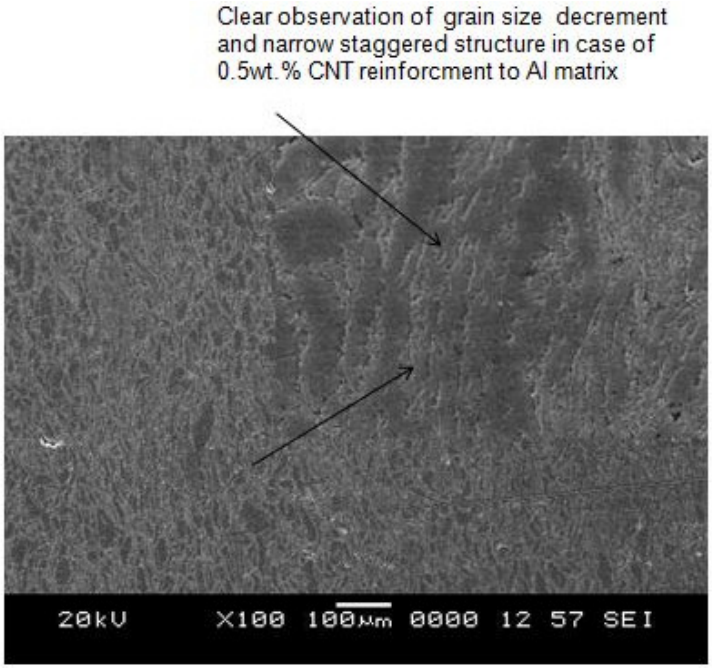

Figure 4.11. SEM microstructure of Al matrix composite with 0.5 wt.% CNT reinforcement

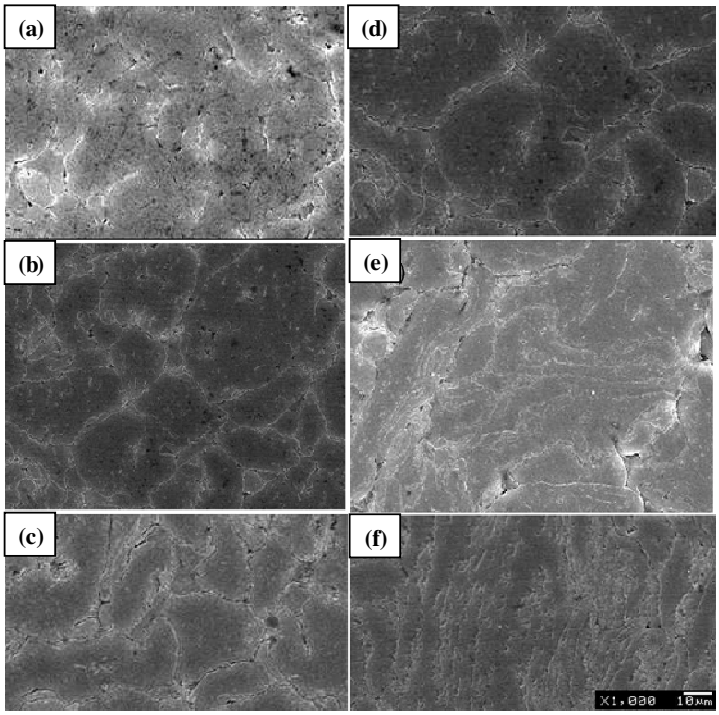

Figure 4.12. SEM micrograph of different 6 layers of FGCL

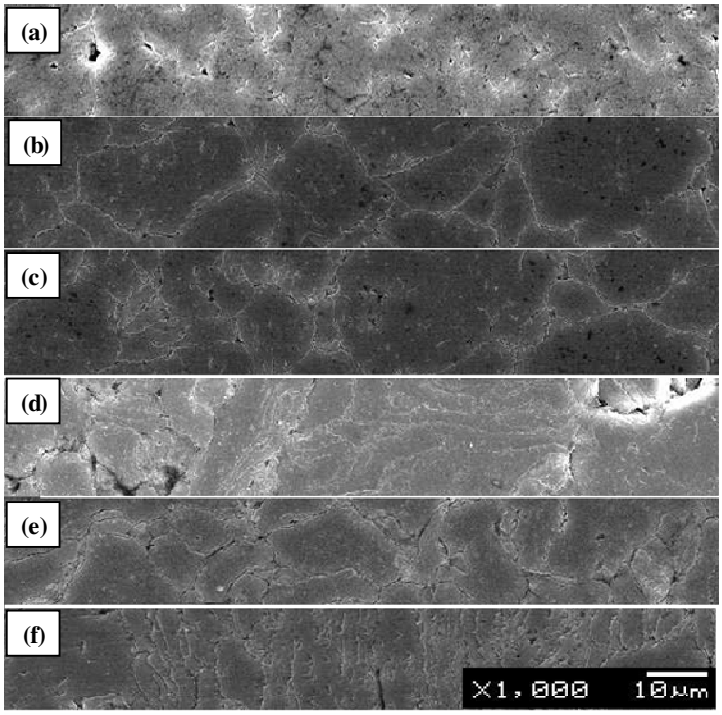

Figure 4.13. SEM images of cross sectional view of Layers of FGCL specimen

Figure 4.7 represents SEM microstructure of 0.1wt.% CNT reinforced Al matrix composite showing clear grain boundaries. Further Figure 4.8 to Figure 4.11 shows 0.2,0.3,0.4,0.5 wt.% CNT reinforced Al matrix composite, respectively. Variation of grain size and increase in hardness of the reinforced layers is observed with the increase in CNT reinforcement. Figure 4.12 shows the SEM image of 6 layers of FGCL and Figure 4.12 shows the cross section view of the FGCL.

4.1.7 EDS analysis

EDS analysis was carried out on cross-section of 6 mm thickness FGCL specimen. The cross section was mirror polished to the required level and then observed under SEM. Microstructure of all the six layers is shown in above Figure 4.13.

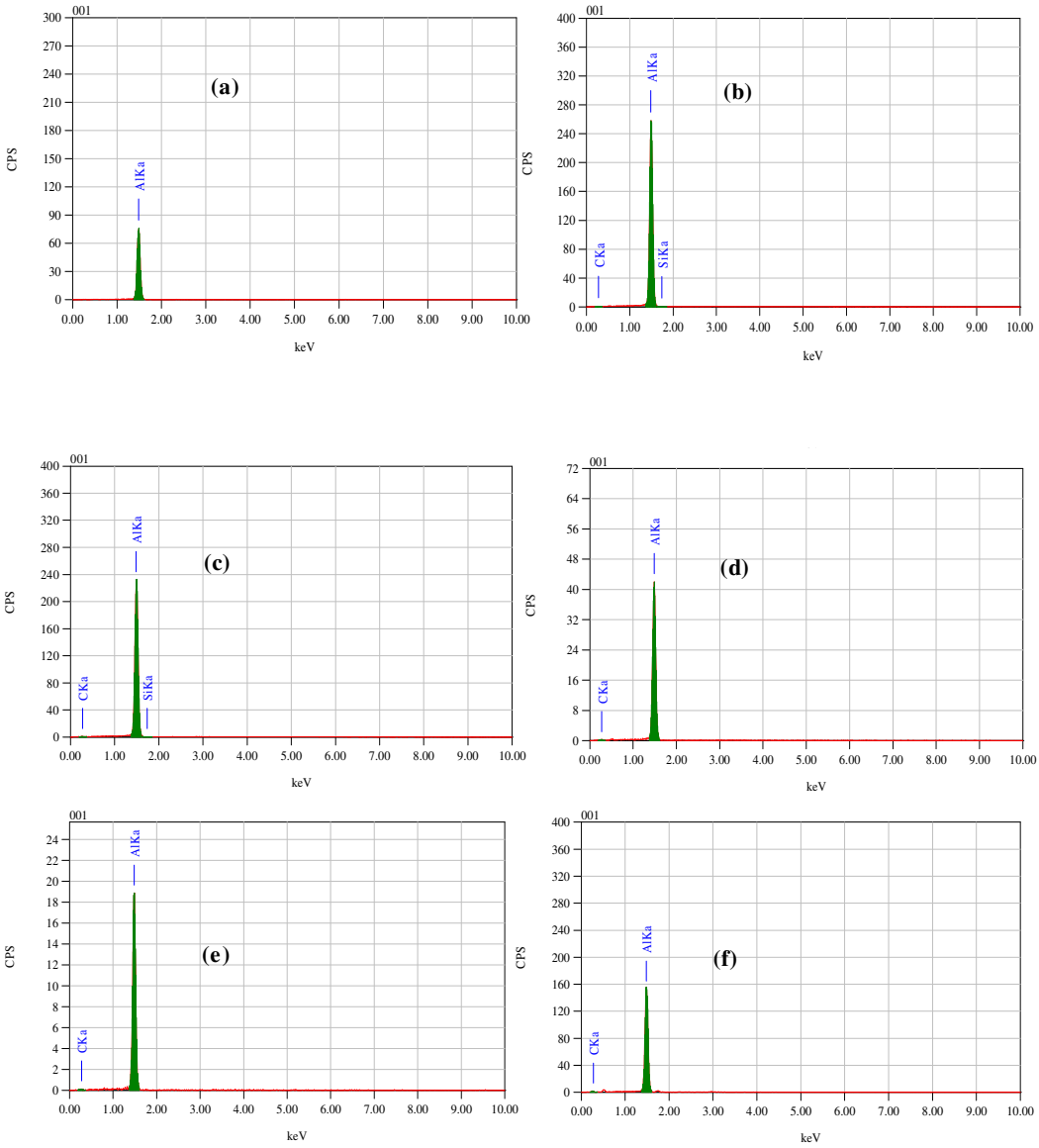

Figure 4.14. EDS analysis of the graded layers

EDS analysis shows the presence of CNT in the respective layers, which in turn is verified by the SEM microstructure variation, represented on figure 4.11. Figure 4.14 (a-e) shows the EDS analysis of the all six layers of the FGCL component.

4.1.8 Discussion

Aluminium-CNT based FGCL was developed using PM technique. The samples were tested to characterize the mechanical behaviour. The powder metallurgy technique is

more economical and simple compared to other methods. The dispersion of the CNT in the matrix plays an important role in determining the material properties. Optical microscopic image and SEM observations revealed CNT distribution was homogeneous (Figure 4.5).

The tensile strength of the CNT/Al composites is mainly affected by the following factors: ductility of matrix, dispersion of CNT and damage of CNTs. Good dispersion of CNT can increase the tensile strength of the composites. As the ball-milling time was increased, the damage of CNTs increased, but the dispersion was not improved. It also resulted in higher impurity content in the composite (Z.Y. Liu et al.212).Because of the afore-mentioned reasons, the ductility of the composites were decreased. It was found that the mechanical properties of the composites are closely related to the interfacial bonding (Nikhil et al 2003). Highly-magnified SEM (2000X) images of the prepared specimen showed that for the composites with 0.4 and 0.5 wt.%, CNT reinforcement, lots of agglomeration of CNTs was observed on the surface (Figure. 4.10), whereas for the reinforcement of 0.5 wt%, no agglomerations of CNTs were found (Figure 4.11). This is due to the uniform distribution of CNT in the matrix material which is evident from the SEM images (Figure 5.10).

The density of nano-composite decreased with increasing weight fraction of CNT. The Al/CNT nano-composite with higher weight fractions of CNT exhibited higher porosities due to the tube-like structure of CNT. The hardness of the composite increased with increasing weight fraction of CNTs from 0 to 0.5% and decreased with addition of more CNT. The introduction of CNT in the Al matrix results in a decrease of the density of composite, whereas the hardness of composite increased by about 84% for 0.5 wt. % CNT. This is due to the staggered structure of grain boundaries and CNT clustering as observed in optical microscope image (Figure 5.10). The variation of grain boundary size and structure is evident from the optical microstructure image (Figure 5.12).

4.1.9 Conclusion

High energy ball-milling was beneficial for the dispersion of CNTs in the Al matrix and the strengthening of the Al matrix. By keeping 10:1 ratio for 15 hr running time with 250

rpm speed is more suitable for uniform distribution of CNT. The developed FGCL specimen exhibited a good interfacial bonding between CNT and Al matrix. Some CNTs were distributed along the grain boundaries and some were located inside the grains. The strengthening of CNTs was improved as the reinforcement of CNT increased up to 0.5 wt. %, and then decreased with further increasing of reinforcement. The mechanical properties of CNT/Al composite are also improved with the reinforcement.

CHAPTER 5
RESULTS AND DISCUSSION

5.1 Overview

This section presents results and discussions of properties under study in two phases. First phase is devoted to characterization of composite materials whilst FGCL characterization and testing are dealt in second phase. For all the tests five replicates are subjected to different loading conditions and the average data values thus evaluated are used for analysis. Composites of different wt.% of CNT reinforced Al specimens are prepared and characterization done as per the ASTM standard. Subsequently, 0.1, 0.2, 0.3, 0.4, 0.5 wt.% CNT reinforced layered Functionally Graded Composite Laminate specimens are prepared for characterization and test results are discussed in the following section.

5.2 Characterization of composites

Pure Al powder (99.5% purity, about 13 μm in diameter) and CNTs (about 10–20 nm in diameter and 5 μm in length), supplied by Chengdu Chemicals, China, were used in the present study.

To obtain a homogeneous distribution of CNT and Al, powders were ball-milled with stainless steel balls using a Planet-Ball-Grinding machine at 250 rpm and the milling time was set to be 15 hr. Bulk hardness of the prepared sample has been studied using Mitutoyo-20 Vickers hardness testing machine. Vickers Hardness test was carried out as per ASTM standard E18-02. The hardness and density of the nanocomposites with different weight fractions of the CNTs are listed in Table 5.1. This variation of Hardness with CNT wt.% is shown in Figure 5.1. A considerable enhancement of the hardness is observed by the addition of the CNTs in the Al matrix. The hardness increases almost linearly with increase of the CNT weight fraction up to 0.5%. At 0.5 wt% of CNT, the hardness of the Al/CNTs nanocomposites was measured to be 68 H_V, which is about 161% higher than that of the pure Al samples. To explain the load carrying capacity of

the Al/CNTs nanocomposites, it was assumed that Al matrix has the ability to transfer and distribute external force to the reinforcement material.

Table 5.1. Density and hardness values

CNT wt. %	Theoretical density (gm/cm^3)	Measured density (gm/cm^3)	Relative density	Hardness(H_V)
0	2.7	2.537	93.9	26±2
0.1	2.695	2.479	91.9	31±1
0.2	2.691	2.454	91.1	37±1
0.3	2.685	2.448	91.1	45±2
0.4	2.681	2.445	91.1	52±3
0.5	2.675	2.421	90.5	68±2

The external load on the Al matrix itself is reduced. Here, the reinforcement material is CNTs, which has high strength, so that the Al/CNTs nanocomposites have mechanical durability greater than that of the raw Al matrix.

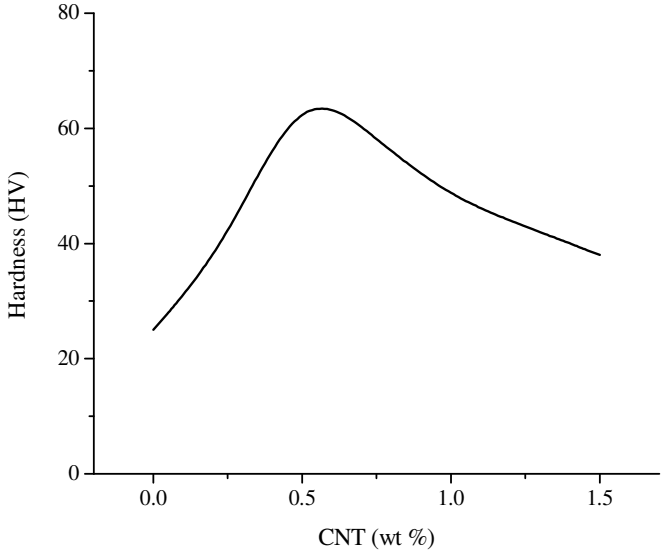

Figure 5.1. Variation of Hardness with CNT wt.%

The above result shows a drastic increase in the bulk hardness value for 0.5 wt.% of CNT reinforcement. This indicates that the CNT reinforcement has affected the agglomeration

of the powder and acted as a bonding agent to certain limit. This was confirmed through SEM micrograph shown in the Figure 4.11 in chapter 4.

The densities of the compact Al and Al-CNT composites were measured by the Archimedes principle with deionized water as the immersion medium and findings are listed in Table 5.1. The densities of the sintered samples decreased with increasing CNTs weight percentage. This expected result is as per the rule of mixtures given that the density of CNTs is less than that of Al. Similar trend is also reported in the literature (Umashankar 2011) for CNT reinforced MMCs. The presence of porous CNTs is the major contributor for densification. Homogeneous bridging of CNTs in the matrix was evident. The microstructure indicated some preferential alignment of CNTs into the matrix material.

The density of compacted samples before sintering and after sintering were measured by considering mass by volume relations. The variation in density for different wt.% of CNT reinforcement in Al is shown in Figure 5.2.

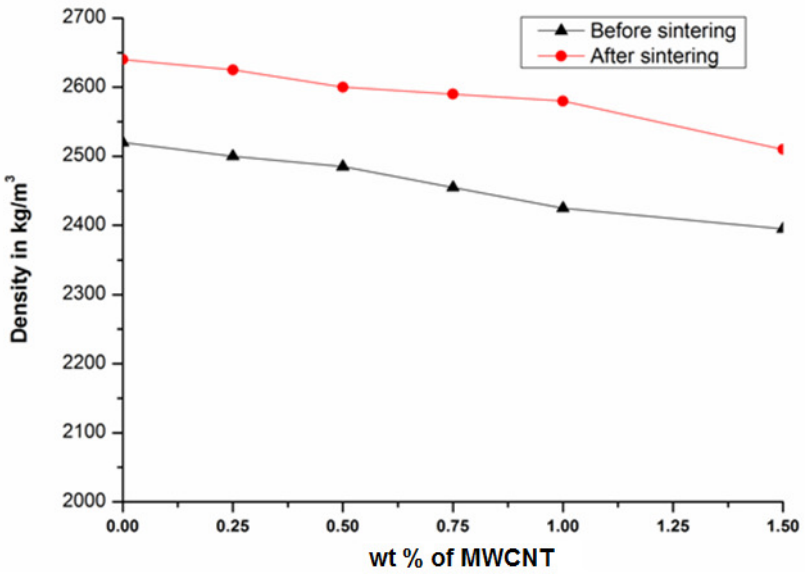

Figure 5.2. Density of samples before and after sintering

5.2.1 Hardness Test

The micromechanical properties of composites were obtained by hardness testing machine. The hardness test was carried out in a CSMTM hardness tester using a Berkovich indenter under load control. The measured average Vickers hardness values in HV (taken from four different sampling points) for pure Al and Al-CNT reinforced FGCL are listed in Table 5.2. The results showed that the hardness values of Al-CNTs composites increase with an increase in CNT weight percentage. Quantitatively, the increase in hardness is very significant: about 129% increase in hardness was observed for 0.5 wt.% CNT reinforcement.

Table 5.2. Microhardness values of FGCL samples

CNT wt %	Microhardness (H_V)
0	31±1
0.1	38±2
0.2	44±1
0.3	53±2
0.4	64±2
0.5	71±2

5.2.2 XRD Analysis

The XRD spectrum of pure Al samples and 0.1, 0.2, 0.3, 0.4, 0.5 wt.% CNT reinforced Al composites are shown in Figure 5.3. These do not exhibit any carbide peak. Similar results were obtained by Kuzumaki et al. 1998 by observing the interfacial structure between CNT and Al using TEM. This indicates that CNT has not reacted with the base material. CNTs have also been identified as suitable reinforcement in Al based composites due to their chemical stability (Kazumaki et al 2002).

5.2.3 Results of EDS Analysis

Figure 5.4 (a) and (b) shows the EDS image of base Al and their composite containing 0.5 wt.% of CNT reinforcements. EDS analysis graph peaks indicate the constituents as elemental compositions.

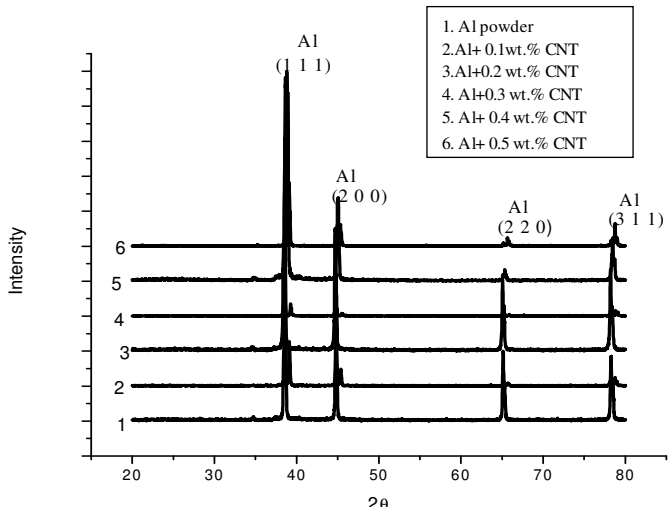

Figure 5.3. XRD patterns of Al and CNT reinforced Al composites

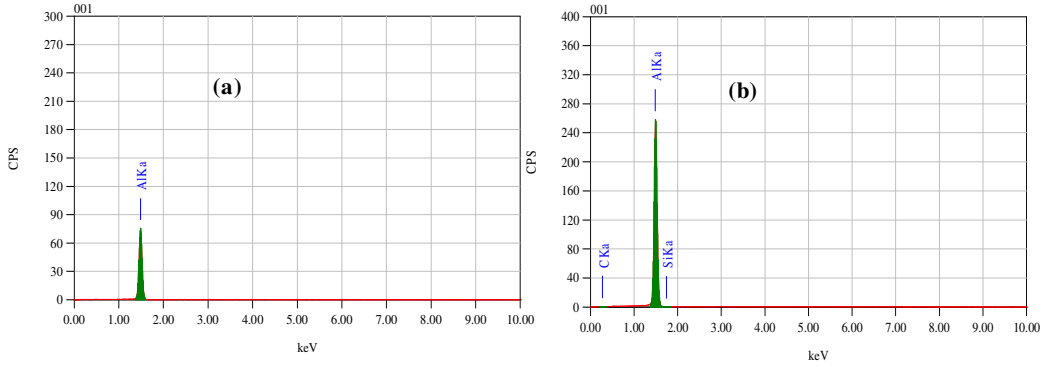

Figure 5.4. Composition of Material found by EDS test (a) Pure Al (b) 0.5wt.% CNT reinforced Al metal matrix composite

5.2.4 Discussion

Figure 4.5 presented in chapter 4 shows the homogeneous distribution of CNTs. It is also observed that CNTs rarely tangled together after sonification. Moreover, the CNTs were slightly damaged in length and outer walls, and no other forms of carbon and metal catalysts were identified during the FE-SEM, EDX.

Two processes are involved in a typical mechanical alloying process: One is cold working of the powders that would lead to a decrease in ductility and the eventual fracturing of the particles; and the other is cold welding of the particles that tends to increase the particle size. In general, once the powders are ball milled, cold welding

becomes the predominant process, resulting in the agglomeration of the particles with an increase in the ball-milling time (Z.Y. Liu et al. 2012). It can be observed that the particles were initially flattened to flake-like ones at an early stage of the mechanical alloying, whereas their size increased slightly (12 hr) in the case of the pure Al powders. However, such flake-like and cold-welded shapes were maintained by increasing the time of ball milling to15 hr.

5.2.5 Microstructure study using Optical Microscope

The etched metallographic specimen of both pure Al and CNT reinforced Al were observed under an optical microscope at magnifications of 10X, 40X and 100X. The Kellers etchant was used to etch the components.

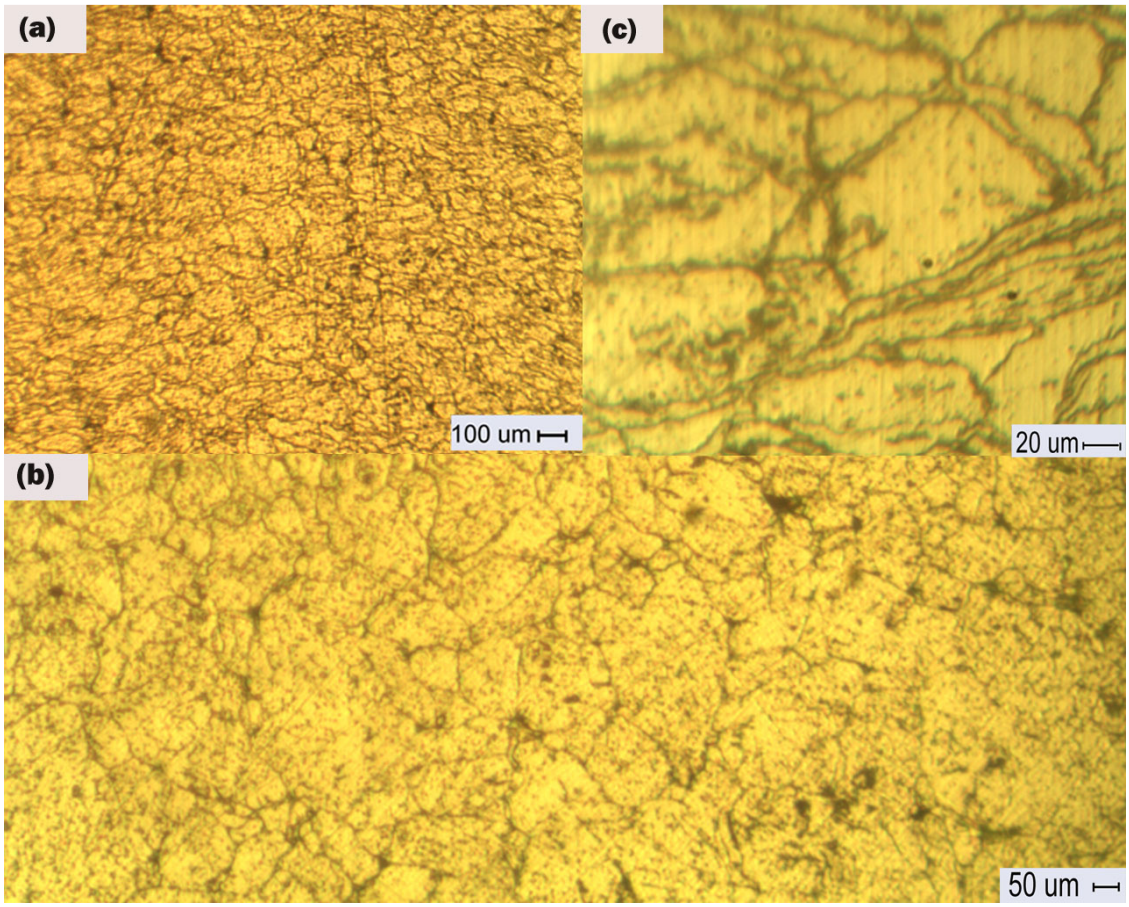

Figure 5.5. (a, b, c) Microstructure of pure Al

Figures 5.5(a,b,c) represent the optical images of pure Al at different magnifications. The microstructure was full plain and clear which indicates no traces of other materials. The optical images corresponding to 0.1, 0.2, 0.3, 0.4, 0.5 wt.% CNT reinforced Al matrix composites is shown in Figure 5.6(a,b,c) to Figure 5.10(a,b,c), respectively. These images clearly shows the variation in distribution of CNT with the increase in the reinforcements.

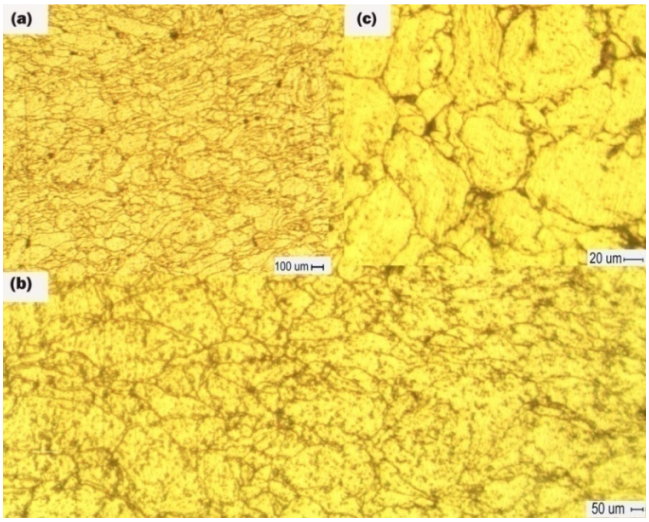

Figure 5.6. (a, b, c) Microstructure of Al matrix composite with 0.1 wt.% CNT reinforcement

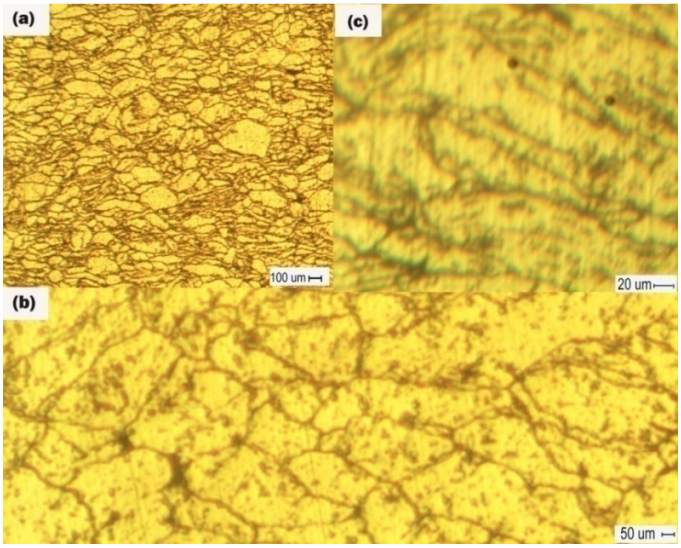

Figure 5.7. (a, b, c) Microstructure of Al matrix composite with 0.2 wt.% CNT reinforcement

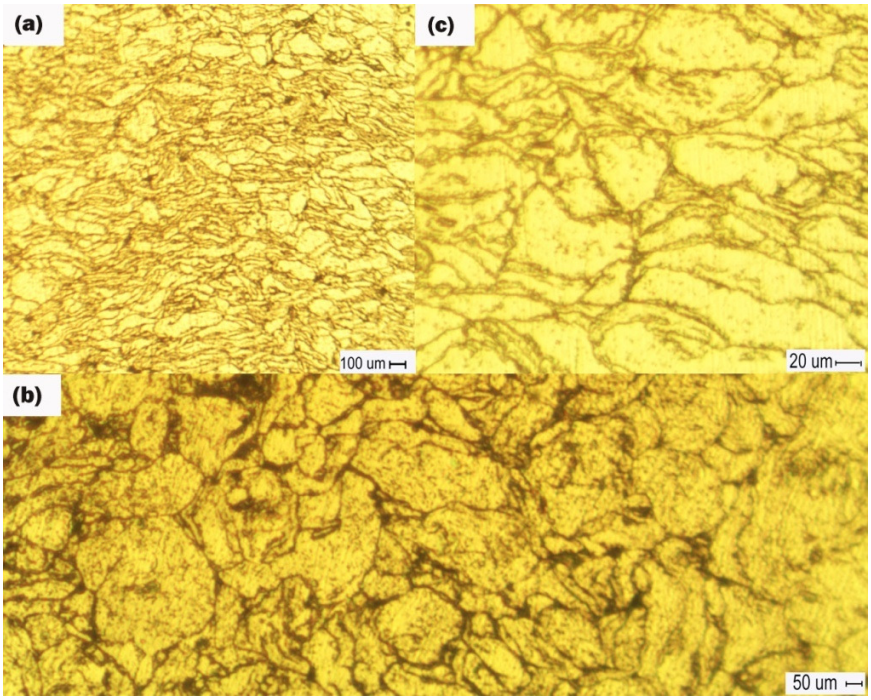

Figure 5.8. (a, b, c) Microstructure of Al matrix composite with 0.3 wt.% CNT reinforcement

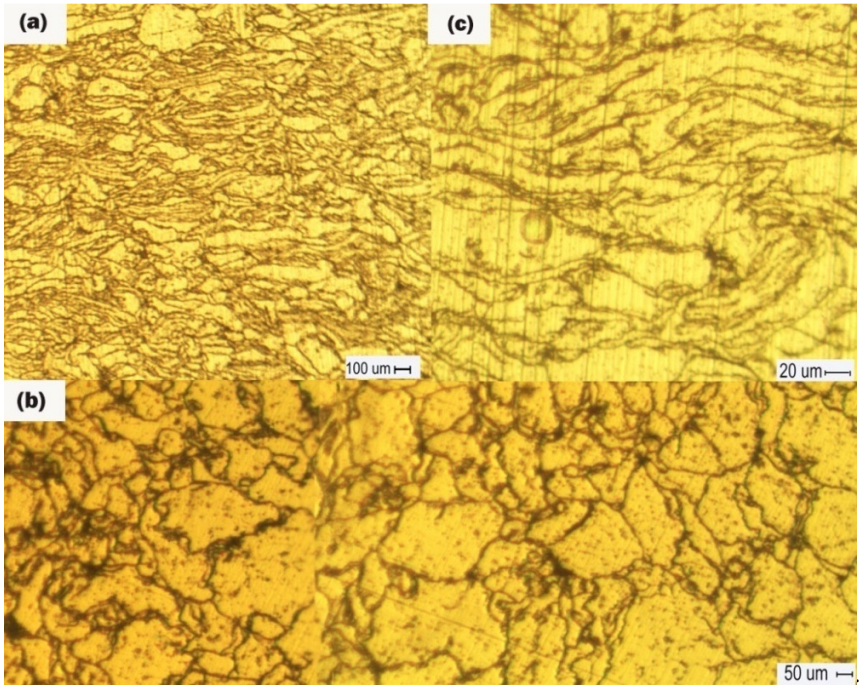

Figure 5.9. (a, b, c) Microstructure of Al matrix composite with 0.4 wt.% CNT reinforcement

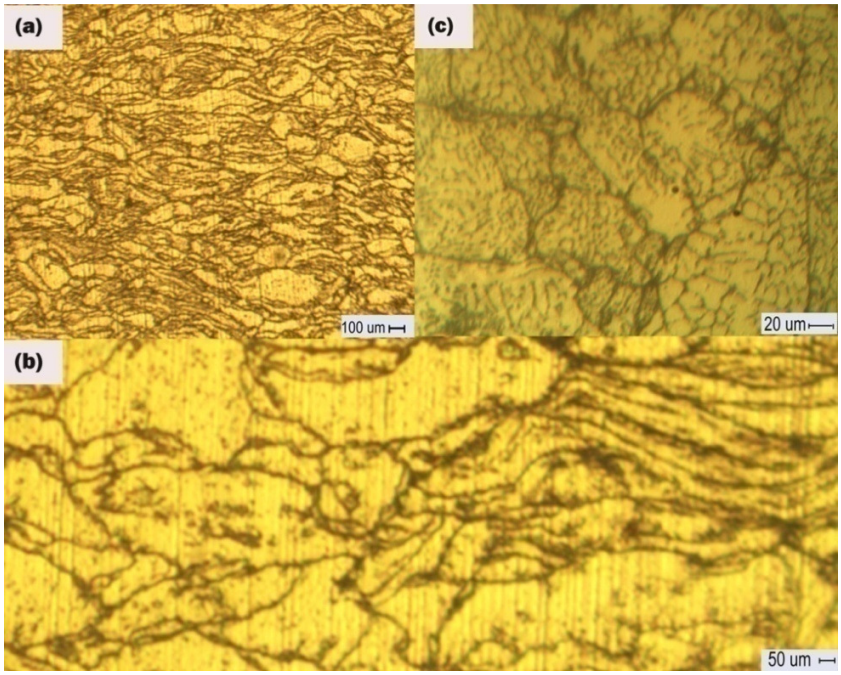

Figure 5.10. (a, b, c) Microstructure of Al matrix composite with 0.5 wt.% CNT reinforcement

Table 5.3. Grain size of Al and its composites

Sl.No	Layers contents	Grain size No(ASTM)	Actual Grain size(µm)
1	Pure Al	3	127
2	Al+0.1wt.%	3.5	106.8
3	Al+0.2wt.%	4	89.8
4	Al+0.3wt.%	4.5	75.5
5	Al+0.4wt.%	5	63.5
6	Al+0.5wt.%	5.5	53.4

The measured grain size of Al and its composites are presented in Table 5.3 (as per ASTM E112-N). It is observed that as the reinforcement is increased from 0.1 wt% to 0.5 wt% of CNT, Grain size continuously decreased from the value of 127 µm to 53.4 µm in FGCL. It is observed from that there is a continuous variation in grain size as the reinforcement is increased from 0.1 to 0.5 wt.% of CNT. Variation in grain size caused a change in hardness value from one end to the other end along the direction.

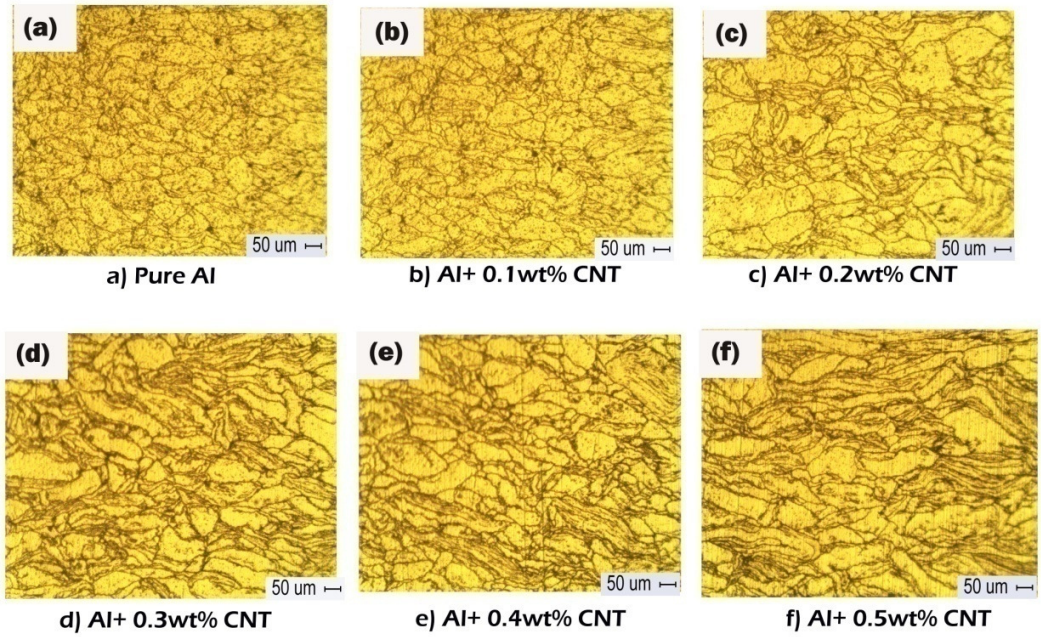

Figure 5.11. Microstructure of a) Pure Al specimen b) 0.1 wt.% CNT reinforced Al metal matrix composite c) 0.2 wt.% CNT reinforced Al metal matrix composite d) 0.3 wt.% CNT reinforced Al metal matrix composite e) 0.4 wt.% CNT reinforced Al metal matrix composite f) 0.5 wt.% CNT reinforced Al metal matrix composite.

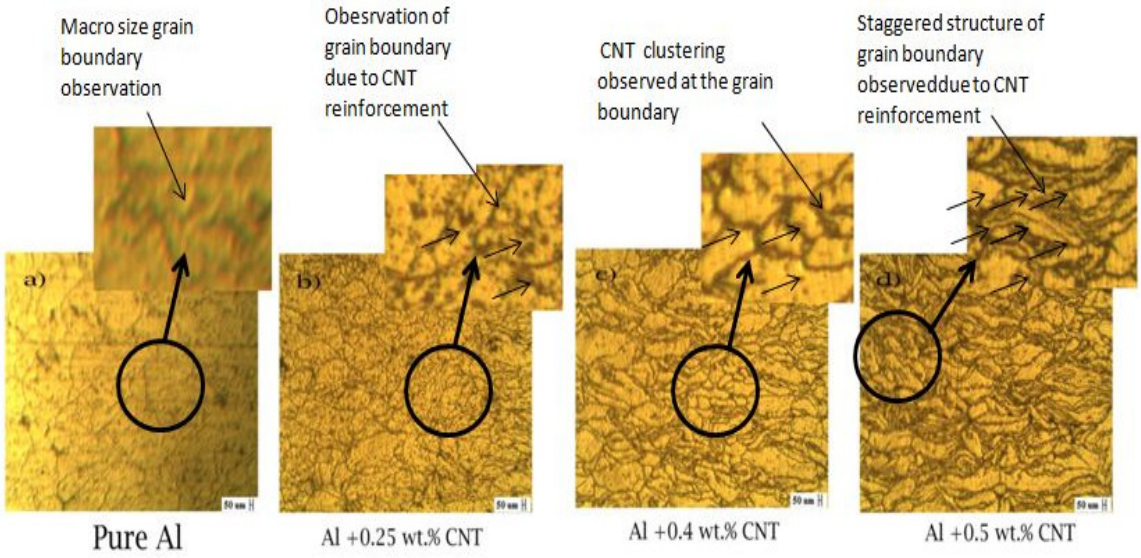

Figure 5.12. Variation of grain size after CNT reinforcement.

5.2.6 Microstructure of FGCL

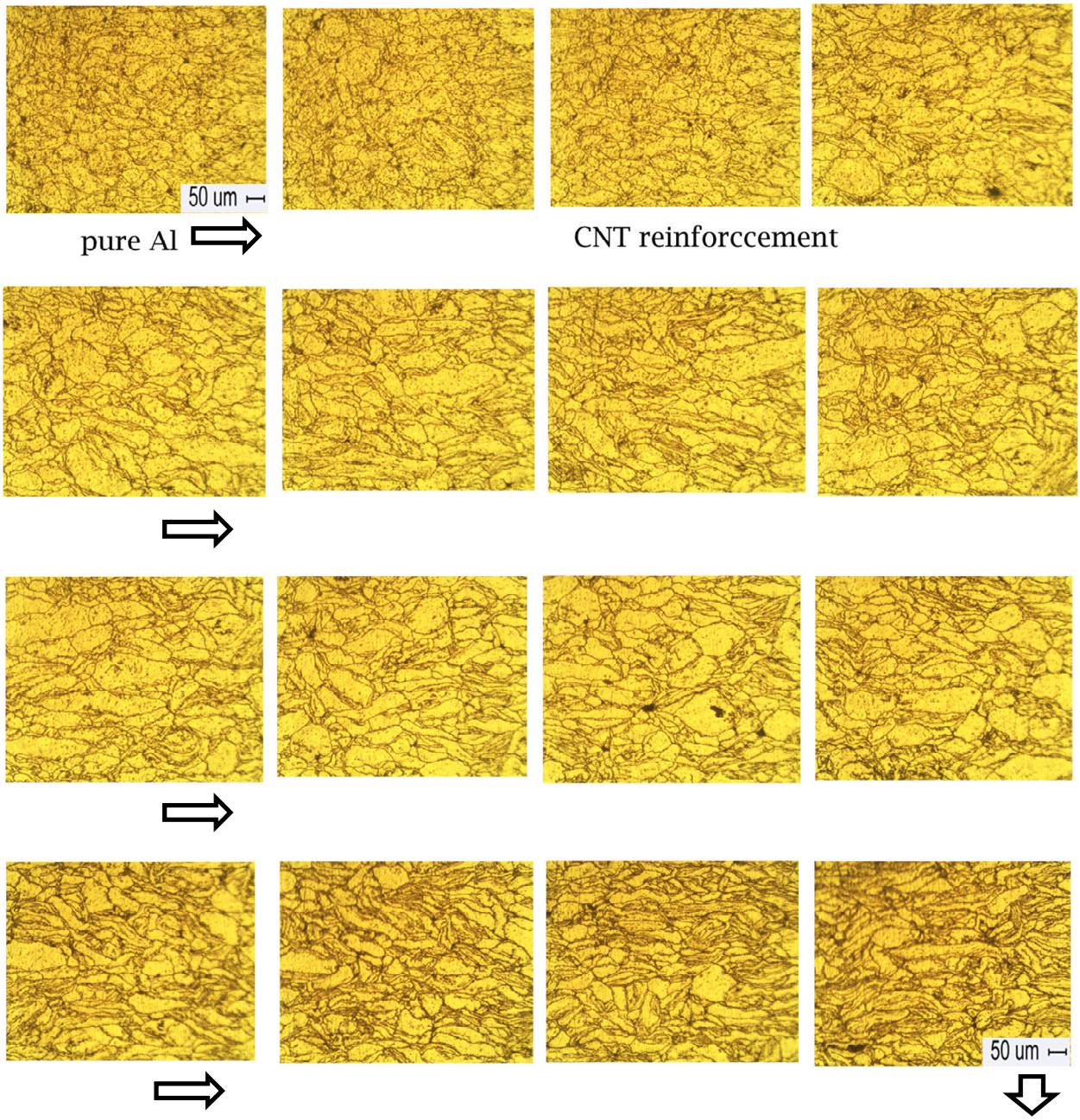

Figure 5.13. Continuous variation of Microstructure of CNT reinforced FGCL

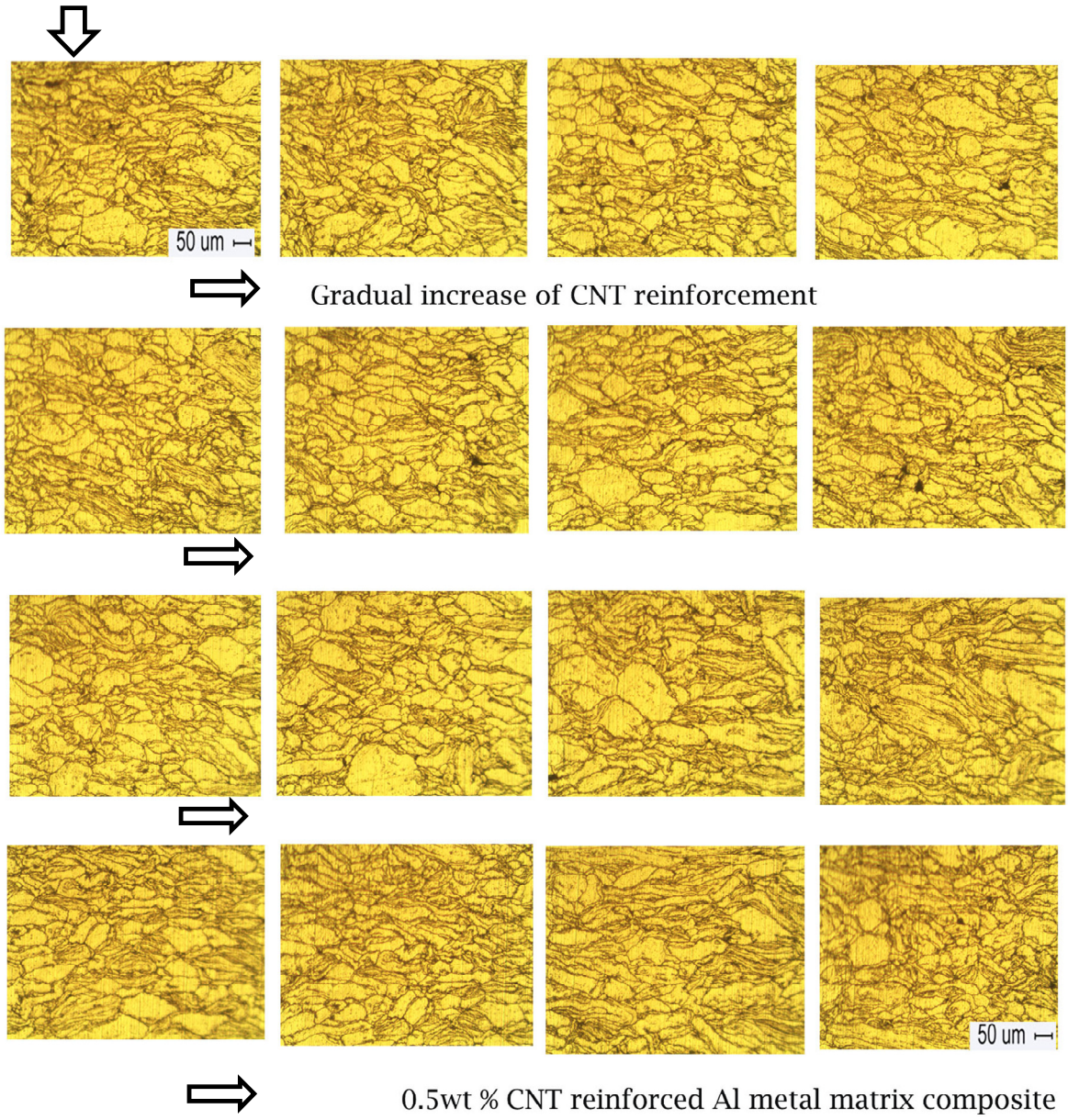

Figure 5.14. Continuous variation of microstructure of CNT reinforced Al FGCL

5.2.7 Conclusion

Aluminium matrix composites reinforced with 0.1, 0.2, 0.3, 0.4 and 0.5 wt.% of CNTs were successfully manufactured using cold compaction followed by sintering techniques. Careful control of sintering temperature has prevented the formation of intermetallic

compounds such as aluminum carbide. The microhardness tests have revealed the enhanced mechanical properties of Al-CNT composites, indicating that the proposed manufacturing method is viable. It is observed that the process adopted is suitable for preparation of layered style of CNT reinforced Al functionally graded composite laminates. Reinforcement of CNT varied from 0.1 wt.% to 0.5 wt.% from one end to other end. This affected micro-hardness on one side which read as 31 HV to micro-harness on the other end which read as 71HV. The microhardness exhibited an improvement of 129% along the direction in the linear manner. As the hardness increases, density of the composite decreases, relatively, which shows that the developed material exhibits property variations along the thickness. Improvement in the hardness is also due to the decrement in the grain size. Grain size continuously decreased from 127 µm to 53.4 µm. There is nearly 57.9 % grain size variation due to the CNT reinforcement to Al matrix. Variation in the microstructure was shown in Figure 5.12. Agglomeration of CNT on the grain boundaries cause the staggered structure for the Al matrix, which leads to reduction in the grain size and improvement in the hardness of the developed material (Figure 5.10). EDS and XRD analysis confirmed the presence of proportional amount of CNT in the Al matrix material.

5.3 Tensile Test performance on FGCL

The physical properties of the CNT reinforced Al Functionally graded composite laminates, like hardness, density and young's modulus varies from one direction to another. Variation of reinforcement is done by varying the percentage content of CNT form one end to the other end. One side has a pure Al while the other end has Al reinforced with 0.5 wt.% of CNT. It is necessary to experimentally evaluate the tensile strength of the prepared laminates in order to assess its tensile strength. The schematic diagram of the rectangular bar specimen for tensile test is shown in figure 5.15. The prepared specimen reshaped as per the ASTM E-8 standards for tensile test is as shown in the figure 5.16.

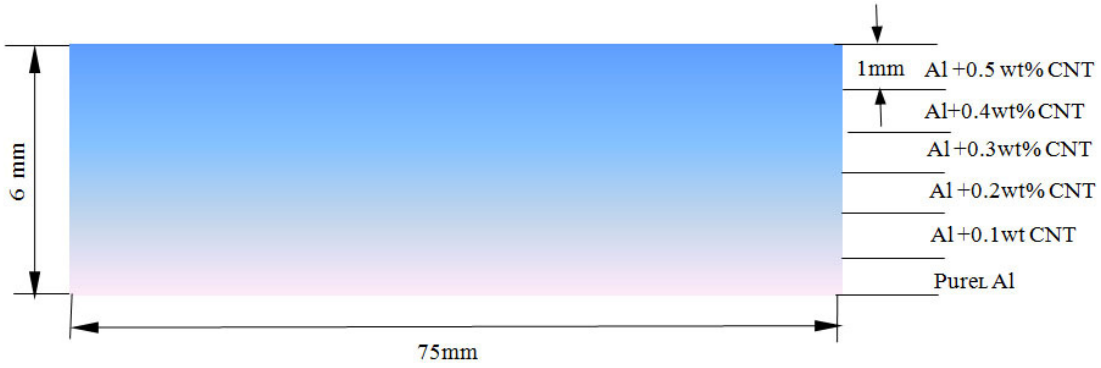

Figure 5.15. Schematic diagram of rectangular FGCL specimen

5.3.1 Tensile behavior of composite material

To evaluate the tensile properties of the Aluminium-CNT reinforced composites, three specimens in each type of composites were prepared as per ASTM-E8 standard. Test was conducted by using computer controlled servo-hydraulic operated INSTRON TESTER of 2 ton capacity at controlled strain rate of 0.001/sec. Figure 5.17 shows the test set up. Young's modulus was calculated by plotting the stress-strain curve. The young's modulus versus wt.% of CNT in the composites is plotted in Figure 5.18.

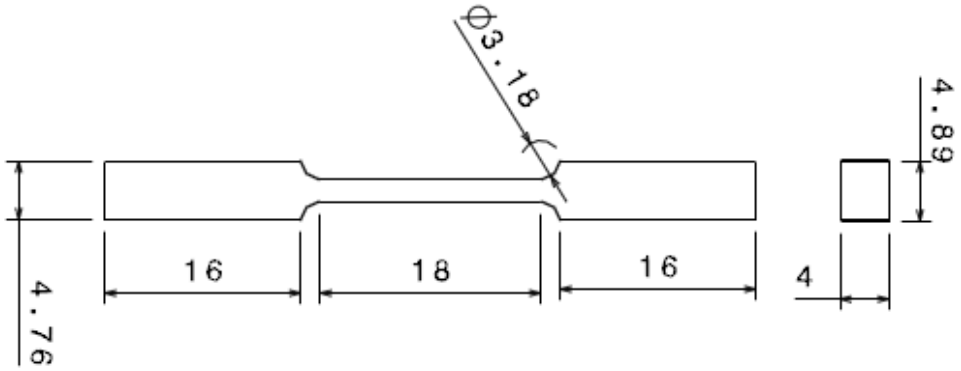

Figure 5.16. Schematic diagram of Tensile test specimen

5.3.2 Experimental set up for tensile test

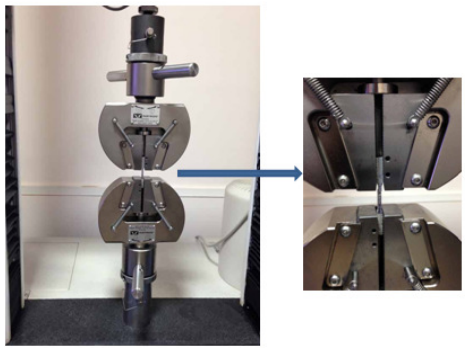

Figure 5.17. Experimental setup for Tensile test

Table 5.4 Young's modulus for different wt.% of CNT in Al

Sl.No	Wt.% of CNT	Young's modulus (GPa)
1	0	58.2±0.1
2	0.25	60.4±0.2
3	0.5	62.9±0.1
4	0.75	57.2±0.2
5	1	55.8±0.1
6	1.25	52.2±0.1
7	1.5	49±0.3

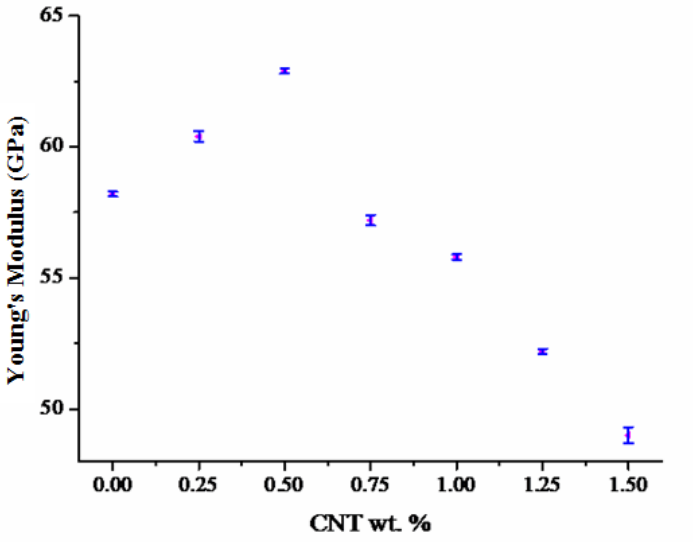

Figure 5.18. Variation in Young's modulus for different wt.% of CNT in Al

The Young's modulus values of all the tested samples are listed in Table 5.4 which shows that the modulus values increased up to a 0.5 wt.% of CNT and it showed a decreasing trend for a weight percentage greater than 0.5%. It is observed that the Young's modulus value increased till CNT reinforcement of 0.5 wt.% and the maximum value was 63.2GPa (Umashankar 2011).

In case of FGCL composite, specimen is made with six different layers. It is difficult to cut the shape as shown in figure 5.16 (Standard specimen for tensile test). Test specimen employed for measuring the Young's modulus schematically represented in figure 5.19 and subjected to bending test (Benjamin D. Chapman 2006).

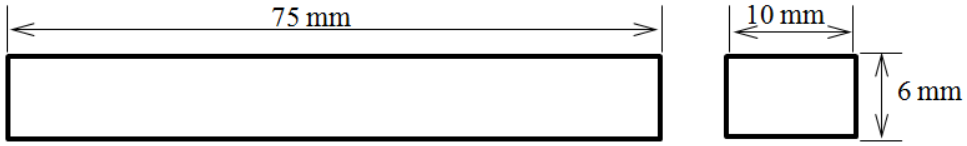

Figure 5.19. Schematic diagram of bending test specimen

Schematic diagram of experiment setup is presented in figure 5.20. The setup was built for experiment as per the standard was shown in figure 5.21.

5.3.3 Experimental set up for Bending test for FGCL

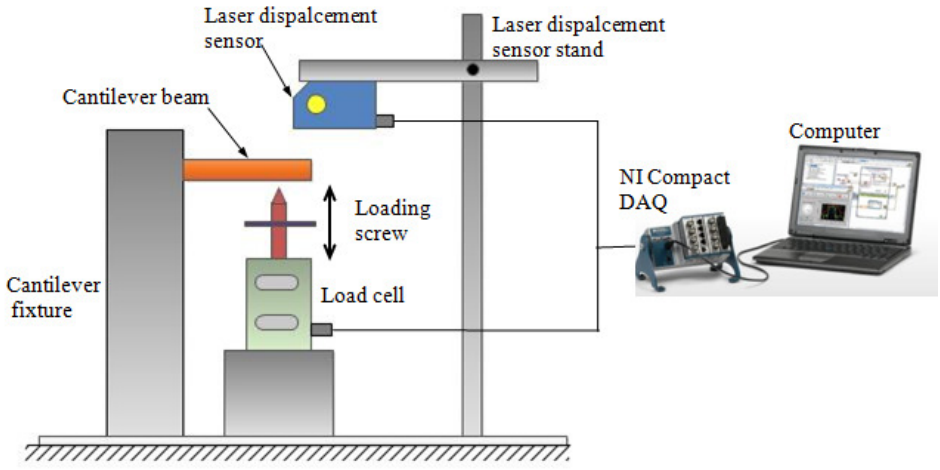

Figure 5.20. Schematic diagram of bending test setup

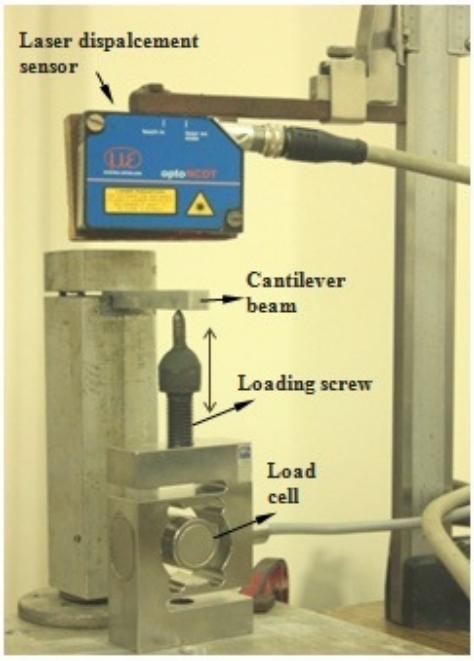

Figure 5.21. FGCL bending test experimental set up

The schematic representation and actual image test set up to evaluate the Young's modulus of FGCL is shown in the Figure 5.20 and Figure 5.21 respectively. This set up is developed on the basis of measurement of Young's modulus from the deflection of cantilever beam for the known load as shown in the Figure 5.22. The Young's modulus of the beam is measured from the following equation (Engineers Edge 2006).

$$E = \frac{Wl^2\left(2l+3b\right)}{6yI} \tag{1}$$

where, W is the force applied (in N), y is the deflection of the cantilever beam, l is the distance of the loading point from the fixed end and b is the distance of loading point from the free end.

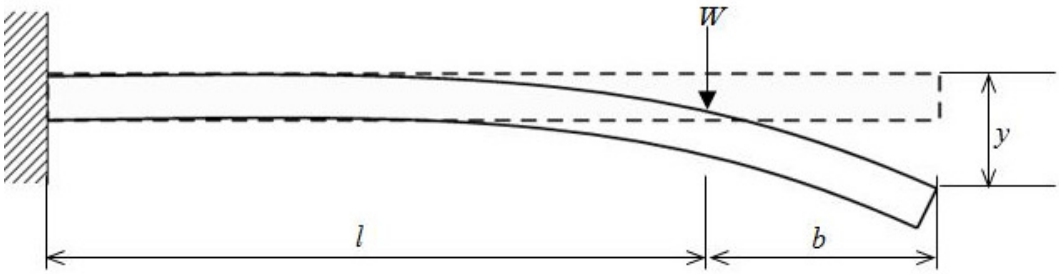

Figure 5.22. Schematic representation of deflection in FGCL beam specimen

The set up comprises of a cantilever fixture to which the test specimen of size 10 mm X 6 mm X 70 mm is fixed. The deflection of the test specimen is measured by a laser displacement sensor (optoNCDT 1402). A point load is applied to cantilever beam through a loading screw mechanism at a distance 45 mm from the fixed end. The load details are gathered by a load cell (HBM S9M/2kN), having one end firmly attached to the support and the other end is connected to the loading screw. The magnitude of point load is adjusted by rotating the loading screw. The signals from the load cell and laser displacement sensor are acquired through NI 9237 and NI 9213 DAQ modules interfaced with labVIEW 2012.

Table 5.5. Young's modulus for Al and Al composites

Material	**Load W in N**	**Loading point *l* (m)**	**Deflection *y*(m)**	**Young's modulus, *E* (GPa)**	**Young's modulus , *E* (GPa) from tensile test**
Pure Al	10	0.045	0.0000534	57.94±0.02	58.20±0.04
0.25 CNT + Pure Al	10	0.045	0.00005158	59.98±0.04	60.40±0.05
0.5 CNT + Pure Al	10	0.045	0.0000498	62.12±0.06	62.90±0.05

The experimental set up is validated by performing bending test on 2024 aluminum specimens of size 10 mm X 6 mm X 70 mm having known material properties. The tested beam has showed the deflection of 0.0425 mm for an applied load of 10N. This measurement has yielded an Young's modulus of 73.7 GPa as compared to the the theoretical value of 73.1 GPa (S.V. Kamat et al. 1989). The difference in Young's modulus estimation was 0.77%

which has suggested that the test setup is able to produce accurate results. The bending tests are extended to compare the experimentally determined Young's modulus of Al-CNT composites from tensile test. The results are listed in the Table 5.5 which has further verified the method of estimating the Young's modulus from bending test.

5.3.4 Conclusion

The bending tests are performed on the FGCL to overcome the difficulties associated with the measurement of Young's modulus through UTM. The tests are performed on a validated bending test set up. The deflection of FGCL cantilever beam is measured for the input load of 10N. Experiments are performed on three identical samples. From the deflection measurements, the Young's modulus of FGCL is found to be 61.48 GPa.

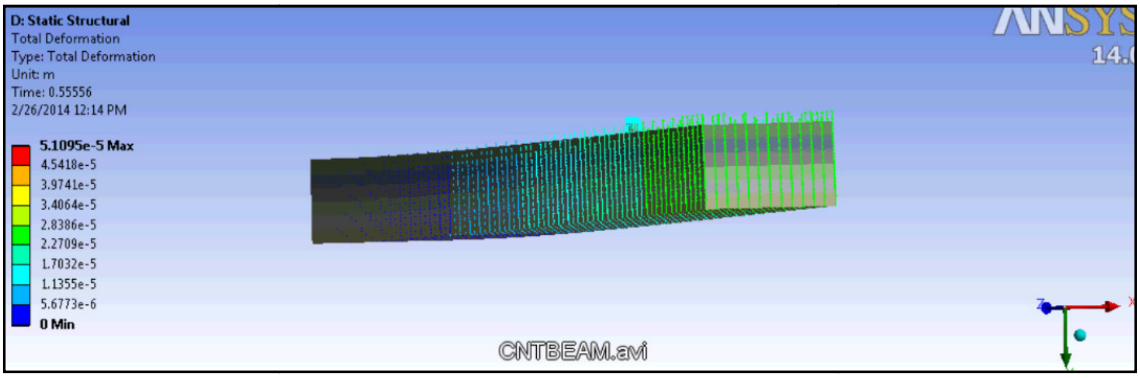

Figure 5.23. ANYSYS(version 14) simulation results of FGCL beam

To verify the experimental results, the FEM simulations are performed on Ansys version-14. A six layers of FGCL beam is modeled by gluing Al-CNT composites with varying CNT reinforcements. The beam is fixed at the one end to represent the cantilever configuration. Each layers are assigned the properties of Al CNT composites obtained from the tensile test. Results were obtained for both plane stress and plane strain and were compared with the experimental results. The Young's modulus of 61.482 GPa calculated for the observed deflection are tabulated in the above table 5.6.

Table 5.6. Young's modulus for FGCL specimen by bending test method

Material	Load W in N	Loading point l (m)	Deflection y(m)	Young's modulus, E (GPa)	Young's modulus, from Ansys simulation E (GPa)
FGCL	10	0.045	0.0000509	61.48±0.02	61.49

5.4 Damping study

Damping property represents the ability of a material to dissipate the energy. The damping characteristics of a material are determined by free or forced vibration tests (Rao SS 2004). Free vibration approach involves the measurement of damping property from the decay in the amplitude of vibration with time in the absence of external disturbance. Force vibration approach involves the measurement of half power points with respect to the measured frequency response functions (FRF) (Monica et al. 1995). The FRF are obtained from the measurement of impulse and response through electrodynamic shaker test and impact hammer tests. The shaker excitation test necessitates the complex experimental set up involving electrodynamic shakers and amplifiers. But the impact hammer tests are preferred choice due to its simplicity and easy to perform (Umut et al. 2011).

In the present damping characterization studies, the impact hammer test is adapted to evaluate the damping properties of FGCL. Tests are performed on FGCL cantilever beam as per the standard test method specified in ASTM E 756-05. The damping characteristics evaluated from the damping ratio corresponding to the fundamental natural frequency of the measured FRF curves (Monica et al. 1995). The damping characteristics of Al-CNT composites are evaluated along with FGCL to compare the variation in damping characteristics.

5.4.1 Experimental set up for damping measurement

Schematic representation of impact hammer test set up to find the damping of the FGCL specimen is shown in Figure 5.24. The set up comprises of a cantilever test specimen of dimensions 75 mm X 10 mm X 6 mm attached to a fixture. The impulse excitations are provided by an impact hammer (PCB, 086C03, sensitivity:1.24 mV/lb) and the response is measured by an accelerometer (YMC, YMC121A100, sensitivity: 100.7 mV/g). The signals are acquired through NI 9234 DAQ with 24-bit resolution. The FRF corresponding to the ratio of impulse and the response is measured from the graphical programming performed in using LabVIEW 2012. The block diagram of the graphical program and the cantilever experimental set up shown in Figure 5.25 and Figure 5.26a, respectively.

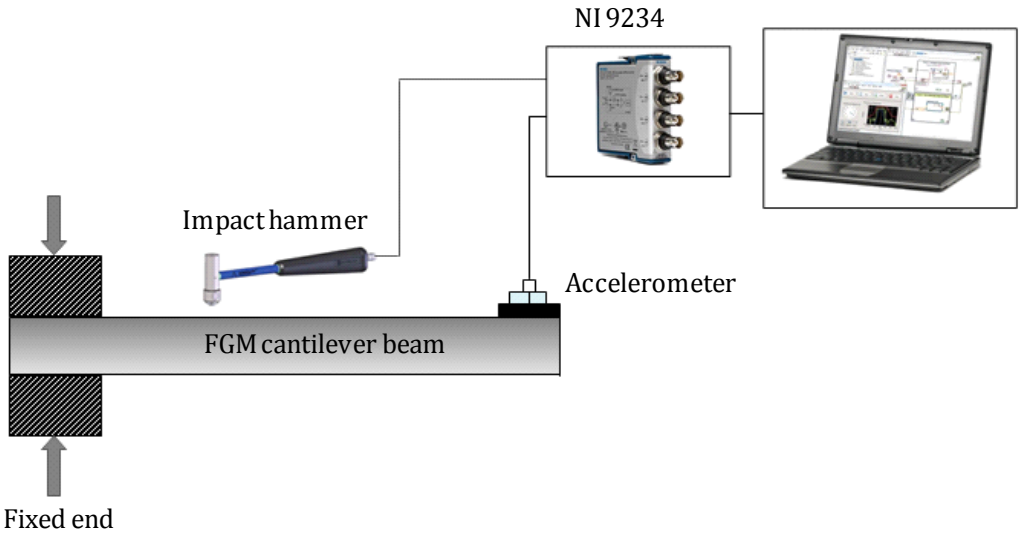

Figure 5.24. Schematic diagram of FGCL beam impact hammer test set up

To validate the experimental set up initial experiments are performed with a specimen having known material properties. To compare the natural frequency of the test specimen, modal analysis is performed for the corresponding boundary conditions in ANSYS version 14.

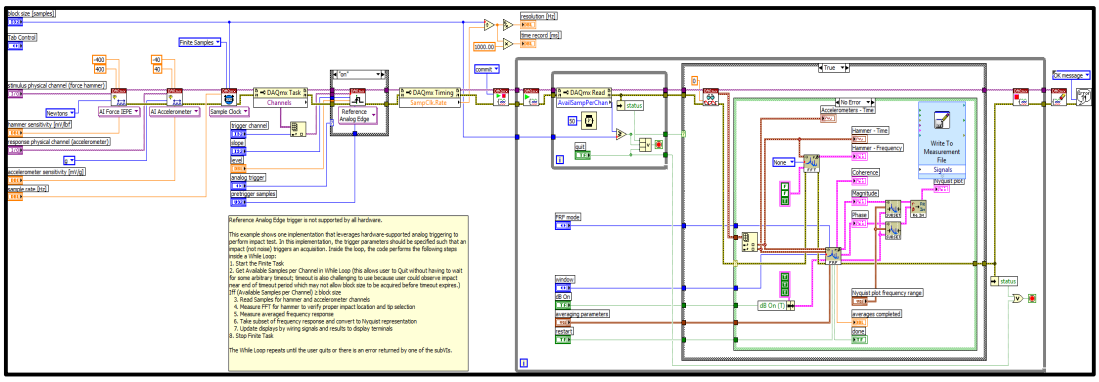

Figure 5.25. Schematic diagram of Lab view block diagram

The natural frequencies obtained from the impact hammer test and from modal analysis showed a close match. Also the loss factor estimated from the half power bandwidth is showed a close match with the actual loss factor. The above analysis validated the impact hammer test set up to characterize the damping characteristics of FGCL. The graphical programming is done using LabVIEW 8.6 to acquire the frequency Response Function shown in figure 5.25 and front panel is shown in Figure 5.26b, respectively.

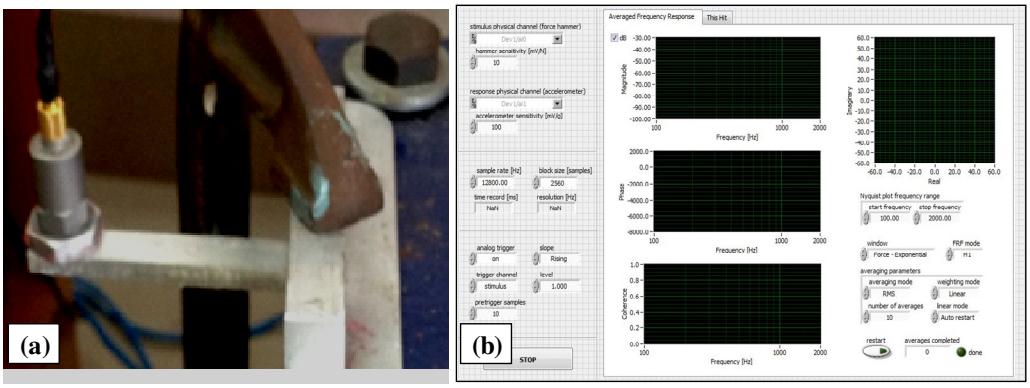

Figure 5.26. (a) Photograph of impulse hammer test setup. (b). Front panel of impact hammer program.

After validating the test set up, impact hammer test is performed on pure Al, Al-CNT samples with 0.25 wt% and 0.5 wt% and FGCL cantilever beams. The experiments were conducted on three identical samples.

5.4.2 Results of damping test

The FRF curves obtained from the impact hammer tests are shown in the Figure 5.27 – Figure 5.30. The natural frequency of the Al, Al-CNT and composite beams estimated from the impact hammer test are listed in table 5.7. These results are verified from the modal analysis performed in ANSYS version-14 using the parameters estimated form tensile test discussed in section 5.3.2. The experimental and simulation results showed a close match indicating satisfactory boundary conditions in the experimental setup.

The damping ratio estimated from the FRFs corresponding to first mode frequency of vibration using half power band width method are tabulated in table 5.8. From the listed values, it can be noticed that the value of damping ratio is higher for 0.5 wt.% CNT reinforcement followed by 0.25 wt.% CNT reinforcement and Al

Table 5.7. Comparison of natural frequencies

Material	Beam dimensions (mm)	1st Mode frequency	
		ANSYS Result in Hz	Experimental Result in Hz
Al	10 X 6 X 75	362	350
0.25wt.% CNT		372	370
0.5wt.% CNT		376	382
FGCL		368	374

This gives an impression that the CNT present in the aluminium provides the additional damping ability. From the SEM images of sintered composite specimens shown in Figure 4.12, it is observed that, with 0.5 wt % CNT reinforcement, the distribution was uniform and denser compared to 0.25 wt.% CNT reinforcement (Amal et al. 2008). This feature of CNT provides more interfacial area between the matrix contents, contributing to enhance the interfacial damping effect in a material compared to pure Al.

Table 5.8. Damping ratio of sintered specimen

Material	Beam dimensions (mm)	Damping ratio
Al	10 X 6 X 75	0.024
0.25wt.% CNT		0.03
0.5wt.% CNT		0.037
FGCL		0.028

The natural frequency of a structure depends on the stiffness and mass of the material. Addition 0.5wt.% CNT has reduced the effective mass of composite beam compared to pure Al beam with same geometrical parameters. This resulted higher natural frequency for 0.5 wt % CNT reinforced beam.

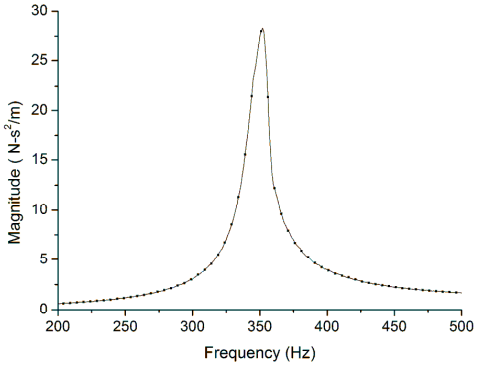

Figure 5.27. Frequency response function (FRF) of Cast Al specimen

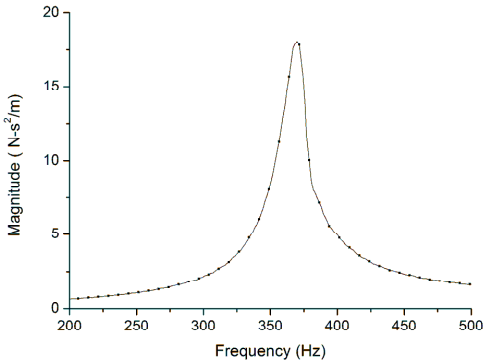

Figure 5.28. Frequency response functionof Al matrix composite with 0.25 wt.% CNT reinforcement

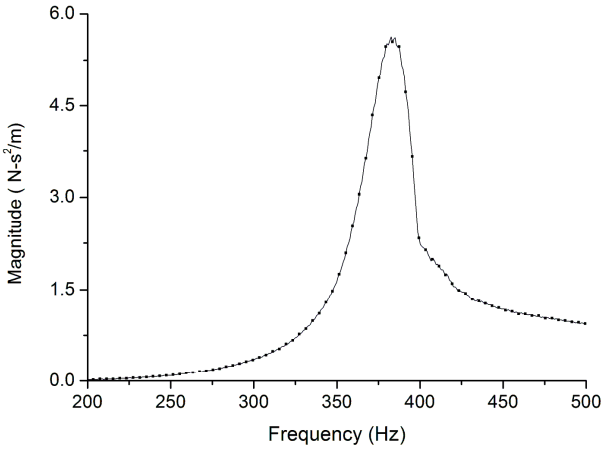

Figure 5.29. Frequency response function of Al matrix composite with 0.5 wt.% CNT reinforcement

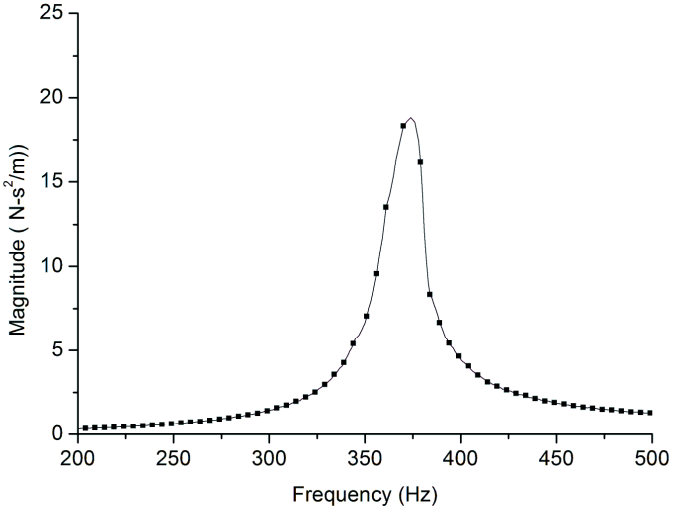

Figure 5.30. Frequency response function of FGCL

The damping ratio of base material and composites is determined separately using the data obtained from all the three tests. Table 5.8 represent the damping ratios of Al, 0.25 wt.% CNT reinforced Al and 0.5 wt.% CNT reinforced Al composites determined from impact hammer tests, respectively (A.D.Nashif,1985).

5.4.3 Discussion

Mechanical properties of PM parts depend on the number of pores, their distribution and size. Fatigue strength and the other mechanical properties increase with decrease in

porosity (Douib 1989). The physical properties depend mainly on pore ratio which is defined as the ratio of volume of void-space to total or bulk volume of material. Corrosion resistance decreases with an increase in pore ratio. Electrical, thermal and magnetic properties change depending on relative density. Porosity increases sound and vibration absorption property. Therefore, most of the studies in powder metallurgy were dedicated to the design of products showing optimal porosity (Caliskan 2000). The difference in the particle size had no significant effect on the pore shape or number of pores per unit area but did have a significant influence on pore size. Porosity (percentage, distribution and size) of PM components depends upon the initial powder size. Small powder particles produce a large number of "small" pores distributed throughout the entire component. Powder particles with a large particle size produces a small number of pores, heterogeneously distributed in the sample and of "large" size. It is also observed that an appropriate selection of average particle size for the preparation of the powder mixture is useful in order to obtain samples with suitable physical properties (Sanchez et al.2003).

Further, the composites produced through PM process showed higher damping ratio compared to their cast counterparts. The optical images of CNT reinforced Al composite by Powder Metallurgy specimen compared with Pure Al microstructure shows that the CNT reinforcements are still finer and distributed more uniformly, accounting for enhancement in interfacial damping. The microstructure of base Pure Al produced by PM method also reveals number of uniformly distributed voids. This feature reduces the energy transmission through the material and helps in more energy absorption within the material. Introduction of reinforcement increases the interfacial area. Depending on the nature of reinforcement, the damping behavior of the base material will change. With the reinforcement of CNT, the damping of the composite is increased and reached a maximum value at 0.5 wt% of reinforcement and then decreases. In addition to providing interfacial area for damping, the nature and distribution of CNT also has a bearing on the composite damping. Since the Multiwall Carbon Nanotube is a hollow material with large L/D ratio, it has higher surface area and provides larger interfacial

contact area between the reinforcement and the matrix material. With higher CNT content and uniform distribution in the matrix, the damping of the composite increase. The damping property of the composite reduces with the increase in agglomeration of CNT. CNT above 0.5 wt.% results in agglomeration and the distribution of reinforcement is not uniform. This results in the decreases of damping ratio. When the CNTs are uniformly dispersed, the hollow feature of Nanotubes automatically creates uniformly distrusted minute pores in the composite. The uniform distribution of CNT depends on the processing technique used.

5.5 Wear study

The friction and wear behavior of CNT reinforced composites is dependent on fabrication, operational and environmental parameters. In particular, the type of CNT employed seems to have crucial influence. Carbon Nanotubes (CNTs), discovered less than 20 years ago, aroused big enthusiasm around the world because of their excellent properties and potential application in many fields. Compared with other filler materials like carbon fibers, CNTs possess an ultra-high strength, modulus which imply their promising application as wearable materials in tribological fields. Friction and wear test results suggest that, composites with CNTs as reinforcing elements exhibit more stable frictional coefficient and lower wear rates, especially light properties of aluminium matrix with low wear rate is added advantage in many application. Based on experimental results conducted on other composites and CNT reinforced matrix, two possible mechanisms about friction and wear process are proposed. In addition, some potential tribological applications of CNT-reinforced functionally graded composites are discussed in brief.

5.5.1 Methodology

The wear test on CNT reinforced Aluminium composite for different weight fraction (0.1 to 0.5wt.%) are conducted. Design of Experiment techniques (Taguchi method) was employed and L27 set of experiments are performed for three different parameters namely CNT wt.%, load and abrasive grit size. The results are analyzed to find the

influencing factors for wear rate. Experimental samples are prepared using conventional Powder Metallurgy technique. Presence of gradation is quantified by weight method. An attempt is made to study the influence of CNT weight fraction, load and abrasive grit size (C/H) of sand paper on wear rate and specific wear rate. The Design of Experiments based upon L9 (27) orthogonal arrays by Taguchi is used. Analysis of variance (ANOVA) and S/N (signal to noise) ratios analysis is performed on the measured data to investigate the influence of material and geometrical parameters on wear rate. An optimal parameter combination is determined which leads to lower wear rate and specific wear rate. The flow chart for wear test experiments is shown in Figure 5.31.

5.5.2 Taguchi Technique

Taguchi's techniques are being used widely in engineering design (Ross, 1996) (Phadke, 1989). It is a powerful tool for the design of high quality systems (Taguchi et.al. 1987; Taguchi, 1993; Ross, 1988; Montgomery 2001). Taguchi's technique focuses on determining the parameter design, which is an engineering method for product or process design that focuses on determining the parameter (factor) settings producing the best levels of a quality characteristic (performance measure) with minimum variation. This method is effective to deal with responses influenced by multiple variables. It drastically reduces the number of experiments that are required to model the response function compared with full factorial design of experiments. It is a technique for designing and performing experiments to investigate processes where the output depends on many factors (variables, inputs) without having to tediously and uneconomically run all possible combinations of values. Taguchi designs provide a powerful and efficient method for designing processes that operate consistently and optimally over a variety of conditions. To determine the best design, it requires the use of a strategically designed experiment, which exposes the process to various levels of design parameters. The major advantage of this technique is to find out the possible interaction between the parameters. The Taguchi technique is advised for process optimization and identification of optimal combination of the factors for a given response (Basavarajappa et. al. 2005).

DOE methods are developed in the early years of 20th century and are being extensively studied by statisticians since then, but they are not easy to use (Phadke, 1989). Taguchi's approach to design of experiments is easy to be adopted and applied for users with limited knowledge of statistics; hence it has gained a wide popularity in the engineering and scientific community. This technique is divided into three main phases, which encompasses all experimentation approaches. The three phases are (1) the planning phase (2) the conducting phase and (3) the analysis phase. Planning phase is the most important phase of the experiment. This technique creates a standard orthogonal array (OA) to accommodate the effect of several factors on the target value and defines the plan of experiments. The experimental results are analyzed using analysis of means and variance to study the influence of factors. Figure 5.29 presents the scheme of the major steps of implementing the Taguchi method (Montgomery, 2001). The effects of CNT content, wear surface (Abrasive grit size) and applied load, on the wear behaviour of the composites were studied. The morphologies of the wear surfaces were investigated using scanning electron microscopy (SEM).

5.5.3 Materials and process

The matrix system consists of pure aluminium and CNT composition by weight fraction. Wear test components of size 4 x 4 mm are prepared by conventional green compact Powder Metallurgy technique. The process flow chart for the wear test is described in Figure 5.31.

5.5.4 Experimental setup and procedure

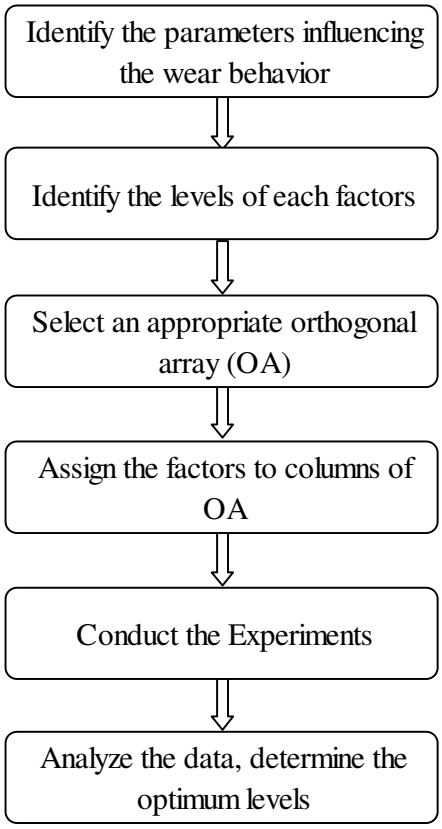

Figure 5.31. Flow chart for wear test experiments

A pin-on-disc test apparatus was used to investigate the dry sliding wear characteristics of the composite as per ASTM G99-95 standards. The wear specimen (pin) of 25 mm diameter and 10 mm height was cut from cast samples, machined and then polished metallographically. The initial weight of the specimen was measured in a single pan electronic weighing machine with least a count of 0.0001 g. During the test the pin was pressed against the counterpart rotating against EN32 steel disc with hardness of 65 HRC by applying the load. After running through a fixed sliding distance, the specimens were removed, cleaned with acetone, dried and weighed to determine the weight loss due to wear. The difference in the weight measured before and after test gave the sliding wear of the composite specimen and then the volume loss was calculated. The sliding wear of the

composite was studied as a function of the volume percentage of the reinforcement, sliding distance, the applied load and the sliding velocity.

5.5.5 Pin-on-disc tests for sliding wear

Figure 5.32. Pin on disc set up of wear test machine

The actual photographs of the pin on wear test machine setup shown in Figure 5.32, with a holder positioned (M.H Bastwros et al. 2013). Specimens underwent the sliding wear tests against abrasive grit size of 400, 800 and 1200 for 10 N, 20 N, 30 N loading using the pin. Tests were carried out at room temperature using water with a disc rotating at a fixed speed of 2 m/s against the samples. The total sliding distance was of 300 m and measurements in the weight of the specimens were taken every 100 m. The abrasive grit was conserved during the whole sliding distance and water was used as lubricant in order to prevent deterioration of abrasive grit (SiC papers) (Ashor Kr.Mishra et al. 2012). For statistical purposes, three runs were performed with different samples for each wear condition using new abrasive grit in each case. The samples were ultrasonically cleaned in methanol, then dried at 60^{o}C for about 30 s and weighted in order to calculate the weight loss of the specimens in each interval of the test. The metallographic study of worn surface and wear debris are performed by scanning electron microscope (JEOL model JSM-7401F).

5.5.6 Design of Experiments

Table 5.9. Taguchi plan of Experiments

$L_{27}(3^3)$	1	2	3
1	1	1	1
2	1	1	2
3	1	1	3
4	1	2	1
5	1	2	2
6	1	2	3
7	1	3	1
8	1	3	2
9	1	3	3
10	2	1	1
11	2	1	2
12	2	1	3
13	2	2	1
14	2	2	2
15	2	2	3
16	2	3	1
17	2	3	2
18	2	3	3
19	3	1	1
20	3	1	2
21	3	1	3
22	3	2	1
23	3	2	2
24	3	2	3
25	3	3	1
26	3	3	2
27	3	3	3

Column 1: 1- 0.0 CNT wt.%, 2- 0.25 CNT wt.%, 3- 0.5 CNT wt.%, Column 2: 1- 10N, 2- 20N, 3- 30N, Column 3: 1- 400 abrasive grit size, 2- 800 abrasive grit size, 3- 1200 abrasive grit size

Design of Experiment is powerful scientific statistical technique to study the effect of multiple variables. This involves a series of steps which must follow a certain sequence for the experiment to yield an improved understanding of process performance (M.R.Doddamani2011). All designed experiments require a certain number of combinations of factors and levels to be tested in order to observe the effect of variables on product quality. Taguchi approach relies on the assignment of factors in specific orthogonal arrays to determine those test combinations. A major step in the DOE process

is the determination of the combination of factors and levels which will provide the desired information (Bala murugan Gopalasamy et al. 2001).

Analysis of the experimental results uses a signal to noise ratio to aid in the determination of the best process design. This technique has been successfully used by researchers in the study of dry sliding wear behaviour of composites. These methods focus on improving the design of manufacturing processes. In the present work, a plan of order for performing the experiments was generated by Taguchi method using orthogonal arrays (R.N. Rao et al. 2010). This method yields the rank of various parameters with the level of significance of influence of a factor or the interaction of factors on a particular output response. In the present investigation a L27 orthogonal array which has 27 rows and 3 columns was selected (Table 5.9) in accordance with the rule that the degrees of freedom of an orthogonal array should be greater than or equal to the sum of wear parameters.

5.5.7 Discussions

Physical properties :Wear Behavior

The aim of the experimental plan is to find the important factors and combination of factors influencing the wear process to achieve the minimum wear rate and coefficient of friction. The experiments were conducted based on an orthogonal array, with the aim of relating the influence of CNT composition, applied load and wear surface(Abrasive grit). These design parameters are distinct and intrinsic feature of the process that influence and determine the composite performance (Ashok Kr. Mishra et.al. 2012). Taguchi recommends analysing the S/N ratio or mean effects using conceptual approach that involves graphing the effects and visually identifying the significant factors (M. R. Doddamani et.al. 2011).

The above mentioned pin on disc test apparatus was used to determine the sliding wear characteristics of the CNT reinforced Al composite. Specimens of size 4 x 4 x 4 mm cube length were cut from the sintered samples, and then machined. The contact surface of the sample (pin) was made flat so that it should be in contact with the rotating disk.

During the test, the pin was held pressed against a rotating polishing paper of different grit sizes by applying load that acts as counterweight and balances the pin.

The track diameter was varied for each batch of experiments. The parameters such as the CNT composition, load, Abrasive Grit size were varied in the range given in Table 5.10 where sliding distance was kept constant. Weight loss method is applied to find the wear rate.

Table 5.10. Orthogonal array L27 (27) of Taguchi

Parameters with their values at three levels			
Level	**CNT wt.%**	**Load (N)**	**Abrasive grit size**
1	0	10	400
2	0.25	20	800
3	0.5	30	1200

Further, weight loss of each specimen was obtained by weighing the specimen before and after the experiment by a single pan electronic weighing machine with an accuracy of 0.0001g after thorough cleaning with acetone solution. The results for various combinations of parameters were obtained by conducting the experiment as per the orthogonal array. The measured results were analysed using the commercial software MINITAB 15 specifically used for design of experiment applications. Table 5.11 shows the experimental results average of two repetitions for wear rate. The selection of orthogonal array depends on three items in order of priority, viz., the number of factors and their interactions, number of levels for the factors and the desired experimental resolution or cost limitations.

Table 5.11. Experimental results obtained for the set of 27 set of Taguchi plan

Test No	CNT (wt %)	Load(N)	Abrasive Grit size	Weight before sliding (g)	Weight after sliding (g)	Weight loss (g)	Wear rate (m^3/m)	Sp.Wear rate (m^3/Nm)
1	0	10	400	0.5872	0.4918	0.0954	1.9116	19.11594
2	0	20	400	0.4716	0.3312	0.1404	2.7663	55.32569
3	0	30	400	0.4605	0.2985	0.162	3.3677	101.0311
4	0.25	10	400	0.5381	0.451	0.0871	1.6834	16.83417
5	0.25	20	400	0.4804	0.4257	0.0547	1.2063	24.12561
6	0.25	30	400	0.4868	0.4173	0.0695	1.4079	42.23555
7	0.5	10	400	0.6423	0.5821	0.0602	1.2147	12.14738
8	0.5	20	400	0.6211	0.5212	0.0999	1.9765	39.52991
9	0.5	30	400	0.5739	0.5121	0.0618	1.2393	37.17964
10	0	10	800	0.7178	0.6312	0.0866	1.664	16.63977
11	0	20	800	0.5905	0.5121	0.0784	1.6007	32.01307
12	0	30	800	0.6671	0.5951	0.072	1.5099	45.29821
13	0.25	10	800	0.5992	0.5412	0.058	1.1799	11.79917
14	0.25	20	800	0.5491	0.5012	0.0479	0.9622	19.2439
15	0.25	30	800	0.6051	0.5345	0.0706	1.424	42.72056
16	0.5	10	800	0.6233	0.5752	0.0481	0.9904	9.904048
17	0.5	20	800	0.6006	0.5652	0.0354	0.7448	14.89648
18	0.5	30	800	0.6651	0.6495	0.0156	0.3089	9.267327
19	0	10	1200	0.5174	0.4752	0.0422	0.818	8.17988
20	0	20	1200	0.6623	0.6123	0.05	0.9637	19.27302
21	0	30	1200	0.5788	0.5312	0.0476	0.9286	27.85798
22	0.25	10	1200	0.6031	0.5712	0.0319	0.6271	6.270887
23	0.25	20	1200	0.6454	0.6123	0.0331	0.6719	13.43835
24	0.25	30	1200	0.599	0.5712	0.0278	0.5628	16.88327
25	0.5	10	1200	0.4579	0.4312	0.0267	0.5313	5.31301
26	0.5	20	1200	0.5766	0.5669	0.0097	0.1907	3.813943
27	0.5	30	1200	0.5402	0.5203	0.0199	0.3928	11.78538

A total of 27 experiments were performed based on the run order generated by the Taguchi model. The response for the model is specific wear rate. In the orthogonal array, first column is assigned to CNT composition, second column is assigned to Load and third column is assigned to paper gird and the remaining columns are assigned to their interactions. The objective of the model is to minimize specific wear rate. The Signal to Noise (S/N) ratio, which condenses the multiple data points within a trial, depends on the type of characteristic being evaluated. The S/N ratio characteristics can be divided into three categories, viz. "nominal is the best‟, "larger the better‟ and "smaller the better" characteristics. In this study, "smaller the better" characteristics was chosen to analyse the dry sliding wear resistance. The S/N ratio for specific wear rate using "smaller the better "characteristic given by Taguchi, is as follows:

5.5.8 Analysis of Variance results for Wear test

The experimental results were analyzed with Analysis of Variance (ANOVA) which is used to investigate the influence of the considered wear parameters namely, CNT composition, applied load and wear surfaces (Abrasive grit) that significantly affect the performance measures. By performing analysis of variance, it can be decided which independent factor dominates over the other and the percentage contribution of that particular independent variable. Table 5.12 and Table 5.13 shows the ANOVA results for specific wear rate for three factors varied at three levels and interactions of those factors. This analysis is carried out for a significance level of $\alpha = 0.05$, i.e. for a confidence level of 95%. Sources with a P-value less than 0.05 were considered to have a statistically significant contribution to the performance measures.

5.5.8.1 Main effects plot for Means

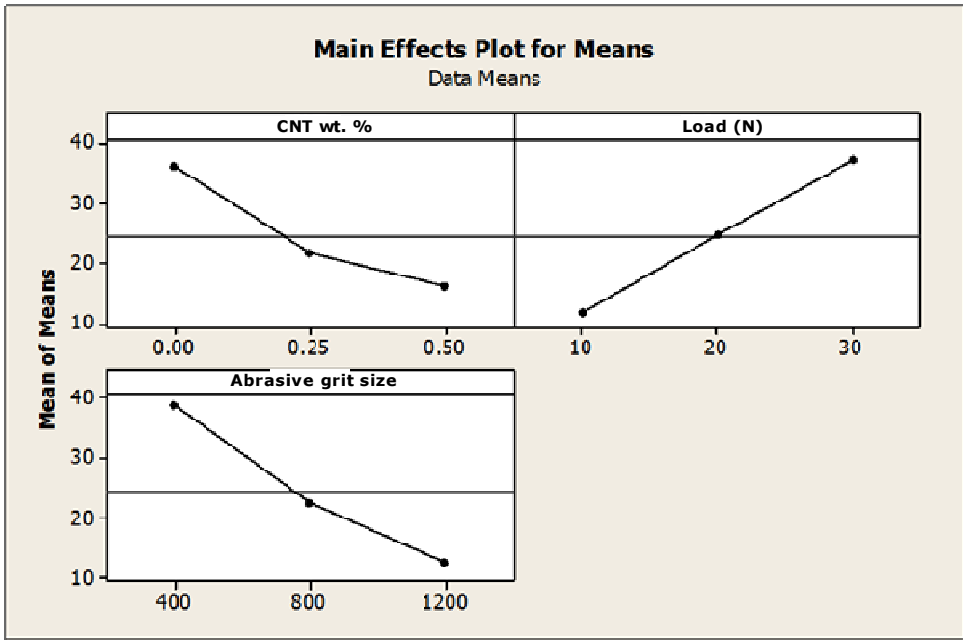

Figure 5.33. Main effects plot for wear test results

5.5.8.2 Interaction plots for means

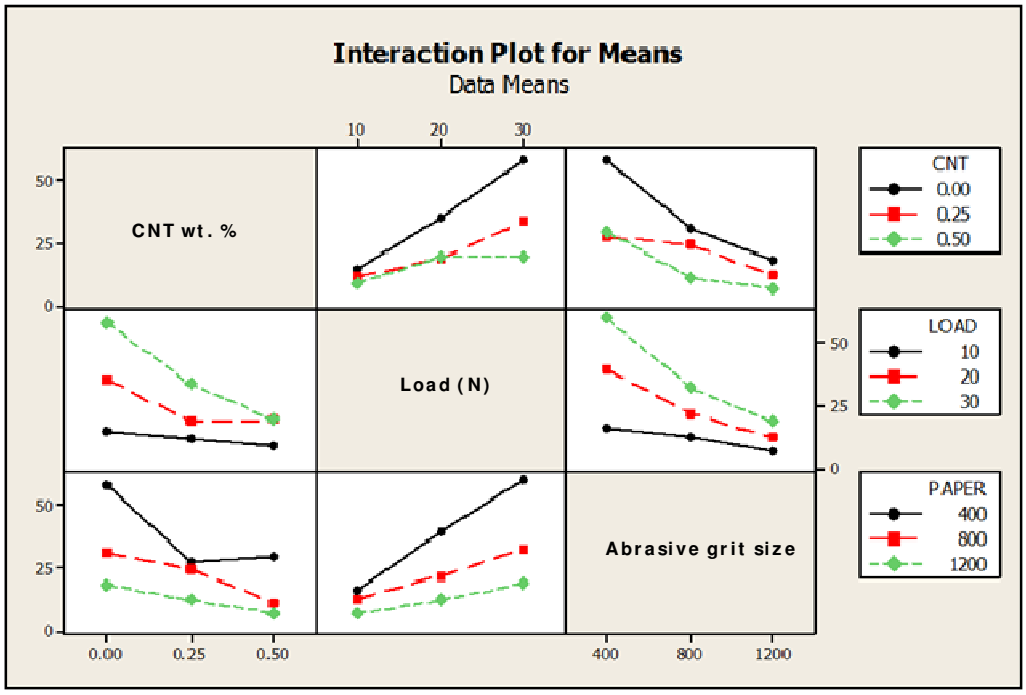

Figure 5.34. Interaction plot of controlling factors

5.5.8.3 Analysis of variance (ANOVA)

Table 5.12. Analysis of Variance for Means

Source	DF	SS	MS	F	P
CNT wt. %	2	1941	970.5	6.1	0.009
Load	2	2890	1444.8	9.08	0.002
Abrasive grit Size	2	3120	1560.1	9.8	0.001
Error	20	3183	159.1	–	–
Total	26	11133	–	–	–

Table 5.13. Analysis of Variance for Means of interaction plot

Source	DF	SS	MS	F	P
CNT wt. %	2	1940.9	970.45	10.27	0.009
Load	2	2889.5	1444.47	15.29	0.002
Abrasive grit Size	2	3120.2	1560.08	16.51	0.001
CNT wt. % * Load	4	927.6	231.9	2.45	0.13
CNT wt. % * Abrasive grit Size	4	658.9	164.73	1.74	0.233
Load * Abrasive grit Size	4	840.3	210.06	2.22	0.156
Error	8	755.69	94.49	–	–
Total	26	–	–	–	–

DF: Degrees of freedom, SS: The sum of squares, MS: The mean sum of squares, F: F-statistic, P: P- Value

The test plan was developed with the aim of relating the specific wear rate with weight fraction of CNT, Load and wear surface (Abrasive grit size). After conducting the experiments as per orthogonal Array, average results for various combinations of parameters are obtained and tabulated (Table 5.11).

Figure 5.33 graphically, represents the effect of the three control factors on wear rate. Analysis of these plots leads to the conclusion that for the combination of 0.5wt.% CNT , 10 N load and abrasive grit size 1200 (smooth paper) gives minimum wear rate yielding better surface with smooth operation. Table 5.13 shows the results of ANOVA analysis for wear rate for three controlling factors. The last column (P) in these tables indicates the probability of significance of control factors. Smaller the value, higher would be the percentage contribution of the factor on the total variation indicating higher degree of influence on the results.

Observations from the ANOVA Table 5.12 shows that, the influence of wear surface (P = 0.001), Load (P = 0.002) and CNT reinforcement (P = 0.009). Wear surface (Abrasive grit size) have a lowest 'P' value and shows the highest influence factor on wear rate followed by load and CNT contribution. Similar observation was made from the ANOVA Table 5.13 for interaction of influencing factors. In which lower P value for interaction of 'CNT wt.% 'and 'Load' (P = 0.13) indicating the higher influencing factor. Figure 5.34 represents the similar trend for interaction of controlling factors in which, for higher CNT wt.% and lower load shows lower specific wear rate. It can be concluded that, contribution of CNT significantly affects the wear rate over load and wear surface.

5.5.8.4 Conclusions

The results for various combinations of parameters were obtained by conducting the experiment as per the orthogonal array. The measured results were analyzed using the commercial software MINITAB version-15 specifically used for design of experiment applications (S. Basavarajappa et.al. 2005). Table 5.11 shows the experimental results average of two repetitions for wear rate. To measure the quality characteristics, the experimental values are transformed into signal to noise ratio. The influence of control parameters such as CNT composition, load and wear surface (Abrasive grit size) on wear rate has been analyzed using ANOVA techniques. It was observed that the wear surface (Abrasive grit size) is a dominant parameter on the wear rate followed by applied load and CNT composition. The analysis of these experimental results using S/N ratios gives the optimum conditions resulting in minimum wear rate and coefficient of friction. Wear

surfaces (Abrasive grit size) (62.5%) has the highest influence on wear rate followed by applied load (37.5%) and CNT composition (1.25%) for Al - CNT metal matrix composites.

5.5.9 Microstructure Analysis of wear surface

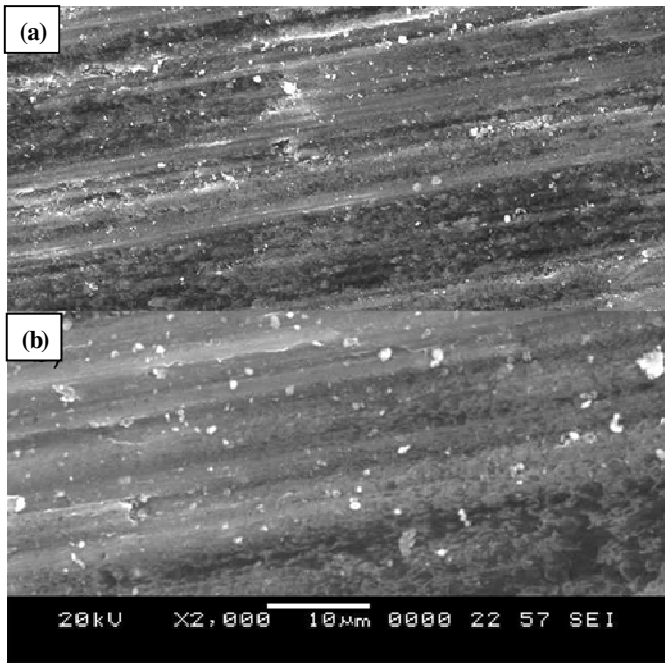

Figure 5.35. (a) SEM micrograph of wear surface of Al subjected to 30N load (a) 500X (b) 2000X

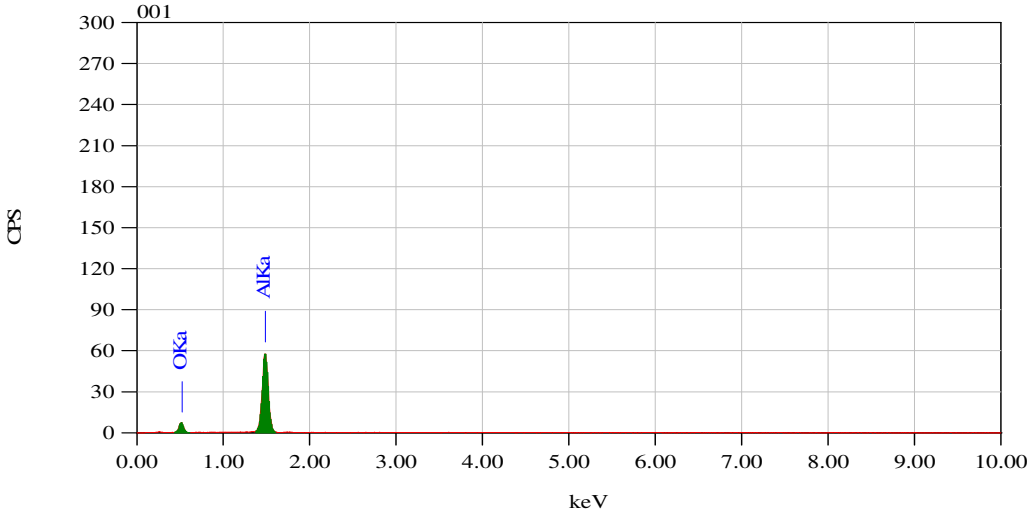

Figure 5.36. EDX of wear surface of Pure Al

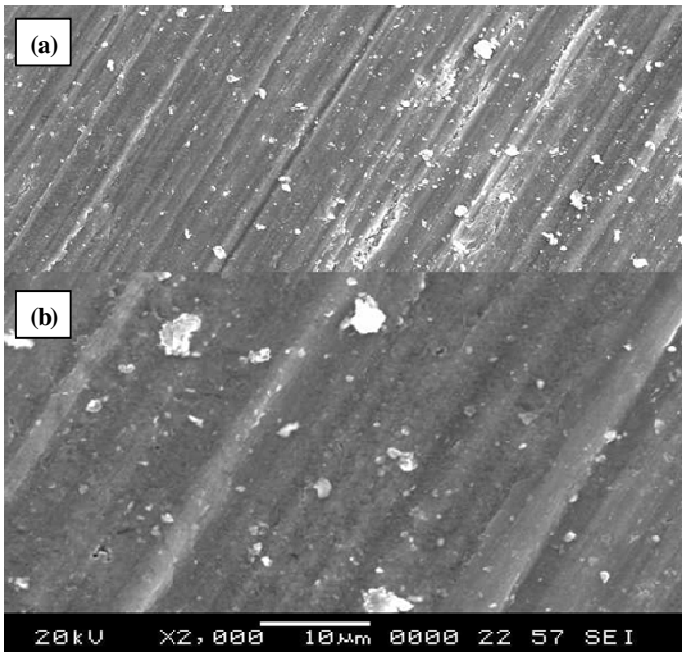

Figure 5.37. (a) SEM micrograph of wear surface of 0.25 wt.% CNT reinforced Al matrix composites subjected to 30N load (a) 500X (b) 2000X

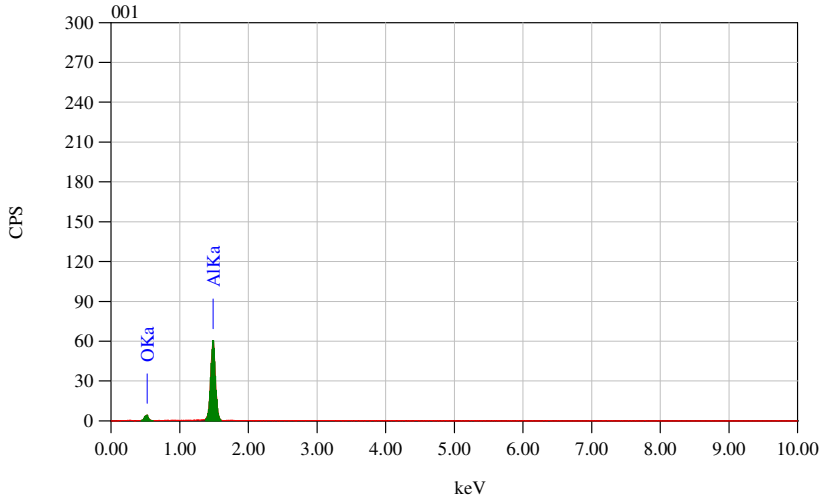

Figure 5.38. EDX of wear surface of 0.25 wt % CNT reinforced Al matrix composite subjected to 30N load.

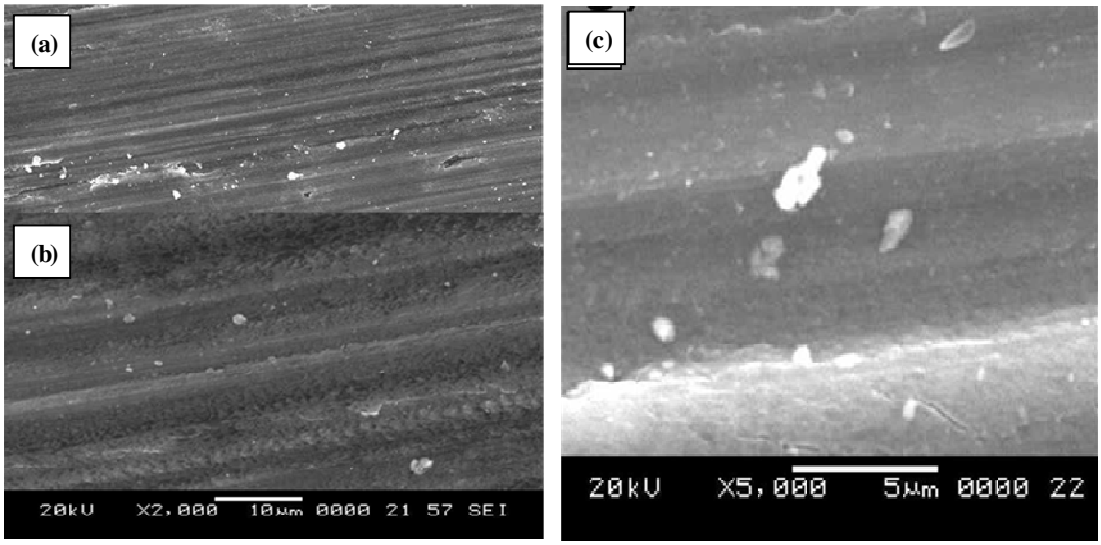

Figure 5.39. (a) SEM micrograph of wear surface of 0.5 wt.% CNT reinforced Al matrix composites subjected to 30N load (a) 500X (b) 2000X. (c) 5000X .

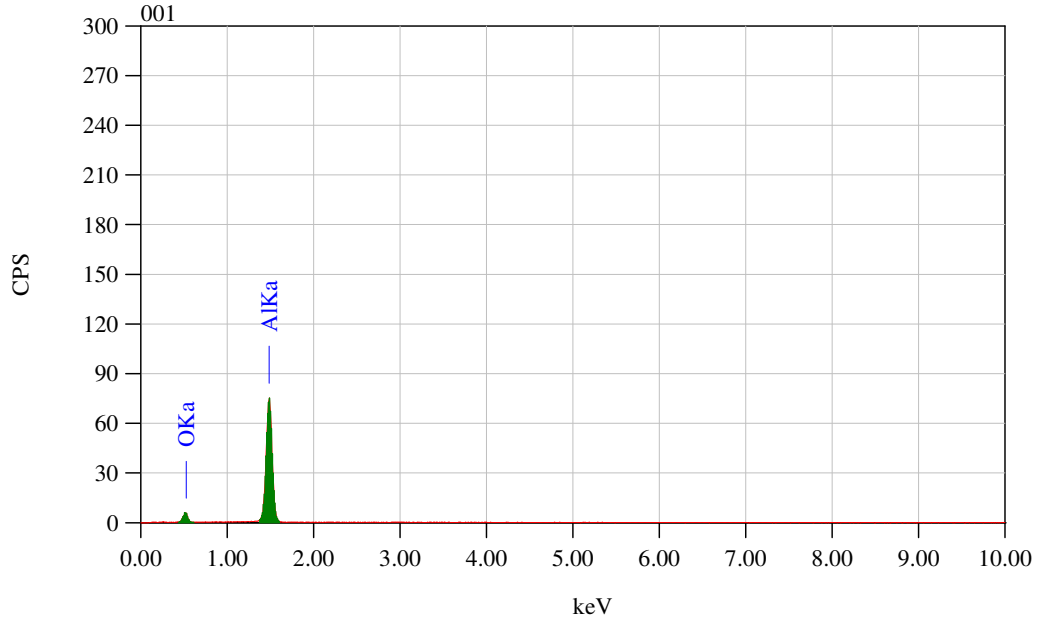

Figure 5.40. EDX of wear surface of 0.5wt.% CNT reinforced Al matrix composite subjected to 30N load

SEM and EDX analysis of worn surfaces and debris revealed contribution of different modes of wear. The intensity of each type of wear was found to be both material and load dependent. The presence of significant amount of "O"(oxides of mixed mechanical layers) on the wear surface and in debris of the composite revealed oxidation conditions prevailed predominantly, especially at higher loads. However, Kim et al. 2009 observed mixed abrasive and adhesive wear for Al-CNT composite with different CNT content at fixed load and sliding speed. As far as the composite is concerned, adhesion of SiC from the counter face was negligible, especially at higher loads. However, the debris contained noticeable amount of C and Si (Figure 5.46). This shows that increased hardness of the composite may cause significant abrasive action on the counter face disk resulting in removal of some SiC particles from the counter face (Abrasive grit). At lower loads, considerable amount of oxygen on the worn surfaces of the composite show formation of stable oxide layer which possibly contributed to better wear resistance of the composite at lower loads. However, at higher loads, excessive fracturing and delamination of the composite disabled the formation of any stable tribolayer and hence the worn surfaces were found to be mainly composed of Al. In their investigation on the wear mechanism in

Al–CNT composites, Zhou et al. (2001) found oxidation as the main wear mechanism. They explained this through the formation of alumina layer on the composite and its subsequent delamination causing abrasion between the specimen and the counter face. This single specific wear mechanism may be due to the fact that they performed all tests under a constant load and sliding speed with varying CNT content. However, M.H. Bastwros et al. (2013) observed mixed abrasive and adhesive wear for Al–CNT composites with different CNT content at fixed load and sliding speed. They also reported minimal oxidation wear for the composite containing 1.0 wt.% CNTs. Micro-ploughing and delamination were reported as the dominant wear modes for Al–CNT composites by A.M. Al-Qutub (2013). At higher loads, they observed more delamination which is in agreement with the present work where delamination intensity sharply increased with increasing load and hard wear surface for Al–CNT composites.

The different modes of wear of Al–CNT composites reported in literature (Popescu. N et al. 2011, R.i.deuis et al. 1996) may be due to different CNT contents, composite fabrication method, and wear test parameters (speed and load). However, the present work clarifies that the wear behavior of Al–CNT composites is largely influenced by the applied load and wear surface (Abrasive grit size).There exists a critical CNT composition of 0.5 wt.% beyond which the CNTs could have a negative impact on the wear resistance of aluminium CNT composites.

5.5.9.1 Analysis of Debris

Figures 5.41, 5.43 and 5.45 shows the morphology of wear debris for pure aluminium and composite at different CNT wt.% composition for 30N loading. Composition of wear debris contain higher percentage of 'C' and 'O'(Oxides of mixed mechanical layers) for pure Al and 0.25 wt.% CNT composite compared to 0.5 wt.% of CNT composite (Zhou et al.2007). This shows the delamination of counter face (Abrasive grit size) is due to wear mechanism. Increase of CNT results in lower percentage of Si particles in composite debris due to low wear rate of counter surface.

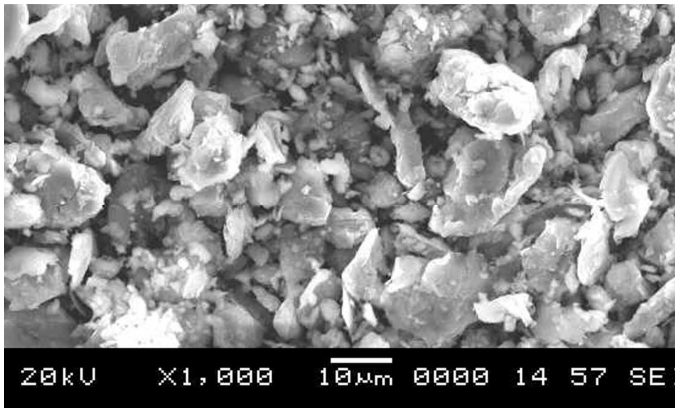

Figure 5.41. SEM image of Wear debris of Al subjected to 30N load

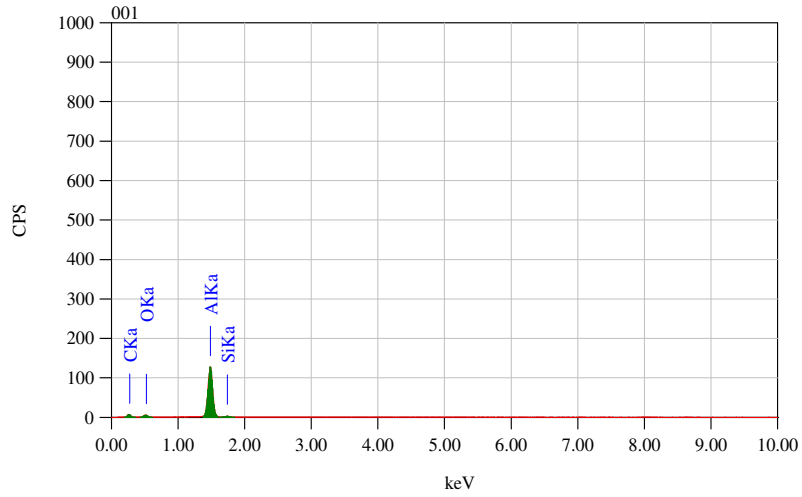

Figure 5.42. EDX of Al wear debris subjected to 30N load

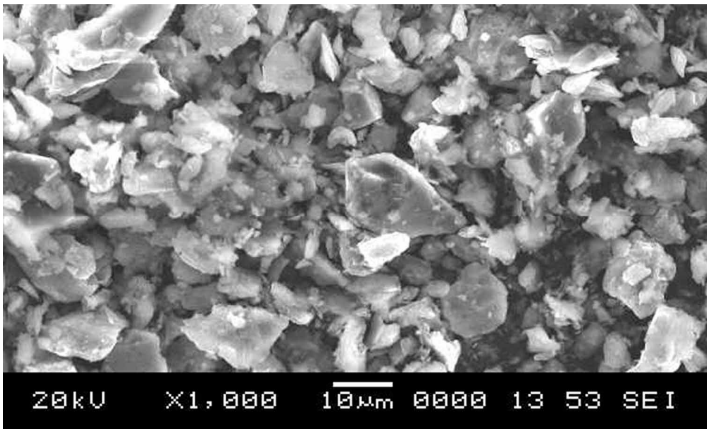

Figure 5.43. SEM micrograph of wear debris of 0.25wt% CNT reinforced Al matrix composite subjected to 30N load

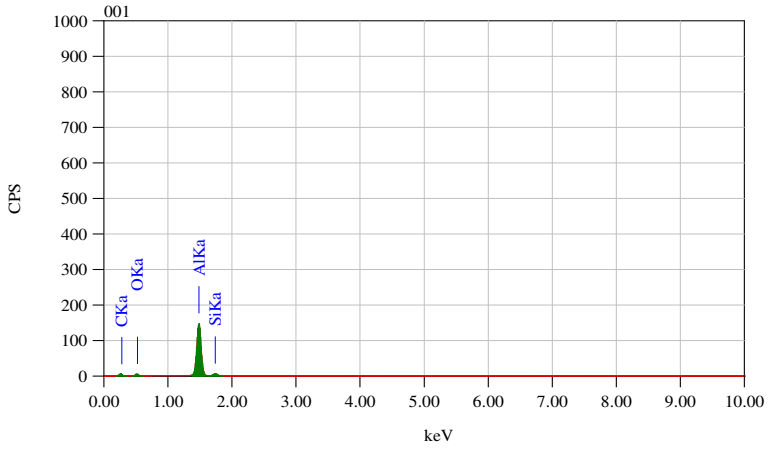

Figure 5.44. EDX of wear debris of 0.25wt% CNT reinforced Al matrix composite subjected to 30N load

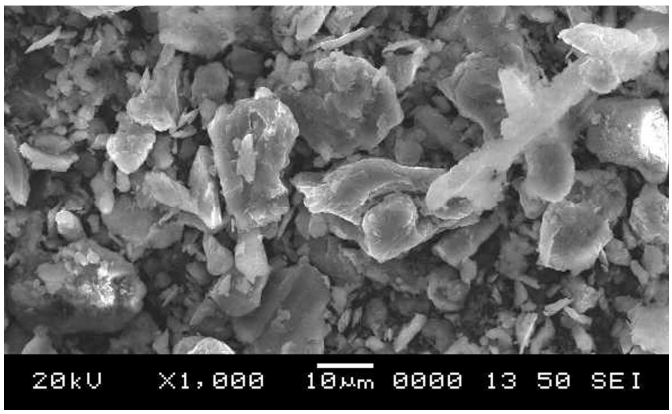

Figure 5.45. SEM micrograph of wear debris of 0.5wt% CNT reinforced Al matrix composite subjected to 30N Load

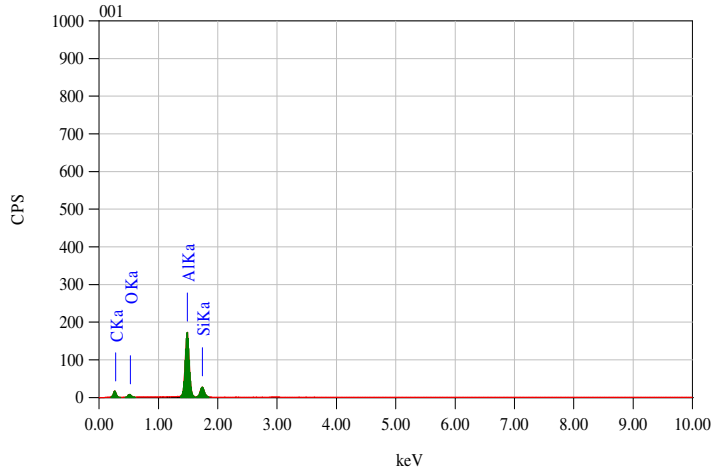

Figure 5.46. EDX of wear debris of 0.5wt% CNT reinforced Al matrix composite subjected to 30N load

Figure 5.42, 5.44 and figure 5.46 shows EDX analysis of the wear debris of pure Al and composite, respectively, at 30 N loading. The Pure Al debris contains significant amount of 'Si'(Silicon) and 'O'(oxides of mixed mechanical layers), whereas almost 75% of the composite debris is composed of Al. The EDX analysis results of debris are in good agreement with those of worn surfaces as both reveal almost similar compositional trend(Al-Qutub et al., 2012). These results show that adhesion and oxidation are dominant wear mechanisms for the monolithic alloy whereas excessive surface wear and delamination remains dominant for the composite.

5.5.9.2 Conclusion

Following conclusions are drawn from the study on dry sliding wear test using Taguchi's technique. Specific wear rate of CNT reinforced Al composites can be successfully analyzed using Taguchi experimental design scheme. Taguchi method provides a simple, systematic and efficient methodology for identifying significant control factors. Wear surfaces (Abrasive grit size) (62.5%) has the highest influence on wear rate followed by applied load (37.5%) and CNT composition (1.25%) for Al - CNT metal matrix composites. This suggests that the sliding surface & applied load have the highest influence on wear rate and CNT reinforcement till 0.5wt.% have significant influence on the wear behavior of composites. The DOE by Taguchi method was successfully used to predict the tribological behaviour of composites.

Increasing incorporation of CNT in weight fraction from 0.1 wt.% to 0.5 wt. % influence the wear rate of the composite. CNT improves the wear resistance of the composite by acting like a protective layer of lubricant between the pin and counter face.

5.6 Thermal Conductivity Test

With increased performance requirements for smaller, more capable, and more efficient systems, thermal challenges have become critical issues in performance design. Improvements in thermal conductivity of the material is critical in design consideration. In response to these critical needs, advanced materials and process improvements in designing new technology are required to provide high thermal transfer efficiency, well-

controlled thermal transient behaviour, environmental compatibility, low weight, fabrication cost acceptable materials. Material with improved thermal efficiency coupled low cost are the need of the hour. This chapter deals with the measurement of thermal conductivity of the different samples. The gradation of CNT reinforcement in aluminium in weight fraction from 0.1 wt.% to 0.5 wt.%. The developed FGCL materials shown 60% improvement in the thermal conductivity over the conventional aluminium material. Its application in thermal design, development of thermal management solutions, advanced thermal management materials selection and component design guideline, as well as environmental compatibility requirements in thermal management provides revolutionary changes in the future needs.

In addition to the technical challenges, market forces such as declining product prices, increased user experience through new devices, longer product life would make these challenges even more complex (Mallik et al. 2005). The challenges in thermal management can be viewed in terms of three different but nonseparable problems (Hannemann 2003).

(1) The product temperature must be maintained at a relatively low level despite high local heat density.

(2) High heat loads must be handled at the assembly or module level.

(3) The thermal environment of the system must be controlled.

As a result, thermal management would be a serious concern behind any new electronic product designs. Two major objectives should be achieved through thermal management: Prevention of catastrophic thermal failure, and extension of the useful lifetime of the system. Catastrophic thermal failure is usually the result of material failure due to overheating, or thermal fracture of a mechanical element in system. The failure rate increases exponentially with operating temperature.

This chapter will give an overview about the thermo physical properties of FGCLs and the measurement methods of these properties. By the combination of a matrix material with a reinforcement such as CNT, special thermophysical properties of the material can be achieved. This allows tailoring the thermo-physical and thermo

mechanical properties of the FGCL material by varying the weight fraction of the inclusion or reinforcement. Therefore the measurement and characterization of thermo physical properties such as density, CTE (Coefficient of Thermal Expansion), specific heat and thermal conductivity or resistivity plays an important role. So, investigations of thermo-physical properties are performed at room temperature but not at higher temperatures or under cycling conditions. This is necessary in order to understand the performance of the material during its use (e.g. the variation of CTE and thermal conductivity with temperature of Cu-C material in a heat sink application).

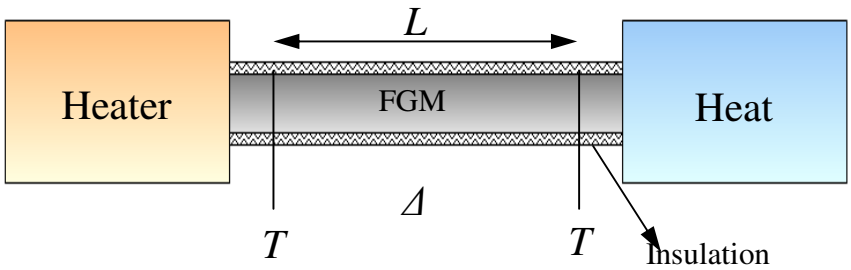

Figure 5.47. Schematic diagram of experimental setup for thermal conductivity measurements

The thermal conductivity (W/mK) of metals, alloys or composites can be measured by comparative method with steady state longitudinal heat flow in a temperature range from room temperature up to about 1000°C. The comparative instrument measures heat flow based upon the known thermal properties of standard reference materials. The test specimen is sandwiched between two identical reference samples. This stack is placed between two heating elements controlled at different temperatures. A guard heater is placed around the test stack to ensure a constant heat flux through the stack and no lateral heat flow losses. As heat flows from the hot element to the cold element the temperature gradient (T/L) across the stack is measured with thermocouples. The schematic diagram of the experimental setup is shown in figure 5.47. Once the specimen reaches a state of thermal equilibrium its thermal conductivity is calculated from the expression(Cengel,2003).

$$\alpha = \frac{L\,Q}{A\,\Delta T}$$

where Q is the heating power of the heater, L is specimen length, A is the area of cross section ΔT is the temperature difference observed. The experimental error is in the range of approximately ± 10 %. The specimen geometry is cylindrical (diameter 25 mm, length approx. 6 mm).

Table 5.14. Thermal conductivity test results on composite and FGCL

Sl.No	Material	Temperature difference (^{o}C)	Thermal conductivity (W/mK)	Percentage increment
1	Pure Al	44	277.76	––
2	Al + 0.1 wt.% CNT	38	321.62	15.79
3	Al + 0.2 wt.% CNT	30	407.38	46.67
4	Al + 0.3 wt.% CNT	25	488.86	76.00
5	Al + 0.4 wt.% CNT	19	643.24	131.58
6	Al + 0.5 wt.% CNT	15	814.77	193.33
7	FGCL	23	531.37	91.30

5.6.1 Conclusion

The thermal conductivity of the CNT reinforced composite increases with CNT weight fraction. Experiments conducted on Al composite revealed that the thermal conductivity was increased which is tabulated in Table 5.14. The thermal conductivity of 0.5 wt.% CNT reinforced composite was about 814.77 W/mK showing an improvement of 193.33% when compare to pure Al samples. In case of FGCL, it observed nearly 531.37 W/mK. The enthalpy of fusion increased with the CNT addition. This suggests that the degree of crystallinity increased with CNT addition. The uniformly dispersed CNT might have served as a seed for the formation of a transcrystallinity layer around CNT. This affects the thermal conductivity of the composite. It can be concluded that MWCNT is suitable for fabricating composites to be used in high temperature environment.

CHAPTER 6
CONCLUSION AND SCOPE FOR FUTURE WORK

This section highlights the significant conclusions derived out of the results presented earlier. Major inferences from both experimental and analytical investigations are discussed below.

Preparation of the layered CNT reinforced Al Functionally graded composite by cold compacting and sintering process by powder metallurgy route was successful with reasonably good physical and chemical properties. The density of the FGCL specimen prepared showed a reasonable improvement, when compared with pure aluminium. Density variation was observed with wt.% of CNT reinforcement, i.e from 0.1 wt.% to 0.5wt.%. The 6 layered FGCL showed 23% weight reduction compared to Pure Al. The void content, evaluated from the measured density is significantly higher with increasing CNT reinforcement. This is possibly because of the tubular structured CNT as reinforced material. Proper mixing and distribution of CNT in Al matrix created porous structure. Hardness test exhibited increase in hardness with increase in reinforcement of CNT weight fraction. A maximum hardness of $68H_V$ was observed for 0.5wt.% CNT reinforcement. Extraordinary changes of about 161% increment in hardness shows the good physical property of the prepared FGCL.

Microstructure observation brought out very interesting effects of CNT reinforcement. Grain size of pure Al was found to be around 127µm and it was reduced to 53.4µm in case of 0.5wt.% CNT reinforcement. There was a grain size decrement by 137.8%, from the top layer of pure Al to the bottom most layer of 0.5wt.% reinforced CNT layer, through the staggered layer structure. Owing to the increased hardness of the developed FGCL in the direction of layering, the staggered structure offers maximum resistance to deformation. These staggered structure offer a maximum resistance to deformation as in result of increment in hardness of the developed FGCL in the direction of layering. Presence of single CNT's on Al particle surface as well clusters of CNT's on the grain boundaries lead to brittle fracture of the FGCL.

With increase in reinforcement, load bearing capacity of FG samples improves under bending load. Young's modulus in FG core sharply increase from 58.2 GPa to 62.9 GPa for 0.5 wt.% CNT reinforcement beyond which it decreases significantly due to improper distribution of CNT's in Al matrix. Bending test was carried out to find the young's modulus for the FGCL material. Modelling of the FG layers in FEM with six layered gradation was considered for the analysis. The analysis results closely match experimental findings of the bending test. Young's modulus is evaluated under dynamic loading condition as 61.4 GPa (with 0.8% difference). An improvement of 5.4% in modulus strength of FGCL produced by CNT reinforcement makes a remarkable change in the future nanotechnology area. It is observed that increase in modulus for higher weight fraction of CNT's is not that encouraging (higher beyond to that of 0.5wt.% CNT).

Damping ratio determined for composite using impact hammer test showed an improvement of 54.1% for 0.5 wt.% CNT reinforcements. Increased damping ratio of 16.6% in the developed FGCL system could mean improved performance in applications involving vibration and energy absorption scenarios in automobile and space shuttle applications.

Taguchi Design of Experiments was employed to study wear mechanism. Observations of wear surface and debris revealed less marginal pullout and smooth tracks with 0.25wt.% CNT reinforcement due to the proper dispersion of CNT's in Al matrix. The other parameter such as load and the abrasive grit size (wear surface) also play a predominant role. Smooth tracks were obtained at 0.25wt.% of CNT with 800 grit size abrasive paper and 10N of load as compared to that of 0.5wt.% CNT with 1200 grit size abrasive paper and 30N of load.

Significant variation in the thermal conductivity of FGCL material (20^{o}C to 30^{o}C temperature difference) makes a huge impact on the future Nanotechnology. CNTs act as a catalyst for heat flow between the Al matrix. Voids between the Al particles are filled with CNTs. These connectivities of CNT across the grain boundaries support the heat flow from one end to other corner.

6.1 Scope for future work

The beneficial effects of the developed FGCL component open up the possibility of implementing a brake rotor with desired properties. In addition to attain better economy and ecology, the general striving for comprehensive safety is one of the central concerns of automotive engineering. As a consequence, the vehicle components which are relevant in terms of active and passive safety are subjected to continuous optimization. Significant higher demands have been made on the braking system during the past years as a result of increased engine power output, average speed and gross vehicle weight rating (vans, trucks etc.) and reduced air drag and rolling resistance of the tyre. To obtain a complete knowledge about where and when competitiveness is located in the production and the use of the brake rotor. A disc brake should acquire a combination of properties such as good thermal capacity, acceptable friction coefficient, good compressive strength, wear resistance and be economically viable.

Table 6.1 Cost analysis of brake rotor

Type of brake disc	Weight of fully machined disc (Kg)	Material cost (USD/disc)
Monolithic cast gray iron	5.571	2.9
Monolithic in ALMMC	2.711	9.23
Core (Al alloy) - Cladding (Al MMC)	2.601	6.14
Bimetal produced by infiltration	3.178	4.88
Bimetal produced by mechanical	3.585	3.96

Because of the amount of energy handled by the brakes can be the equivalent of many times the power developed by the engine and they are often called upon to decelerate the vehicle in a fraction of the time that the engine is normally expected to take to accelerate it, an advanced brake disc material should meet several requirements which cannot be provided by a single phase material. Varuzan Kevorkijan (2002) reported the analysis of development of bimetal brake discs with a cast gray iron friction cladding and an aluminium alloy core. Economic benefits are listed in the above Table 6.1.

The economic analysis performed above (Varuzan Kevorkijan, 2002) demonstrates that layered composite structure consisting of cast gray iron friction cladding and an aluminium alloy core could provide many more economic benefits than the monolithic alloy or locally reinforced Al MMC. But cast iron has only one serious disadvantage in this application - it is too heavy in comparison with aluminium-based materials (R.O.Rourke et al. 2001). So, an alternative approach might be to provide standard wear properties and reduce the weight with an aluminium alloy core. Cast iron can be welded, brazed or joined by other well practiced techniques of joining aluminium to ferrous alloys. This generates thermal stresses due to the differential thermal expansion and contraction during and after braking. The heating and cooling process also lead to corrosion problems.To overcome all the problems, core would be replaced with CNT reinforced Al FGCL as shown below.

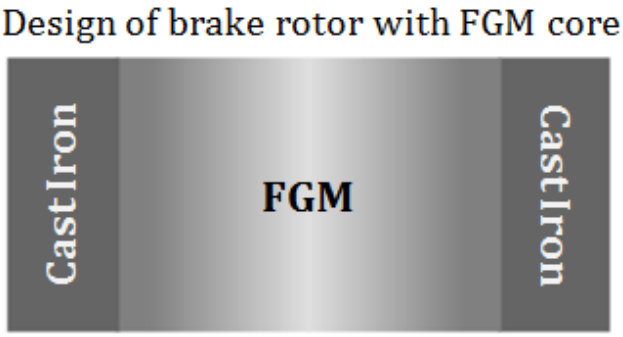

Figure 6.1. Design of brake rotor with FGCL core

Further optimization of the bimetal brake disc towards decreasing the thickness and brake disc volume is necessary to achieve the targeted market price. More promising results may be produced due to the good mechanical property and chemical resistance of the produced FGCL systems.

References

C.Y. Lin, C. Bathias, H. B. McShane, and R. D. Rawlings, (1999), “Production of silicon carbide Al 2124 alloy functionally graded materials by mechanical powder metallurgy technique”, Powder Metallurgy, Vol. 42 No. 1 29.

Cemal Cakir, M., Yahya Isik. (2005). “Finite element analysis of cutting tools prior to fracture in hard turning operations”, Materials and Design, 26,105–112.

Cho, J.R. and Ha, D.Y. (2001). “Averaging and finite-element discretization approaches in the numerical analysis of functionally graded materials”. Materials Science and Engineering, A302, 187–196.

Cho, J.R. and Park, H.J. (2002), “High strength FGM cutting tools: finite element analysis on thermo elastic characteristics.”Journal of Materials Processing Technology, 351-356.

Jaworska, L., Rozmus, M., Krolicka, B. and Twardowska.A. (2006). “Functionally graded cermets”. Journal of Achievements in Materials and Manufacturing Engineering, 17, 73-76.

Dobrzanski, L.A and Dolsanska, B. (2010). “Hardness to toughness relationship on WC-Co tool gradient materials evaluated by Palmqvist method.”Internatiojal Scientific Journal, 43(2), 87-93.

A.Daoud, M.T. Abou El-khair (2009), “Wear and friction behavior of sand cast brake rotor made of A359-20 vol% SiC particle composites sliding against automobile friction material”, Tribology International, vol. 43, pp. 544-553.

A.Fernandez-Canteli, A. Arguellesa, J. Vina, M. Ramulu, A.S. Kobayashi (2002)," Dynamic fracture toughness measurements in composites by instrumented Charpy testing: influence of aging", Composites Science and Technology, 62.1315–1325.

A.J. Ruys, E. B. Popov, D. Sun, J. J. Russell, C. C. J. Murray(2000) “Functionally graded electrical/thermal ceramic systems”, Journal of the European Ceramic Society, vol. 21, pp. 2025-2029.

A.P. Meyer, P. Hottebart, p. Malletroit (1994), " Cast Metal Matrix Composites, American Foundrymen's Society”, Des plaines, III inois, USA, pp. 111-132.

Abdel. H.A. and Ali.Y, (1994). “Experimental determination of dynamic forces during transient orthogonal cutting”, Journal of Materials Processing Technology, 55,162-170.

Amal.E, Alshorbagy, Eltaher, M.A. and Mahmoud, F.F, (2011). “Free vibration characteristics of a functionally graded beam by finite element method”, Applied Mathematical Modelling, 35,412–425.

Andrew.J, Goupee and Senthil.S.V, (2006). “Optimization of natural frequencies of bidirectional functionally graded beams”, Struct Multidisc Optim, 32,473–484.

ASM Speciality handbook (1993), Aluminum and Aluminum Alloys, Materials Park, OH, pp. 428-429.

By Hansang Kwon, Christopher R. Bradbury and Marc Leparoux (2011), “Fabrication of Functionally Graded Carbon Nanotube-Reinforced Aluminum Matrix Composite”, Advanced engineering materials13, No. 4.

C. Tatar, N. Ozdemir (2010), “Investigation of thermal conductivity and microstructure of the α-Al2O3 particulate reinforced aluminium composites (Al/Al2O3-MMC) by powder metallurgy method”, in Physica *B:* Condensed Matter, vol. 405, pp. 896-899.

Calard,V (1998), "Approaches statistics - probability of the mechanical behavior of ceramic matrix composites", PhD, University Bordeaux, Doctoral School of Physical Sciences and Engineering.

Chakrabortya, A., Gopalakrishnana, S. and Reddy, J.N. (2003), “A new beam finite element for the analysis of functionally graded materials.” International Journal of Mechanical Sciences, 45,519–539.

Chandrupatla, T.R. and Delegundu, D. (1997). “Introduction to Finite Element in Engineering”, Trentice Hall of India Pvt. Ltd., New Delhi.

Cho, J.R. and Park, H.J. (2002), “High strength FGM cutting tools: finite element analysis on thermo elastic characteristics.”Journal of Materials Processing Technology, 351-356.

Clausen A.H, Borvik.T, Hopperstad O.S, Benallal, (2004), "Flow and fracture characteristics of aluminium alloy aa5083 h116 as function of strain rate, temperature and triaxiality", Mat Sci Eng, A364:260-272.

Corran, Shadbolt PJ, and Ruiz C (1983),"Impact loading of plates an experimental investigation", International Journal of Impact Engineering, 1(1):3-22.

Fata, A, and Nikuei, B. (2010). “The Effect of the Tool Geometry and Cutting Conditions on the Tool Deflection and Cutting Forces”, World Academy of Science, Engineering and Technology, 69,161-66.

Fatemeh Farhatnia and Gholam-Ali. (2009). “Numerical and analytical approach of thermo-mechanical stresses in FGM beams”, Proceedings of the World Congress on Engineering 2009 Vol II, London.

G. Cueva, A. Sinatora, W. L. Guesser, A. P. Tschiptschin (2003), “Wear resistance of cast irons used in brake disc rotors”, Wear, vol. 255, pp. 1256-1260.

G.L. Manjunath and S. Surendran (2013), " Dynamic fracture toughness of aluminium 6063 with multilayer composite patching at lower temperatures", Vol. 8, No. 2, 163–175, Ships and Offshore Structures.

G.S. Cole (1994), Cast Metal Matrix Composites, American Foundrymen's Society, DesPlaines, lllinois,USA, pp.9-19.

I. Low (1998), “Synthesis and properties of in situ layered and graded aluminium titanate-alumina composites”, Materials Research Bulletin, vol. 33, pp. 1475-1482.

I.M.hutchings, S.Wilson, A.T.Alpas (2000), " Comprehensive composite Materials, Vol.3, Metal Matrix Composites", Elsevier, Amsterdam, pp.447.

J. A. E. Bell, A.E.M. Warner, T. F. Stephnson,E. Siegrist (1996), "Processing properties and Applications of Cast Metal Matrix Composites", Warrendale, PA,USA , pp. 247-258.

J.E.Hatch (Ed.)(1984), " Aluminium Properties and Physical Metallurgy", American Society for Metals, Ohio.

Jabbari, M., Sohrabpour, S. and Eslam, M.R. (2002). “Mechanical and thermal stresses in a functionally graded hollow cylinder due to radially symmetric loads”, International Journal of Pressure Vessels and Piping, 79,493–497.

Kapuria.S, Bhattacharyya.M and Kumar.A.N.(2008). “Bending and free vibration response of layered functionally graded beams: A theoretical model and its experimental validation”, Composite Structures, 82, 390–402.

Krishnan Narasimha Prasad.B.S. and Deepak.G.B,(1995),"Development of a graded TiCN coating or cemented carbide cutting tools-a design approach", Wear 188, 123-129.

Logan.L,(2004), "A First Course in the Finite Element Method", Thomson Asia Pte Ltd.,

Banglore.Rajasekaran.S,(2008). "Finite element analysis in engineering design".Chand, s. publication, Chennai.

M. A. Iqbal, N. K. Gupt (2008), " Energy absorption characteristics of aluminum plates subjected to projectile impact", Latin American Journal of Solids and Structures, 5. 259-287.

M.Kemal Apalak, Recep Gunes, Selim Eroglu, (2007), "Thermal residual stresses in an adhesively bonded functionally graded tubular single lap joint", International Journal of Adhesion & Adhesives 27, 26–48.

Mahmoud Nemat-Alla, (2009) "Reduction of thermal stresses by composition optimization of two-dimensional functionally graded materials", Acta Mech 208, 147–161.

Marom and Bonder SR (1979), "Projectile perforation of multi-layered beams", Int. Journal of Mechanical Sciences, 21:489-504.

Mesut Simsek. (2010). "Fundamental frequency analysis of functionally graded beams by using different higher-order beam theories", Nuclear Engineering and Design, 240,697–705.

Mustafa Yaman. (2006), "Finite element vibration analysis of a partially covered cantilever beam with concentrated tip mass", Materials and Design 27,243–250.

Naghdabadi.R. and Hosseini Kordkheili.S.A, (2005),"A finite element formulation for analysis of functionally graded plates and shells", Archive of Applied Mechanics, 74,375-386.

Nikhil Gupta, Sandeep Kumar Gupta, Benjamin J. Mueller, (2008), "Analysis of a Functionally Graded Particulate Composite under Flexural Loading Conditions", Vol.485, No.1-2, PP. 439-447.

P. J. Blau, C. Brian. Jolly, J. Qu, W. H. Peter, C. A. Blue (2007), "Tribological investigation of titanium-based materials for brakes", Wear, vol.263, pp. 1202–1211.

P.V. Vasconcelos , F.J. Lino b, A. Magalhaes C, R.J.L. Neto (2005), " Impact fracture study of epoxy-based composites with aluminium particles and milled fibres", Journal of Materials Processing Technology, 170. 277–283.

Petyt. M, (1990), "Introduction to Finite Element Vibration Analysis", Cambridge university press, New York.

Piovan.M.T. and Machado.S.P. (2011), "Thermoelastic dynamic stability of thin-walled beams with graded material properties", Thin-Walled Structures, 49, 437–447.

Piovan. M.T and Sampaio. R. (2008), "Vibrations of axially moving flexible beams made of functionally graded materials", Thin-Walled Structures, 46,112–121.

Pompe.W, Worch and Epple.B. (2003), "Functionally graded materials for biomedical applications." Materials Science and Engineering, A362, 40–60.

Ramamurti.V,(2000), "Computer Aided Mechanical Design and Analysis", Tata Mcgraw-Hill, New York.

Reddy.J.N,(2005), "An Introduction to the Finite Element Method", Tata Mcgraw-Hill, New York.

Rosso.M, Porto.G and Geminiani. A(1999), "Studies of graded cemented carbides components", International Journal of Refractory Metals & Hard Material, 17, 187-192.

S. Bueno, L. Micele, C. Melandri, C. Baudin, G. De Portu (2011), "Improved wear behavior of alumina-aluminium titanate laminates with low residual stresses and large grained interfaces" , Journal of the European Ceramic Society, vol. 31, pp. 475-483.

S. Bueno, R. Moreno, C. Baudin (2004), "Design and processing of Al_2O_3- Al_2TiO_5 layered structures" , Journal of the European Ceramic Society, vol. 25, pp. 847-856.

S. N. Aqida, M. I. Ghazali, J. Hashim (2004), "Effects of porosity on mechanical properties of metal matrix composite: an overview", Journal of materials Technology, vol. 40, pp. 17-32.

S. Y. Zhang, F. P. Wang (2006) “Comparison of friction and wear performances of brake material dry sliding against two aluminium matrix composites reinforced with different SiC particles”, Journal of Materials Processing Technology, vol. 182, pp. 122-127.

Sharifi Hyun.S.H and Yoo.H (1999), “Dynamic modelling and stability analysis of a xially oscillating cantilever beams”, Journal of Sound and Vibration, 228(3), 543-558.

Sina.S.A, Navazi.H.M and Haddadpour. H (2009), “An analytical method for free vibration analysis of functionally graded beams”, Materials and Design, 30,741–747.

Suk-Hwan Suh, Jung-Hoon Cho andJean-Yves Hascoet (1996), “Incorporation of Tool Deflection in Tool Path Computation: Simulation and Analysis”, Journal of Manufacturing Systems, 15(3), 190-199.

Suleyman.Y. and Faruk. U. (2005), “Design, development and testing of a turning dynamometer for cutting force measurement”, 1-21,312-317.

Tahani. M, Torabizadeh. M.A and Fereidoon.A (2006), “Nonlinear analysis of functionally graded beams”, Journal of Achievements in Materials and Manufacturing Engineering, 18,315-318.

Thomas. M. and Beauchamp. Y (2003), “Statistical investigation of modal parameters of cutting tools in dry turning”, International Journal of Machine Tools & Manufacture, 43, 1093–1106.

Tomkow. J. and Marchelek. K (1995), “Modelling cutting process in dynamic stability analysis of machine tools” International Journal of Machine Tools and Manufacture, 35(4), 535-545.

Toshio Nomura, Hideki Moriguchi and Keiichi Tsuda(1999), “Material design method for the functionally graded cemented carbide tool”, International Journal of Refractory Metals & Hard Material, 17, 397-404.

Turner, CE (1973), "Fracture Toughness and Fracture Specific Energy: A Re-analysis of Results", Materials Science and Engineering, 11, pp. 275-282.

Vu-Khanh,T. Yu(1997) "Mechanisms of brittle-ductile transition in toughened thermoplastics", Theoretical and Applied Fracture Mechanics, 26, 177-183

W. Pompe, H. Worch , M. Epple , W. Friess , M. Gelinsky , P. Greil , (2003), "Functionally graded materials for biomedical applications", Materials Science and Engineering, A362,40–60.

Walter Lengauera and Klaus Dreyerb (2002), "Functionally graded hard metals", Journal of Alloys and Compounds, 33, 194–212.

William G. Cooley, BS Captain, USAF,(2001), "Application of functionally graded materials in aircraft structures", AFIT/GAE/ENY/05-M04.

Xian-Fang Li, Bao-LinWang and Jie-Cai Han (2010) "A higher-order theory for static and dynamic analyses of functionally graded beams", Arch Appl Mech, 80, 1197–1212.

Ying-An Kanga and Xian-FangLia (2009), "Bending of functionally graded cantilever beam with power-law non-linearity subjected to an end force", International Journal of Non-Linear Mechanics, 44, 696 – 703.

Zaid A.O, EL-Kalay A, and Travis F.W(1973), "An examination of the perforation of mild steel plates by flat ended cylindrical projectile", International Journal of Mechanical Sciences, 15:129-143.

Zheng Zhong, Tao Yu (2007), "Analytical solution of a cantilever functionally graded beam", Composites Science and Technology, 67,481–488.

Appendix-I

CODE FOR CALCULATING YOUNGS MODULUS BY USING SIMPLE POWER LAW FOR A BEAM

The material property of the FGCL beam assumed to vary through thickness according to the power law distribution.

$P(z) = (P_u - P_l)\,(Z/h + 1/2)^k + P_l$ ---------(1) (Kim.J et al. 2002)

But the gradation was step wise, we could use the simple power law distribution

$E = E_{filler}\ V_{filler} + E_{matrix}\ V_{matrix}$ ----------(2)

Moment of inertia of the beam calculated using :

$$I = \frac{b\,h^3}{12} + A\bar{y}^2 \quad \text{---------(3)}$$

Deflection calculation using

$$y = \frac{Wl^2\left(2l + 3b\right)}{6EI} \quad \text{----------(4)}$$

Step 1.: Calculated weight fraction of CNT

```
W_cnt1=0.1/100;

W_cnt2=0.2/100;

W_cnt3=0.3/100;

W_cnt4=0.4/100;

W_cnt5=0.5/100;
```

E_AL=58;

E_CNT=1400;

al_density=2.537;

cnt_density=1.6;

Step 2: Converted weight fraction to volume fraction

V_cnt1=W_cnt1/(W_cnt1+(1-W_cnt1)*(cnt_density/al_density));

V_cnt2=W_cnt2/(W_cnt2+(1-W_cnt2)*(cnt_density/al_density));

V_cnt3=W_cnt3/(W_cnt3+(1-W_cnt3)*(cnt_density/al_density));

V_cnt4=W_cnt4/(W_cnt4+(1-W_cnt4)*(cnt_density/al_density));

V_cnt5=W_cnt5/(W_cnt5+(1-W_cnt5)*(cnt_density/al_density));

Step 3: Calculation of Young's modulus for each layer of laminates

E1=E_AL*(1-V_cnt1)+E_CNT*V_cnt1

E2=E_AL*(1-V_cnt2)+E_CNT*V_cnt2

E3=E_AL*(1-V_cnt3)+E_CNT*V_cnt3

E4=E_AL*(1-V_cnt4)+E_CNT*V_cnt4

E5=E_AL*(1-V_cnt5)+E_CNT*V_cnt5

Step 4: Calculation of effective Moment of intertia

y=(10*1*5.5+10*1*4.5+10*1*3.5+10*1*2.5+10*1*1.5+10*1*0.5)/(6*10*1)

I1=((10*1^3)/12)+10*1*(5.5-y)^2;

I2=((10*1^3)/12)+10*1*(4.5-y)^2;

I3=((10*1^3)/12)+10*1*(3.5-y)^2;

I4=((10*1^3)/12)+10*1*(2.5-y)^2;

I5=((10*1^3)/12)+10*1*(1.5-y)^2;

I6=((10*1^3)/12)+10*1*(0.5-y)^2-8

I=I1+I2+I3+I4+I5+I6

Step 5: Calculation of Deflection by using simple bending equation

Deflection= (10*45^2*(2*45+3*25))/(6*E6*10^3*I)

Technical research papers published based on this thesis

Category details:

1. Journal paper 2. International conference 3. National Conference

Sl. No	Title of the paper	Authors	Name of the journal	Month & Year of publication	Category
1	Fabrication of Functionally Graded Carbon Nanotube-Reinforced Aluminium Matrix Laminate by Mechanical Powder Metallurgy Technique-Part I	Gururaja Udupa S.Shrikantha Rao K.V.Gangadharan	J Material Science Engineering ISSN:2169-0022 JME,an open acces journal	May, 2015	1
2	A review of Carbon Nanotube Reinforced Aluminium Composite and Functionally Graded composites as a Future material for Aerospace	Gururaja Udupa S.Shrikantha Rao K.V.Gangadharan	International Journal of Modern Engineering and research	Jully, 2014	1
3	Future applications of Carbon Nanotube reinforced Functionally Graded Composite materials	Gururaja Udupa S.Shrikantha Rao K.V.Gangadharan	IEEE : International conference on Advances in Engineering,Science and Management(ICAESM-2012) ISBN: 978-81-909042-2-3 ©2012 IEEE	March 30,31. 2012	2
4	Functionally graded Composite materials: An overview	Gururaja Udupa S.Shrikantha Rao K.V.Gangadharan	Procedia Material Science 5 (2014) 1291-1299(ICAMME 2014)doi:10.1016/j.mspro2014. 07442	March , 2014	2
5	Future applications of Carbon Nanotube reinforced Functionally Graded Composite materials	Gururaja Udupa S.Shrikantha Rao K.V.Gangadharan	IEEE – International Conference on Advances in engineering, Science and Management	March, 2012	2
6	A review of Carbon Nanotube Reinforced Aluminium Composite and Functionally Graded composites as a Future material for Aerospace	Gururaja Udupa S.Shrikantha Rao K.V.Gangadharan	National Conference on Advances in Material science and future prospects	October, 2013	3